

Code CFTs and Topological Matter

E.H Saidi^{1,2,3}, **R. Sammani**^{1,2}

¹*LPHE-MS, Science Faculty, Mohammed V University in Rabat, Morocco*

²*Hassan II Academy of Science and Technology, Kingdom of Morocco*

³*Centre of Physics and Mathematics, CPM- Morocco.*

E-mail: e.saidi@um5r.ac.ma, rajae.sammani@um5.ac.ma

ABSTRACT: In this paper, we propose a novel framework for modeling topological phases of matter using code-based Narain conformal field theories (NCFTs). We show that the algebraic structure of the NCFTs naturally embeds into critical lattice quantum field theory, yielding emergent topological features characteristic of gapless fermionic systems with non-zero Chern numbers. We develop a new representation of construction A of code CFT in terms of root and weight lattices of Lie algebras, focusing in particular on SU(2) and SU(3). We then derive the spectrum of particle states occupying the lattice and, with the help of fermionisation techniques, demonstrate that it hosts fermionic excitations with Dirac cones akin to tight binding systems namely the Haldane model of quantum anomalous hall effect on a honeycomb geometry.

KEYWORDS: Chern-Simons theory, code/Narain CFTs, root/weight lattices, fermionisation, tight binding model on honeycomb, Dirac cones and topological matter.

Contents

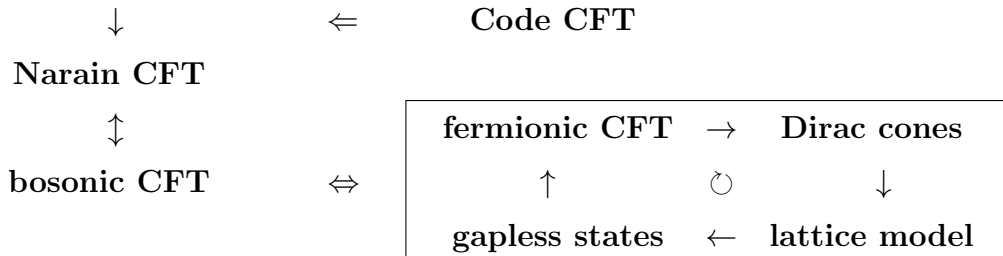
1	Introduction	3
2	The triplet $(\Lambda_k, \Lambda_{k\mathcal{C}}, \Lambda_k^*)$ from $SU(2)$ lattices	6
2.1	Narain CFT with $c_{L/R} = 1$	7
2.1.1	Models with CS level $k=2$	8
2.1.2	Lattices of $SO(4)$	12
2.2	Models with CS level $k>2$	13
2.3	From scalars in continuum to lattice QFT	16
2.3.1	Case of one real 2D scalar field $X = X(\tau, \sigma)$	16
2.3.2	Lattice extension	17
3	Extension to $SU(3)$ Lattices	19
3.1	Realisation at level $k=3$	19
3.2	The triplet $(\Lambda^{\text{su}_3}, \Lambda_{\mathcal{C}}^{\text{su}_3}, \Lambda^{*\text{su}_3})$	22
4	Particles in NCFTs and path to topological matter	24
4.1	Particles in $SU(2)$ based model	25
4.1.1	Exhibiting the $SU(2)$ symmetry	26
4.1.2	About the even integer condition	28
4.2	Particles in the $SU(3)$ based model	30
4.2.1	Momenta $P_{L/R}$ and $SU(3)$ symmetry	30
4.2.2	Ground configurations and $SU(3)$ representations	32
5	Lattice fermions and topological phases	33
5.1	KK/W system on the lattice	35
5.1.1	Fermionisation	35
5.1.2	Hamiltonian Eq(5.9) in reciprocal space	37
5.2	Dirac cones and gapless states	38
6	Conclusion and discussion	40
A	From code-CFT to Narain ensemble	43
B	Construction A of code Narain CFT	49
C	Lattices $\Lambda^{\text{su}_3}, \Lambda_{\mathcal{C}}^{\text{su}_3}, \Lambda^{*\text{su}_3}$ for $k<3$ and $k>3$	52

1 Introduction

Condensed matter systems, especially in their lattice QFT formulations, have long provided a testing ground for concepts originating in high energy physics theory [1, 2]. These models allow the realizability of theoretical frameworks that are otherwise difficult or even impossible to test. Beyond the experimental validation, they also offer insights on testable predictions that may open pathways towards the development of potential technologies [3].

In this work, we introduce a novel approach to modeling topological phases of matter by proposing code-based conformal field theories (CFTs) [4]-[13] as a new class of realizations. Exploiting recent constructions of Narain CFT as a coding theory [13]-[24] where one can systematically build and analyze Narain CFTs using self-dual additive codes defined over discrete abelian groups, we demonstrate that the associated algebraic data can be leveraged to model topologically non trivial phases of matter [25]-[40]. We show that the framework of code based Narain CFT is not only mathematically rich but also physically relevant with emergent topological properties [41]-[51] characteristic of a gapless fermionic system having a non zero Chern number [52, 53]. In doing so, we provide a new framework for describing topological matter as a code based CFT.

AB Chern-Simons



For every even self dual code \mathcal{C} , one can construct a triplet of lattices $\Lambda_{\mathbf{k}}^{r,r} \subset \Lambda_{\mathbf{k}\mathcal{C}}^{r,r} \subset (\Lambda_{\mathbf{k}}^{r,r})^*$ realizing the Narain CFT with $U(1)^{c_L} \times U(1)^{c_R}$ where $c_L = c_R = r$ [4]-[16] that admits a holographic dual given by the AB Chern-Simons (CS) theory with coupling constant $k \in \mathbb{N}^*$ (CS level) [21]; report to *appendix A* for a comprehensive review. These constructions allow to perform explicit calculations of generalised Narain partition functions using code based algorithms [24]. The structure of the even self dual codes \mathcal{C} enables to build discrete sets $\Lambda_{\mathbf{k}\mathcal{C}}^{r,r}$ sitting in $\mathbb{R}^{r,r}$ which in turn realise $2r$ dimensional Narain lattices Λ_{NARAIN} . In this setting, the discrete group $G_{\mathbf{k}}^{r,r}$ is identified with the discriminant $\Lambda_{\mathbf{k}}^{r,r*}/\Lambda_{\mathbf{k}}^{r,r}$ taken in this study to be $\mathbb{Z}_{\mathbf{k}}^r \times \mathbb{Z}_{\mathbf{k}}^r$ and can be interpreted in terms of the symmetries of unit cells of the real lattice $\Lambda_{\mathbf{k}}^{r,r}$, its dual $\Lambda_{\mathbf{k}}^{*r,r}$ and the even self

dual $\Lambda_{k\mathcal{C}}^{r,r}$. This construction, referred to as Construction A [54], permits to generate KK and winding states, related via duality, and populating a lattice (a honeycomb for SU(3) with $k=2$) that hosts fermionic hoppings. The resulting lattice model is shown to mimic that of Haldane theory with Dirac cones.

Our investigation unfolds through the following steps:

(a) **the SU(2) construction:** We begin by showing that construction A of the $c_{L/R} = 1$ Narain theory admits a natural interpretation in terms of the root $R^{\text{su}_2} := R_k^{\text{su}_2}|_{k=2}$ and weight $W^{\text{su}_2} = W_k^{\text{su}_2}|_{k=2}$ lattices of SU(2) and their fibrations as given by eq(A.6) which is valid for generic values of k , including the special level $k=2$. Recall that the group SU(2) has rank $r=1$, and for $k=2$, the associated discriminant $W^{\text{su}_2}/R^{\text{su}_2}$ is isomorphic to \mathbb{Z}_2 . This implies that the unit cell of W^{su_2} contains two different types of sites (represented by a two-colored grid), whereas R^{su_2} has only one type of sites. This distinction is depicted in Figure 17. In this illustrative image, we graphically represent the lattice sequence $\Lambda_2^{1,1} \subset \Lambda_{2\mathcal{C}}^{1,1} \subset \Lambda_2^{*,1,1}$ using different color codings: (i) four colors for the largest lattice $\Lambda_2^{*,1,1} = W_2^{\text{su}_2} \times W_2^{\text{su}_2}$, (ii) two colors for the intermediate $\Lambda_{2\mathcal{C}}^{1,1} = R_2^{\text{su}_2} \times W_2^{\text{su}_2}$; and (iii) one color for the smallest one $\Lambda_2^{1,1} = R_2^{\text{su}_2} \times W_2^{\text{su}_2}$. For generic values of the CS level k , the graphical

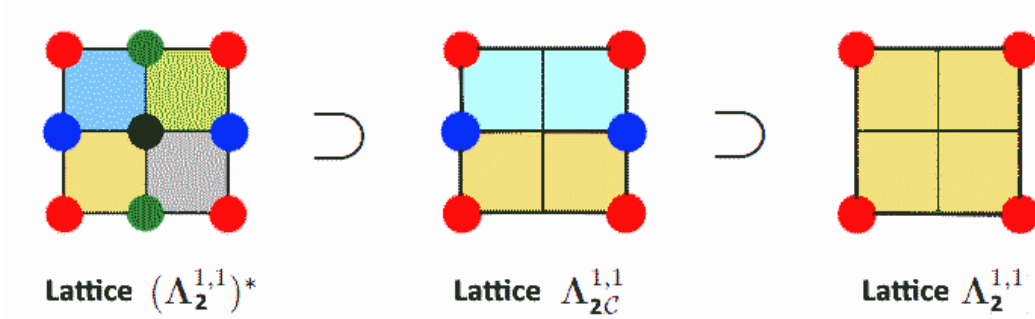


Figure 1: The unit cells of the 2D lattices of construction A of the $c_{L/R} = 1$ theory. The lattice sites are color coded with the number of colors reflecting the density of the lattice: k^2 colors for $\Lambda_k^{1,1*}$, k colors for $\Lambda_{k\mathcal{C}}^{1,1}$ and one color for $\Lambda_k^{1,1}$. The areas of the unit cells are exhibited in increasing order. On left, $\Lambda_2^{1,1*}$ with 4 unit cells. In middle, the $\Lambda_{2\mathcal{C}}^{1,1}$ with 2 unit cells. On right, the unit cell of $\Lambda_2^{1,1}$.

representation of the triplet $\Lambda_k^{1,1} \subset \Lambda_{k\mathcal{C}}^{1,1} \subset \Lambda_k^{1,1*}$ in $\mathbb{R}^{1,1}$ requires k^2 colored sites. They can be remarkably realized via the fibrations

$$\begin{aligned}
 \Lambda_k^{1,1} &= R_k^{\text{su}_2} \times R_k^{\text{su}_2} & \Lambda_k^{\text{su}_2} &= R_k^{\text{su}_2} \times R_k^{\text{su}_2} \\
 \Lambda_{k\mathcal{C}}^{1,1} &= R_k^{\text{su}_2} \times W_k^{\text{su}_2} & \Lambda_{k\mathcal{C}}^{\text{su}_2} &= R_k^{\text{su}_2} \times W_k^{\text{su}_2} \\
 \Lambda_k^{*,1,1} &= W_k^{\text{su}_2} \times W_k^{\text{su}_2} & \Lambda_k^{*\text{su}_2} &= W_k^{\text{su}_2} \times W_k^{\text{su}_2}
 \end{aligned} \quad \Leftrightarrow \quad (1.1)$$

In these expressions, the root lattice $\mathbf{R}_k^{\text{su}2}$ is isomorphic to the 1D lattice $\sqrt{k}\mathbb{Z}$ while the weight lattice $\mathbf{W}_k^{\text{su}2}$ is its dual $\frac{1}{\sqrt{k}}\mathbb{Z}$. The coset structure $\mathbf{W}_k^{\text{su}2}/\mathbf{R}_k^{\text{su}2} \simeq \mathbb{Z}_k$ shows that $\mathbf{W}_k^{\text{su}2}$ can be interpreted as a union of k (shifted) sublattices of $\mathbf{R}_k^{\text{su}2}$ distant by some weight vectors as explicitly illustrated in sections 3 and 4. The sites of these lattices Λ describe quantum particle states $|\psi_{a,n}^{b,m}\rangle$ labeled by four indices: ground configuration indices (a,b) , Kaluza n and windings m modes.

- (b) **The SU(3) extension:** We construct novel realisations of construction A of code CFT, extending beyond the SU(2) based configurations [55]-[58] discussed previously. In this extension, we build upon the SU(2) results to generalise the lattice realisation (A.6) to higher dimensional Lie algebras especially those of rank 2 such as SU(3), SO(5) and G2. Focussing on the interesting case of SU(3), the relevant 4D lattices are embedded in $\mathbb{R}^{2,2}$ with hierarchy $\Lambda_k^{\text{su}3} \subset \Lambda_{k\mathcal{C}}^{\text{su}3} \subset \Lambda_k^{*\text{su}3}$ and representation:

$$\begin{aligned}\Lambda_k^{\text{su}3} &= \mathbf{R}_k^{\text{su}3} \times \mathbf{R}_k^{\text{su}3} \\ \Lambda_{k\mathcal{C}}^{\text{su}3} &= \mathbf{R}_k^{\text{su}3} \times \mathbf{W}_k^{\text{su}3} \\ \Lambda_k^{*\text{su}3} &= \mathbf{W}_k^{\text{su}3} \times \mathbf{W}_k^{\text{su}3}\end{aligned}\tag{1.2}$$

We distinguish three cases according to the value of the Chern-Simons level k of the holographic dual of the Narain CFT: (i) **Case $k=3$:** At this level, the discriminant group is $\mathbb{Z}_3 \times \mathbb{Z}_3$ with \mathbb{Z}_3 being the group centre of SU(3). The 4D lattice $\Lambda_3^{\text{su}3} = \mathbf{R}_3^{\text{su}3} \times \mathbf{R}_3^{\text{su}3}$ is made out of the fibration of two hexagonal lattices while its dual $\Lambda_3^{*\text{su}3} = \mathbf{W}_3^{\text{su}3} \times \mathbf{W}_3^{\text{su}3}$ is constructed from the fibration of two triangular lattices. (ii) **Case $k>3$:** the results obtained for $k=3$ extends naturally to higher values $k>3$ for which the discriminant satisfies $\mathbf{W}_k^{\text{su}3}/\mathbf{R}_k^{\text{su}3} \simeq \mathbb{Z}_k$. (iii) **Case $k<3$:** for low levels $k = 1, 2$, the situation is subtler. While the CS level $k=1$ is somehow "exotic" because the condition $\mathbf{R}_k^{\text{su}3} \subseteq \mathbf{W}_k^{\text{su}3}$, as we will discuss, is violated. This bound holds only for $k \geq \sqrt{3}$ therefore ruling out $k=1$ but allowing $k=2$ for which the weight lattice $\mathbf{W}_2^{\text{su}3}$ is given by the 2D honeycomb while the $\mathbf{R}_2^{\text{su}3}$ is an hexagonal lattice.

- (c) **Emergence of topological properties:** After establishing a new formulation of the framework in terms of algebraic data, we exploit the new setting to develop a path towards topological phases of matter by linking Narain CFT to critical lattice QFT. We start by modeling the particles sitting at the intersection of the lattice $\Lambda_{\mathcal{C}}$ grid in terms of KK $|KK_{\mathbf{m}}\rangle$ and winding states $|W_{\mathbf{m}}\rangle$ akin to tight-binding systems in condensed matter physics. Our primary focus remains on SU(2) based

code CFTs with central charge giving quantized left/right momenta for particle states, organizing into $SU(2)$ representations, and labeled by ground state and excitation quantum numbers. This reveals a Hilbert space containing k^2 vacuum states and associated excitations, a decoupling of energy and momentum sectors, in addition to a globally defined topological index depending on k .

Proceeding, we analyze the particle content in the $SU(3)$ Chern-Simons (CS) theory at level $k=2$. We show that the corresponding weight lattice decomposes into two sublattices forming a honeycomb structure, interconnected via a Z_2 symmetry. This later also relates the KK modes residing on one sublattice to the winding modes populating the other. Using fermionisation techniques [62–64], we introduce Dirac fermions as propagations on the honeycomb lattice with a tight binding Hamiltonian that breaks inversion symmetry. We prove that our lattice model mimics that of Haldane theory [33, 34] with Dirac cones therefore demonstrating that NCFTs can be realised as gapless fermionic systems having non zero Chern numbers. This in turn closes the loop and establishes a direct link between code CFT and topological matter.

The organisation is as follows: In [section 2](#), we present construction A in code-CFTs realising Narain conformal theories and show how the three lattices $(\Lambda_k, \Lambda_{k\mathcal{C}}, \Lambda_k^*)$ can be linked to the root R^{su_2} and the weight W^{su_2} lattices of $SU(2)$ and their cross products. New results for this $SU(2)$ based building are obtained. In [section 3](#), we extend the construction to $SU(3)$ and derive realisations of the triplet $(\Lambda_k^{\text{su}_3}, \Lambda_{k\mathcal{C}}^{\text{su}_3}, \Lambda_k^{\text{su}_3*})$ while distinguishing three intervals $k=3$, $k>3$ and $k<3$. In [section 4](#), we give applications aiming to establish a link between the Narain CFTs and lattice quantum matter at Dirac points. Here, we investigate the properties of particle states in the $SU(2)$ and the $SU(3)$ based CFTs while in [section 5](#) we draw the way to Chern matter by giving explicit examples. [section 6](#) is devoted to conclusion and discussions. [Appendix A](#), [Appendix B](#) and [Appendix C](#) contain technical details of our calculations and supplementary material supporting the main text.

2 The triplet $(\Lambda_k, \Lambda_{k\mathcal{C}}, \Lambda_k^*)$ from $SU(2)$ lattices

In this section, we demonstrate how the three lattices Λ , Λ^* and $\Lambda_{\mathcal{C}}$ used in the construction A, *reviewed in appendix B*, can be linked to the root R^{su_2} , the weight W^{su_2} lattices of $SU(2)$ and their cross products. This identification will lay the groundwork foundation for the next section where we extend the study to a broader class of lattices associated

with general Lie algebras \mathfrak{g} going beyond $SU(2)$. This will lead to novel realisations of the triplet $(\Lambda^{\mathfrak{g}}, \Lambda_{\mathcal{C}}^{\mathfrak{g}}, \Lambda^{*\mathfrak{g}})$ in higher dimensions.

2.1 Narain CFT with $c_{L/R} = 1$

To start, we focus on the case $r=1$ (i.e. central charge $c_{L/R} = 1$) to clearly present the core idea of the construction. The extension to $r>1$ follows directly from (B.14) and will be briefly commented later. To that purpose, we define¹ $R_k = \sqrt{k}\mathbb{Z}$ and $W_k = \frac{1}{\sqrt{k}}\mathbb{Z}$ with integer $k>1$; they naturally satisfy the inclusion property $R_k \subset W_k$ and have a discriminant group given by W_k/R_k , which upon substitution becomes $\frac{1}{\sqrt{k}}\mathbb{Z}/(\sqrt{k}\mathbb{Z})$ isomorphic to the abelian group $\mathbb{Z}/(k\mathbb{Z}) \simeq \mathbb{Z}_k$ giving therefore

$$W_k/R_k \simeq \mathbb{Z}_k \quad (2.1)$$

This coset space will later be given a compelling geometric interpretation. By viewing W_k as the product $\mathbb{Z}_k \times R_k$, one may think of it as a superposition of k sheets of 1D sublattices, each isomorphic to R_k . Formally, we have

$$W_k \simeq \underbrace{R_k \cup R_k^{[\lambda]} \cup \dots \cup R_k^{[(k-1)\lambda]}}_{k \text{ components}} \subset \mathbb{R} \quad (2.2)$$

where we have set $R_k^{[\varepsilon\lambda]} = R_k + \varepsilon\lambda$ and $R_k^{[0]} = R_k$. These sheets are related to one another by the symmetry \mathbb{Z}_k , generated by the algebraic k -cycle $(1, 2, \dots, k)$ which can be represented by the matrix

$$T = \begin{pmatrix} 0 & 1 & \dots & 0 \\ \vdots & \ddots & \ddots & \vdots \\ 0 & 0 & 0 & 1 \\ 1 & 0 & 0 & 0 \end{pmatrix}_{k \times k}, \quad T^k = I_{id} \quad (2.3)$$

For the special case $k = 1$, we have $R_1 = \mathbb{Z}$ and $W_1 = \mathbb{Z}$ so that $R_1 \simeq W_1$; their discriminant \mathbb{Z}_1 is therefore trivial and given by the identity element I_{id} . From the perspective of code CFT, this case $k = 1$ corresponds to the trivial code [5, 23]

$$\mathcal{C} = \{c = (0, 0)\} \subseteq \mathbb{Z}_k \quad (2.4)$$

Recall that a generic codeword c , defined by the pair (a, b) with components taking integer values $a, b = 0, \dots, k-1$, belongs to an even self dual code \mathcal{C} . In terms of the sets R_k and W_k , the lattice Λ_k is then given by the cross product $R_k \times R_k$ while its dual Λ_k^*

¹ In general, one may take $R_k = \sqrt{k}(\mathfrak{a}\mathbb{Z})$ and $W_k = \frac{1}{\sqrt{k}}(\mathbb{Z}/\mathfrak{a})$ with respective parameters \mathfrak{a} and $1/\mathfrak{a}$.

is $W_k \times W_k$ thus satisfying the inclusion $\Lambda_k \subset \Lambda_k^*$ due to $R_k \subset W_k$. The motivation for using R_k and W_k stems from their interesting interpretation as the root R_k and weight W_k lattices of $SU(2)$ which naturally leads to the 2D lattices Λ_k and Λ_k^* imagined as follows

Lattice	$SU(2)$	$SU(2) \times SU(2)$
root	R_k	$\Lambda_k = R_k \times R_k$
weight	W_k	$\Lambda_k^* = W_k \times W_k$

(2.5)

To illustrate this structure, we first consider the particular case $k=2$ for which $R_2 = \sqrt{2}\mathbb{Z}$ and $W_2 = \frac{1}{\sqrt{2}}\mathbb{Z}$. Then, we proceed to the generic case $k > 2$.

2.1.1 Models with CS level $k=2$

For the particular $k=2$ case, the discrete spaces Λ_2 , Λ_{2C} and Λ_2^* constructed out of R_2 and W_2 are two dimensional lattices embedded in $\mathbb{R}^{1,1}$. To set the stage, we provide a preview of their graphic description in the Figures 2-3. The Λ_2 and Λ_2^* are given by square lattices characterised, respectively, by parameters α and λ which will be determined later. In the two illustrations of Figure 2, we employ distinct colors to

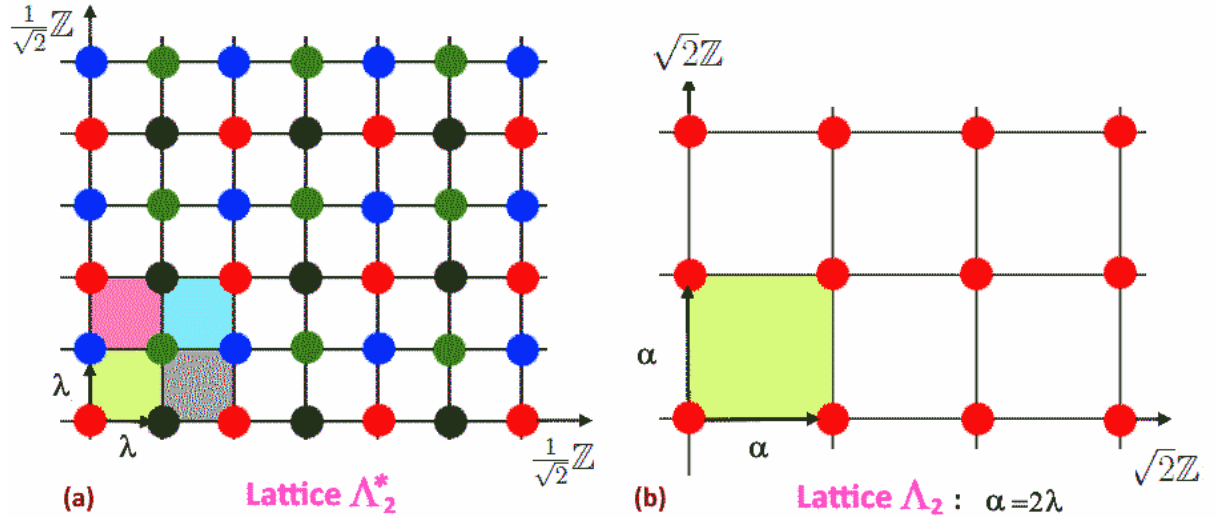


Figure 2: Graphic descriptions of the lattice Λ_2 and its dual Λ_2^* . On right, the sites in Λ_2 are painted in red with the unit cell highlighted in pistachio. In the left, the sites of Λ_2^* are color coded in black, green, blue and red to illustrate the embedding property $\Lambda_2 \subset \Lambda_{2C} \subset \Lambda_2^*$. The graphics of Λ_{2C} is given by the Figure 3.

designate the sites of Λ_2 and its dual Λ_2^* . For the real lattice Λ_2 , the sites are painted in red; its unit cell, shaded in pistachio, has an area equal to 2 (i.e $uc\Lambda_2 = 2$). As for the dual lattice Λ_2^* , we use four colors (black, green, blue and red) to explicitly display

the embedding hierarchy

$$\Lambda_2 \subset \Lambda_{2\mathcal{C}} \subset \Lambda_2^* \quad \Leftrightarrow \quad uc\Lambda_2 > uc\Lambda_{2\mathcal{C}} > uc\Lambda_2^* \quad (2.6)$$

The area of the unit cell for Λ_2^* is equal to $1/2$ (i.e. $uc\Lambda_2^* = 1/2 = uc\Lambda_2/4$) which is the reciprocal of the unit cell area of the real Λ_2 . For completeness, we also give an anticipatory graphic representation of the even self dual lattice $\Lambda_{2\mathcal{C}}$ satisfying the embedding property (2.6). Its unit cell area is equal to 1 (i.e. $uc\Lambda_{2\mathcal{C}} = 1$), a value that we use as *a criterion of self duality*. The graphic of $\Lambda_{2\mathcal{C}}$ is depicted in Figure 3 where its lattice sites are distinguished in red and blue.

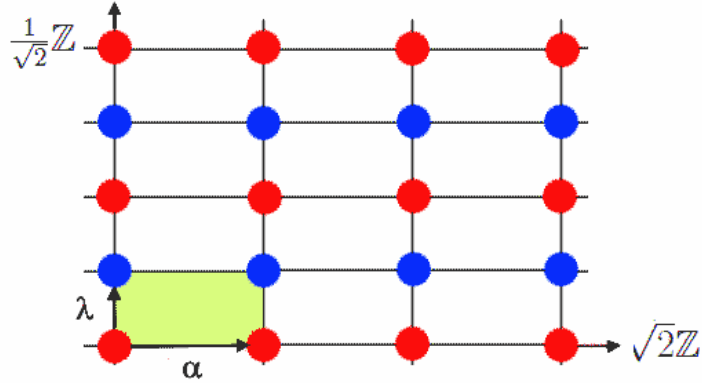


Figure 3: The structure of the lattice $\Lambda_{2\mathcal{C}}$ with sites shown in two different colors. The even self dual lattice contains the Λ_2 made by red sites. Sites in blue belong to $\Lambda_{2\mathcal{C}}/\Lambda_2 \simeq \Lambda_2 + \lambda$. Physically, red sites will be thought of as filled by KK particle states and the blue ones by winding modes; see section 4 for details.

The set of red sites represents the sublattice Λ_2 contained into $\Lambda_{2\mathcal{C}}$ while the blue sites describe the complement $\Lambda_{2\mathcal{C}}/\Lambda_2$ which, up to a global shift λ , is isomorphic to Λ_2 . Hence, we have the decomposition

$$\begin{aligned} \Lambda_{2\mathcal{C}} &= \Lambda_2 + (\Lambda_{2\mathcal{C}}/\Lambda_2) \\ &\simeq \underbrace{\Lambda_2 + (\Lambda_2 + \lambda)}_{2 \text{ superposed } \Lambda_2\text{s}} \end{aligned} \quad (2.7)$$

To derive the results illustrated in Figures 2-3, we start with eq(B.9) which shows that the lattices Λ_2 and Λ_2^* , realised in terms of R_2 and W_2 , have the following factorised structure

$$\Lambda_2 = R_2 \times R_2' \quad , \quad \Lambda_2^* = W_2 \times W_2' \quad (2.8)$$

Since $W_2/R_2 \simeq \mathbb{Z}_2$, the discriminant Λ_2^*/Λ_2 is isomorphic to the discrete group $\mathbb{Z}_2 \times \mathbb{Z}_2$. To elucidate the $SU(2)$ interpretation of the lattices Λ_2 , Λ_{2C} , Λ_2^* , we reconsider the discrete sets $\sqrt{2}\mathbb{Z}$ and $\frac{1}{\sqrt{2}}\mathbb{Z}$ as follows:

(1) **sublattice** $\sqrt{2}\mathbb{Z}$.

The presence of $\sqrt{2}$ viewed as $\sqrt{1^2 + 1^2}$, suggest that the discrete set $\sqrt{2}\mathbb{Z}$ correspond to a 1D sublattice of the ambient square lattice $\mathbb{Z} \times \mathbb{Z}$ with canonical basis vectors $(\mathbf{e}_1, \mathbf{e}_2)$ and lattice spacing $\mathbf{a} = \mathbf{b} = 1$. This sublattice can be realised in two equivalent ways:

(i) As the *diagonal 1D sublattice* with coordinates (n, n) where $n \in \mathbb{Z}$; see red dots in Figure 4.

(ii) As the *anti-diagonal sublattice* with coordinates $(n, -n)$; see the blue dots in the same Figure 4. These (anti) diagonal lines in $\mathbb{Z} \times \mathbb{Z}$ have slopes $\frac{b}{a} = \pm 1$ and spacing $c = \sqrt{a^2 + b^2} = \sqrt{2}$.

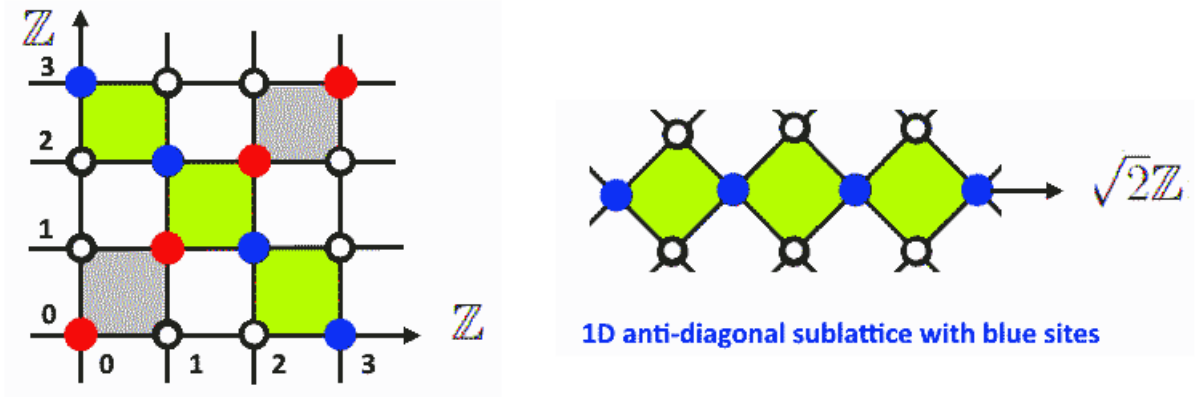


Figure 4: On top, the square lattice $\mathbb{Z} \times \mathbb{Z}$. (anti-) diagonal 1D sublattice $\pm\sqrt{2}\mathbb{Z}$ is given the (blue) red sites. In bottom, the anti-diagonal 1D sublattice to be used below.

For our purposes, we adopt the anti-diagonal realisation of $R_2 \sim \sqrt{2}\mathbb{Z}$ with sites $(n, -n)$. This sublattice is generated by the vector $\boldsymbol{\alpha} = \mathbf{e}_1 - \mathbf{e}_2$ with components $(1, -1)$ satisfying $\boldsymbol{\alpha}^2 = 2$ and norm $\|\boldsymbol{\alpha}\| = \sqrt{2}$. We can therefore define the 1D sublattice like

$$R_2 \simeq \mathbb{Z}\boldsymbol{\alpha} \quad (2.9)$$

By using the unit vector $\mathbf{u} = \frac{1}{\sqrt{2}}(\mathbf{e}_1 - \mathbf{e}_2)$ in the direction of R_2 , we may also write $\boldsymbol{\alpha} = \sqrt{2}\mathbf{u}$ and then $R_2 \simeq (\sqrt{2}\mathbb{Z})\mathbf{u}$.

(2) **sublattice** $\frac{1}{\sqrt{2}}\mathbb{Z}$.

This lattice, denoted $W_2 = \frac{1}{\sqrt{2}}\mathbb{Z}$, is dual to $\sqrt{2}\mathbb{Z}$. It is generated by $\boldsymbol{\lambda} = \frac{1}{2}\boldsymbol{\alpha}$ with components $(\frac{1}{2}, -\frac{1}{2})$, euclidian length $\boldsymbol{\lambda}^2 = 1/2$ and norm $\|\boldsymbol{\lambda}\| = 1/\sqrt{2}$; precisely the inverses of the corresponding root quantities $\boldsymbol{\alpha}^2$ and $\|\boldsymbol{\alpha}\|$. The lattice W_2 sits along *the*

anti-diagonal line of the square lattice $\frac{1}{2}\mathbb{Z} \times \frac{1}{2}\mathbb{Z}$ with lattice spacing $\tilde{\mathbf{a}} = \frac{1}{2}$ leading to $\tilde{c} = \sqrt{\frac{1}{4} + \frac{1}{4}} = \frac{1}{\sqrt{2}}$. Thus

$$W_2 \simeq \mathbb{Z}\boldsymbol{\lambda} \quad (2.10)$$

Again, in terms of the unit vector \mathbf{u} , we also find $\boldsymbol{\lambda} = \frac{1}{\sqrt{2}}\mathbf{u}$ implying $W_2 \simeq (\frac{1}{\sqrt{2}}\mathbb{Z})\mathbf{u}$. For illustration, see the Figure 5.

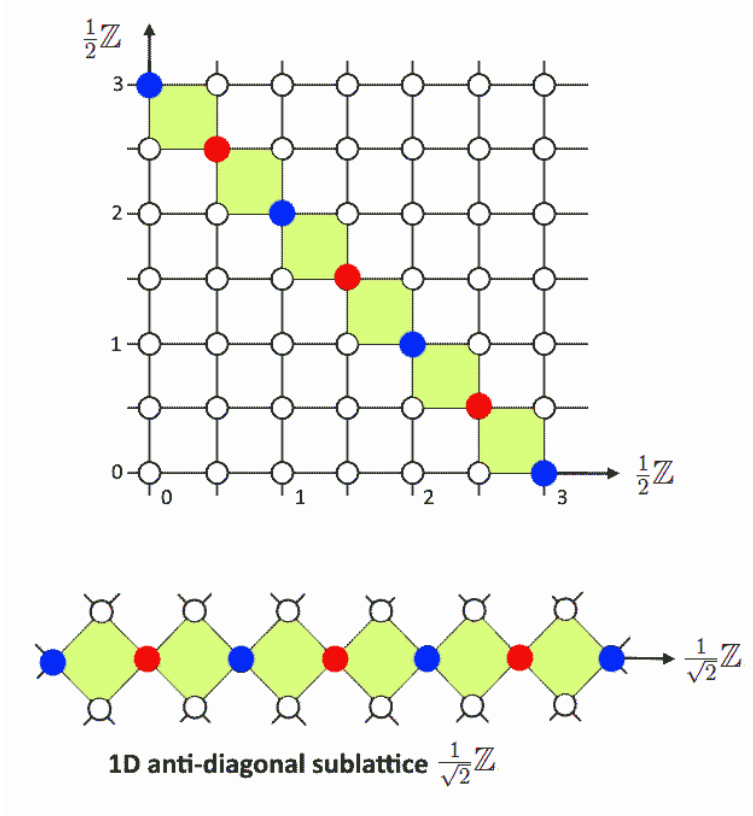


Figure 5: On top, we give the $\frac{1}{2}\mathbb{Z} \times \frac{1}{2}\mathbb{Z}$ and anti-diagonal 1D with blue and red sites. In bottom, we find the anti-diagonal 1D lattice $\frac{1}{\sqrt{2}}\mathbb{Z}$ containing $\sqrt{2}\mathbb{Z}$ as a sublattice.

In this parametrisation of $\sqrt{2}\mathbb{Z}$ and $\frac{1}{\sqrt{2}}\mathbb{Z}$, the generators $\boldsymbol{\alpha}$ and $\boldsymbol{\lambda}$ are very remarkable in the sense they are familiar in Lie algebra theory. When endowed with the euclidian metric δ_{ij} , $\boldsymbol{\alpha}$ and $\boldsymbol{\lambda}$ correspond to the simple root and the fundamental weight vectors of $SU(2)$ with $\boldsymbol{\alpha}^2 = 2$ and $\boldsymbol{\lambda}^2 = 1/2$ and obeying the duality relation $\boldsymbol{\alpha} \cdot \boldsymbol{\lambda} = 1$. Therefore, we can accordingly characterise the lattices $R_2 = \sqrt{2}\mathbb{Z}$ and $W_2 = \frac{1}{\sqrt{2}}\mathbb{Z}$ as follows:

$$R_2 = \{\mathbf{x}_n = n\boldsymbol{\alpha} \mid n \in \mathbb{Z}\}, \quad \langle \mathbf{x}_n, \mathbf{x}_n \rangle = 2n^2 \quad (2.11)$$

$$W_2 = \{\mathbf{k}_m = m\boldsymbol{\lambda} \mid m \in \mathbb{Z}\}, \quad \langle \mathbf{x}_n, \mathbf{k}_m \rangle = nm \quad (2.12)$$

From the relation $\boldsymbol{\lambda} = \frac{1}{2}\boldsymbol{\alpha}$, the dual weight lattice W_2 splits into two subsets W_2^{even} and W_2^{odd} as described below:

- (i) the W_2^{even} , generated by *even* integers $m = 2\mu$, gives vectors $\mathbf{k}_{2\mu} = 2\mu\boldsymbol{\lambda}$ which are isomorphic to root vectors $\mu\boldsymbol{\alpha}$; as such, we have $W_2^{even} \simeq R_2$. This corresponds to the blue 1D lattice in Figure 5.
- (ii) the subset W_2^{odd} , made of *odd* vectors $\mathbf{k}_{2\mu-1} = (2\mu+1)\boldsymbol{\lambda}$ that read also like $(\mu + \frac{1}{2})\boldsymbol{\alpha}$, describes root vectors $\mu\boldsymbol{\alpha}$ shifted by a fundamental weight $\boldsymbol{\lambda} = \frac{1}{2}\boldsymbol{\alpha}$. Thus W_2^{odd} is isomorphic to $R_2 + \boldsymbol{\lambda}$; it corresponds to the red 1D lattice in Figure 5. Hence, W_2 decomposes into the superposition

$$\begin{aligned} W_2 &= W_2^{even} \cup W_2^{odd} & W_2^{even} &\simeq R_2 \\ &= R_2 \cup \{R_2 + \boldsymbol{\lambda}\} & W_2^{odd} &\simeq R_2 + \boldsymbol{\lambda} \end{aligned} \quad (2.13)$$

in agreement with the discriminant $W_2/R_2 \simeq \mathbb{Z}_2$.

2.1.2 Lattices of SO(4)

Here, we use equation (2.8) to construct the two dimensional lattices Λ_2 , $\Lambda_{2\mathcal{C}}$ and Λ_2^* along with their respective characteristic matrices represented by the same symbols Λ , $\Lambda_{\mathcal{C}}$ and Λ^* .

A. the triplet $(\Lambda_2, \Lambda_{2\mathcal{C}}, \Lambda_2^*)$ and SO(4) lattices

Using the above results, the 2D lattices $\Lambda_2 \simeq R_2 \times R_2$ and $\Lambda_2^* \simeq W_2 \times W_2$, given by eq(2.8), can be naturally interpreted as the 2D root R_2^{so4} and the 2D weight W_2^{so4} lattices of $SU(2) \times SU(2)'$. This group is isomorphic to SO(4), which possesses two orthogonal simple roots $(\boldsymbol{\alpha}, \boldsymbol{\alpha}')$ and two orthogonal fundamental weight vectors $(\boldsymbol{\lambda}, \boldsymbol{\lambda}')$. Within this view, the site vectors \mathbf{v}_n and \mathbf{w}_m in the lattices Λ_2 and Λ_2^* are therefore parameterised by pairs of integers (n, n') and (m, m') as follows

$$\begin{aligned} \Lambda_2 &= \{\mathbf{v}_n = n\boldsymbol{\alpha} \oplus n'\boldsymbol{\alpha}'\} & \Lambda_2 &= \{\mathbf{v}_n = \sqrt{2}(n^1\mathbf{u}_1 + n^2\mathbf{u}_2)\} \\ \Lambda_2^* &= \{\mathbf{w}_m = m\boldsymbol{\lambda} \oplus m'\boldsymbol{\lambda}'\} & \Lambda_2^* &= \{\mathbf{w}_m = \frac{1}{\sqrt{2}}(m^1\mathbf{u}_1 + m^2\mathbf{u}_2)\} \end{aligned} \quad (2.14)$$

where $\boldsymbol{\alpha} = \sqrt{2}\mathbf{u}_1$, $\boldsymbol{\alpha}' = \sqrt{2}\mathbf{u}_2$ and $\boldsymbol{\lambda} = \frac{1}{\sqrt{2}}\mathbf{u}_1$, $\boldsymbol{\lambda}' = \frac{1}{\sqrt{2}}\mathbf{u}_2$. They are represented in Figure 2. Notice that in terms of the components $\mathbf{u}_1 = (1, 0)$ and $\mathbf{u}_2 = (0, 1)$ with Lorentzian product $\mathbf{u}_i^T \eta \mathbf{u}_j = \eta_{ij}$, we have

$$v_n^i = \sqrt{2}u_j^i n^j \quad , \quad w_m^i = \frac{1}{\sqrt{2}}u_j^i m^j \quad (2.15)$$

The characteristic matrices follow as $(\Lambda_2)_j^i = \sqrt{2}u_j^i$ and $(\Lambda_2^*)_j^i = \frac{1}{\sqrt{2}}u_j^i$. From the relationships (2.14), we deduce the realisation of $\Lambda_{2\mathcal{C}} \simeq R_2 \times W_2$ reading like

$$\Lambda_{2\mathcal{C}} = \{\mathbf{u}_{n,m} = n\sqrt{2}\mathbf{u}_1 + \frac{m}{\sqrt{2}}\mathbf{u}_2\} \quad (2.16)$$

The lattice picture is depicted by the Figure 3.

B. characteristic matrices

Using the components of the vectors \mathbf{v}_n and \mathbf{w}_m given by (2.15), the characteristic matrices of the real and dual lattices are respectively given by $\Lambda_2 = \sqrt{2}I_{2 \times 2}$ and $\Lambda_2^* = \frac{1}{\sqrt{2}}I_{2 \times 2}$. To express the matrix $\Lambda_{2\mathcal{C}}$, it is convenient to decompose the identity matrix $I_{2 \times 2}$ in terms of the projectors ϱ_1 and ϱ_2 defined as follows

$$\varrho_1 = \begin{pmatrix} 1 & 0 \\ 0 & 0 \end{pmatrix}, \quad \varrho_2 = \begin{pmatrix} 0 & 0 \\ 0 & 1 \end{pmatrix} \quad (2.17)$$

In term of these ϱ_i 's, the characteristic matrices of the triplet $(\Lambda_2, \Lambda_{2\mathcal{C}}, \Lambda_2^*)$ can be written as

$$\Lambda_2 = \sqrt{2}\varrho_1 + \sqrt{2}\varrho_2, \quad \Lambda_2^* = \frac{1}{\sqrt{2}}\varrho_1 + \frac{1}{\sqrt{2}}\varrho_2, \quad \Lambda_{2\mathcal{C}} = \sqrt{2}\varrho_1 + \frac{1}{\sqrt{2}}\varrho_2 \quad (2.18)$$

2.2 Models with CS level $k > 2$

For higher values of the integer k , while keeping the central charge $c_{L/R} = 1$, the root $\boldsymbol{\alpha}$ and the fundamental weight vector $\boldsymbol{\lambda}$ are respectively replaced by a dilated $\tilde{\boldsymbol{\alpha}}$ and a compressed $\tilde{\boldsymbol{\lambda}}$ satisfying the euclidian properties:

$$\tilde{\boldsymbol{\alpha}}^2 = k > 2, \quad \tilde{\boldsymbol{\lambda}}^2 = \frac{1}{k} < \frac{1}{2}, \quad \tilde{\boldsymbol{\alpha}} \cdot \tilde{\boldsymbol{\lambda}} = 1 \quad (2.19)$$

These newly scaled vectors $\tilde{\boldsymbol{\alpha}}$ and $\tilde{\boldsymbol{\lambda}}$ generate 1D sublattices $\tilde{\mathbf{R}}_k$ and $\tilde{\mathbf{W}}_k$ extending the root and the weight lattices \mathbf{R}_2 and \mathbf{W}_2 of $SU(2)$. An interesting way to realise this

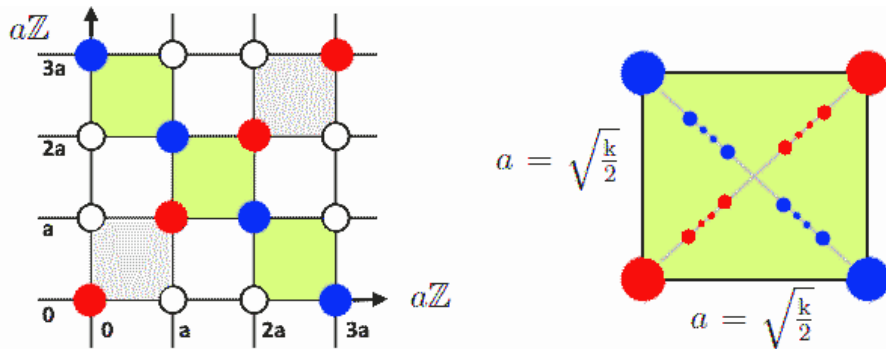


Figure 6: On the left, we represent the square lattice $a\mathbb{Z} \times a\mathbb{Z}$ with parameter $a = \sqrt{\frac{k}{2}}$. It contains the 1D root lattice $\tilde{\mathbf{R}}_k$. Here, the 1D (anti) diagonal lattices are represented in red and blue colors. On the right, a unit cell having k charges. A similar figure is valid for the weight lattice $\tilde{\mathbf{W}}_k$ sitting in $\frac{1}{a}\mathbb{Z} \times \frac{1}{a}\mathbb{Z}$; see the Figure 7 for $k=3$.

structure is obtained using a square lattice with scaled spacings $\mathbf{a}_x = \mathbf{a}_y = \sqrt{k/2}$. In

this case, the vectors $\tilde{\alpha}$ and $\tilde{\lambda}$ relate to the canonical simple root and the fundamental weight vector via $\tilde{\alpha} = \sqrt{k/2}\alpha$ and $\tilde{\lambda} = \sqrt{2/k}\lambda$ and consequently

$$\tilde{\lambda} = \frac{1}{k}\tilde{\alpha} \quad \Rightarrow \quad \tilde{\alpha} = k\tilde{\lambda} \quad (2.20)$$

In this realisation, the root lattice $R_k = \sqrt{k}\mathbb{Z}$ is generated by $\{\mathbf{x}_n = n\tilde{\alpha}\}$, depicted in Figure 5, it is a 1D sublattice of $\sqrt{k/2}\mathbb{Z} \times \sqrt{k/2}\mathbb{Z}$ with sites

$$\mathbf{x}_n = n\tilde{\alpha} = \sqrt{\frac{k}{2}}n\alpha \quad (2.21)$$

Setting $a_x = a_y = a$, the leading prime values for the CS level correspond to

$$\begin{array}{cccccc} a = & 1 & \frac{3}{2} & \frac{5}{2} & \frac{7}{2} & \frac{11}{2} & \frac{13}{2} \\ k = & 2 & 3 & 5 & 7 & 11 & 13 \end{array} \quad (2.22)$$

The dual weight lattice $W_k = \frac{1}{\sqrt{k}}\mathbb{Z}$ is defined by $\{\mathbf{k}_m = m\tilde{\lambda}\}$ with $m \in \mathbb{Z}$; it is a 1D sublattice embedded in $\sqrt{\frac{2}{k}}\mathbb{Z} \times \sqrt{\frac{2}{k}}\mathbb{Z}$. By substituting $\tilde{\lambda} = \frac{1}{k}\tilde{\alpha}$, we get $\mathbf{k}_m = \sqrt{\frac{2}{k}}m\lambda$ that reads also like

$$\mathbf{k}_m = m\tilde{\lambda} = \frac{m}{k}\tilde{\alpha} \quad , \quad m \in \mathbb{Z} \quad (2.23)$$

By setting $m = kn + \varepsilon$ with $\varepsilon = 0, \dots, k-1 \pmod{k}$, we end up with $\mathbf{k}_m = n\tilde{\alpha} + \varepsilon\tilde{\lambda}$ showing that W_k is a superposition of k sheets labeled by ε . For odd integers $k=2j+1$, the values of $\varepsilon \in \{-j, \dots, j\}$ reflect that the $2j+1$ sheets making W_{2j+1} form an irreducible representation of $SU(2)$ with isospin j . For illustration, see Figure 7 regarding $k=3$ and $W_3/R_3 \simeq \mathbb{Z}_3$ where the three sheets are colored in blue, red and green.

In conclusion, the two dimensional lattices $(\Lambda_2, \Lambda_{2C}, \Lambda_2^*)$, depicted in Figures 2 and 3, extend for Chern-Simons levels $k > 2$ like

$$\begin{array}{lcl} \Lambda_k & = & \{\mathbf{v}_n = n\tilde{\alpha} \oplus n'\tilde{\alpha}'\} = \{\mathbf{v}_n = \sqrt{k}(n\mathbf{u}_1 + n'\mathbf{u}_2)\} \\ \Lambda_k^* & = & \{\mathbf{w}_m = m\tilde{\lambda} \oplus m'\tilde{\lambda}'\} = \{\mathbf{w}_m = \frac{1}{\sqrt{k}}(m\mathbf{u}_1 + m'\mathbf{u}_2)\} \end{array} \quad (2.24)$$

where \mathbf{u}_i are as previously defined. Substituting $\tilde{\lambda} = \frac{1}{k}\tilde{\alpha}$ and $\tilde{\lambda}' = \frac{1}{k}\tilde{\alpha}'$ while setting $m = kn + \varepsilon$ and $m' = kn' + \varepsilon'$ with $\varepsilon, \varepsilon' = 0, \dots, k-1$, we get

$$\mathbf{w}_m = (n\tilde{\alpha} + n'\tilde{\alpha}') + \varepsilon\tilde{\lambda} + \varepsilon'\tilde{\lambda}' \quad (2.25)$$

showing that the dual Λ_k^* is a union of $k \times k$ sheets of 2D lattices isomorphic to the real Λ_k . For odd integers $k=2j+1$, these sheets form a representation of $SO(4)$ with isospin pair (j, j) . Moreover, the even self dual lattice Λ_{kC} engendered by the vectors $n\tilde{\alpha} + m\tilde{\alpha}' + \varepsilon\tilde{\lambda}'$ is composed of k sheets isomorphic to Λ_k . It can also be expressed like

$$\Lambda_{kC} = \{\mathbf{u}_{n,m} = n\sqrt{k}\mathbf{u}_1 + \frac{m}{\sqrt{k}}\mathbf{u}_2\} \quad (2.26)$$

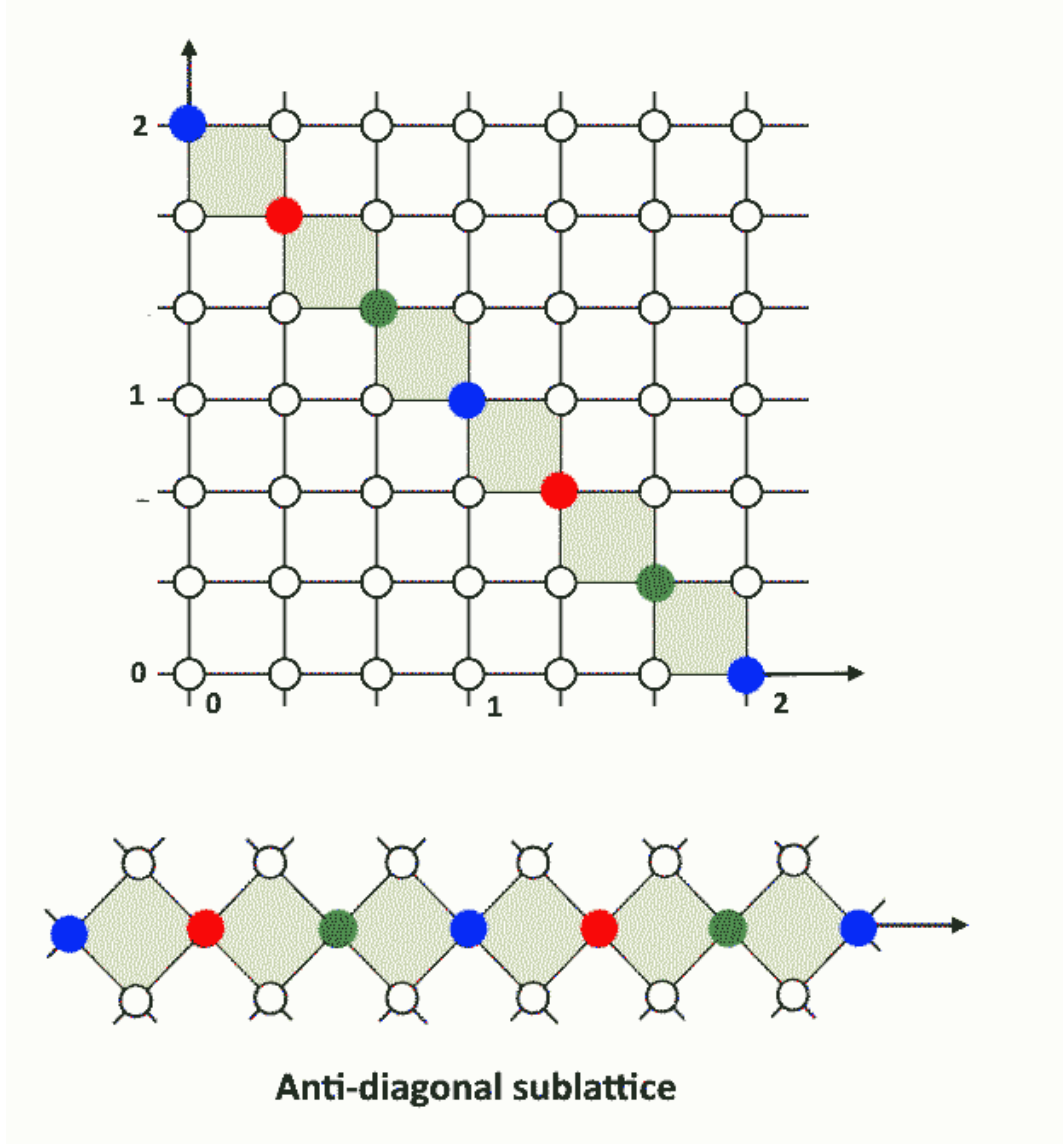


Figure 7: On top, the square lattice $\frac{1}{a}\mathbb{Z} \times \frac{1}{a}\mathbb{Z}$ with $a = \sqrt{\frac{k}{2}}$. It contains the 1D weight lattice \tilde{W}_3 given by the superposition of three 1D sublattices $\mathbb{R}_3 \cup \{\mathbb{R}_3 + \boldsymbol{\lambda}\} \cup \{\mathbb{R}_3 + 2\boldsymbol{\lambda}\}$ distinguished by the colors: blue, red and green. For $k=3$, the value $2\boldsymbol{\lambda}$ can be imagined as corresponding to $-\boldsymbol{\lambda}$.

The corresponding characteristic matrix $(\Lambda_k)_C$ of the even self dual lattice and the induced metric $(g_{\Lambda_{kC}}) = \Lambda_{kC}^T \eta \Lambda_{kC}$ read as follows

$$\Lambda_{kC} = \begin{pmatrix} \sqrt{k} & 0 \\ 0 & \frac{1}{\sqrt{k}} \end{pmatrix}, \quad g_{\Lambda_{kC}} = \begin{pmatrix} 0 & 1 \\ 1 & 0 \end{pmatrix} \quad (2.27)$$

with determinant $\det \Lambda_{kC} = 1$.

Finally, we note that the generalisation to higher orders $r > 1$, with central charge values $c_{L/R} = r$, follows straightforwardly. A detailed study is omitted here.

2.3 From scalars in continuum to lattice QFT

In this subsection, we outline the key steps by which the lattices introduced earlier will be maneuvered in our study. This construction provides a formal pathway towards a non perturbative description of topological matter that we will further develop later on (see section 5). Focussing on the scalar fields (a fermionic description will be introduced subsequently via fermionization techniques), the transition from scalars in continuum to a non perturbative lattice framework can be summarised as follows:

2.3.1 Case of one real 2D scalar field $X = X(\tau, \sigma)$

We start from the 2D field action $\mathcal{S}(X) = \int_{\mathcal{M}_2} d^2\xi \mathcal{L}(X)$ in continuum with quadratic lagrangian density given by $\frac{1}{2}(\partial_\mu X)(\partial^\mu X) + \frac{1}{2}m^2 X^2$ where we have added the term $m^2 X^2$ as a possible quadratic term. In the interesting limit $m \rightarrow 0$ (required by conformal invariance), the field equation of the scalar (bosonic string) field reads like $(\frac{\partial^2}{\partial\tau^2} - \frac{\partial^2}{\partial\sigma^2})X = \mathcal{O}(m^2) \simeq 0$; it remarkably factorises as follows

$$\left(\frac{\partial}{\partial\tau} - \frac{\partial}{\partial\sigma}\right)\left(\frac{\partial}{\partial\tau} + \frac{\partial}{\partial\sigma}\right)X \simeq 0 \quad \Rightarrow \quad \begin{cases} \frac{\partial}{\partial\xi_L} \frac{\partial}{\partial\xi_R} X \simeq 0 \\ \frac{\partial}{\partial\xi_R} \frac{\partial}{\partial\xi_L} X \simeq 0 \end{cases} \quad (2.28)$$

and admits solutions in terms of left and right moving modes corresponding to the usual splitting $X = X_L + X_R$ with $X_L = X(\xi_L)$ and $X_R = X(\xi_R)$. In the euclidian metric, the real coordinates $\xi_{L/R}$ get replaced by the complex variables z, \bar{z} .

- *Matrix equation:*

By defining $V_L \simeq \partial_L X$ and $V_R \simeq \partial_R X$, commonly interpreted as the left J_L and right J_R chiral currents but thought of below as just the components of a 2D "vector" field \mathcal{V} in the limit $m \rightarrow 0$, the above equations of motion (2.28) become $\partial_R V_L \simeq 0$ and $\partial_L V_R \simeq 0$. For finite m , we have $V_{L/R} = (\partial_{L/R} + \frac{m^2}{\partial_{R/L}})X$. Setting $\mathcal{V} = (V_L, V_R)$, one can recast the dynamics into a 2×2 matrix equation like $(\gamma^L \partial_L + \gamma^R \partial_R) \mathcal{V} \simeq 0$ with γ^L and γ^R reading from the following expression

$$\begin{pmatrix} 0 & \partial_L \\ \partial_R & 0 \end{pmatrix} \begin{pmatrix} V_L \\ V_R \end{pmatrix} \simeq \begin{pmatrix} 0 \\ 0 \end{pmatrix} \quad (2.29)$$

from which we deduce the operators

$$\mathcal{D} \simeq \begin{pmatrix} 0 & \partial_L \\ \partial_R & 0 \end{pmatrix}, \quad \mathcal{D}^2 \simeq \begin{pmatrix} \partial_L \partial_R & 0 \\ 0 & \partial_R \partial_L \end{pmatrix} \quad (2.30)$$

• *Fourier transform:*

In the reciprocal space $\partial_{L/R} = \frac{i}{\hbar} q_{L/R}$ and where the fields V_L and V_R are expanded in Fourier series² like $\sum_q e^{iq \cdot \xi} \tilde{V}_L$ and $\sum_q e^{iq \cdot \xi} \tilde{V}_R$, the above matrix relation can be brought to the form

$$\sum_{(q_L, q_R)} \begin{pmatrix} 0 & q_L \\ q_R & 0 \end{pmatrix} \begin{pmatrix} e^{iq \cdot \xi} \tilde{V}_L \\ e^{iq \cdot \xi} \tilde{V}_R \end{pmatrix} \simeq \begin{pmatrix} 0 \\ 0 \end{pmatrix} \quad (2.31)$$

Notice the emergence of the *Dirac-like*³ matrix operators \mathcal{D} in (2.30) and the reciprocal $\tilde{\mathcal{D}}$ in (2.31) which generally appear in fermionic theories. This hints at a possible generalization to a non-perturbative regime, where the non linear (differential) operator $\hat{\mathcal{D}}$ involves oscillating (trigonometric) functions like for instance

$$\hat{\mathcal{D}} = \begin{pmatrix} 0 & \sin q_L \\ \sin q_R & 0 \end{pmatrix} \rightarrow \tilde{\mathcal{D}} = \begin{pmatrix} 0 & q_L \\ q_R & 0 \end{pmatrix} \quad (2.32)$$

with eigenvalues given by $\delta_{\pm} \sim \pm \sqrt{|\sin q_L \sin q_R|}$ which tends to $\pm \sqrt{|q_L q_R|}$ for small values $q_{L/R} \rightarrow 0$.

2.3.2 Lattice extension

In the (euclidian) lattice field description, the continuum fields $V_L(\xi) \equiv V^+(\xi)$ and $V_R(\xi) \equiv V^-(\xi)$ are discretized in terms of the two following: (i) The lattice components $V_{\xi_n}^+ \equiv V_n^+$ and $V_{\xi_n}^- \equiv V_n^-$ with discrete coordinates $\xi_n = n^i \mathbf{e}_i$ where $(\mathbf{e}_1, \mathbf{e}_2)$ are generators of the 2D lattice. And (ii) their *Fourier transforms* given by the expansions $\sum_{\mathbf{k}} e^{i\mathbf{k} \cdot \xi_n} \tilde{V}_{\xi_n}^+$ and $\sum_{\mathbf{k}} e^{i\mathbf{k} \cdot \xi_n} \tilde{V}_{\xi_n}^-$. Borrowing ideas from tight binding modeling of condensed matter [34]-[39], the quadratic lattice hamiltonian describing neighboring interactions read as follows

$$H = \sum_{\xi_n, \xi_m} \left(V_{\xi_n}^{+\dagger}, V_{\xi_n}^{-\dagger} \right) \begin{pmatrix} t_{\xi_n, \xi_m}^{--} & t_{\xi_n, \xi_m}^{-+} \\ t_{\xi_n, \xi_m}^{+-} & t_{\xi_n, \xi_m}^{++} \end{pmatrix} \begin{pmatrix} V_{\xi_m}^+ \\ V_{\xi_m}^- \end{pmatrix} + hc \quad (2.33)$$

where the complex $t_{\xi_n, \xi_m}^{\pm\pm}$ are coupling functions that can be thought of as constants for convenience. By using the Fourier transforms while restricting the interactions to the first nearest neighbours ($\xi_m = \xi_n + \theta_j$ with $j = 1, \dots, d$) and assuming off-diagonal hopping parameters for illustration (eg: $H = t \sum_{\xi_n} \sum_j V_{\xi_n}^{-\dagger} V_{\xi_n + \theta_j}^+ + hc$), it reads in the Fourier space like $H = \sum_{\mathbf{k}} \tilde{V}_{\mathbf{k}}^{\dagger} H_{\mathbf{k}} \tilde{V}_{\mathbf{k}}$ with 2×2 matrix $H_{\mathbf{k}}$ given by

$$H_{\mathbf{k}} = \begin{pmatrix} 0 & f_{\mathbf{k}} \\ f_{\mathbf{k}}^* & 0 \end{pmatrix}, \quad f_{\mathbf{k}} = t \sum_j e^{i\mathbf{k} \cdot \theta_j} \quad (2.34)$$

² For exact $m=0$ (CFT), one uses Laurent expansions and the powerful properties of complex analysis.

³ By using fermionisation ideas, the real bosonic components $V_{L/R}$ can be expressed in terms of complex fermionic fields as $\psi_{L/R} \psi_{L/R}^*$.

where we have set $k_j = \mathbf{k} \cdot \boldsymbol{\theta}_j$ and for which the eigenvalues $E_{\mathbf{k}}^{\pm}$ are given by $\pm \sqrt{f_{\mathbf{k}}^* f_{\mathbf{k}}}$; see eq(5.15) for an interesting concrete model. For the toy example where we only consider the two first closest neighbors given by $k_1 = \mathbf{k} \cdot \boldsymbol{\theta}_1 = k$ and $k_2 = \mathbf{k} \cdot \boldsymbol{\theta}_2 = -k$, we get $f_{\mathbf{k}} = t \cos k$ with $t = t_1 + it_2$ and consequently

$$H_{\mathbf{k}} = \begin{pmatrix} 0 & t \sin\left(\frac{\pi}{2} - k\right) \\ t^* \sin\left(\frac{\pi}{2} - k\right) & 0 \end{pmatrix} \quad (2.35)$$

with eigenvalues

$$E_{\pm} = \pm \sqrt{tt^* \cos^2 k} \quad , \quad -\frac{\pi}{2} \leq k \leq \frac{3\pi}{2} \quad (2.36)$$

For this toy example, the zero modes of $H_{\mathbf{k}}$, which follow from the solving the condition $f_{\mathbf{k}} = 0$, are given by $\kappa_{\pm} = \pm \frac{\pi}{2} \bmod 2\pi$. Around these zeros while setting $q = \kappa_{\pm} - k \ll 1$, the non perturbative Hamiltonian $H_{\mathbf{k}}$ reduces to the $h_{\mathbf{q}}$ given by

$$h_{\mathbf{q}} = \begin{pmatrix} 0 & tq \\ t^*q & 0 \end{pmatrix} + \mathcal{O}(q^3) \quad (2.37)$$

which is linear in momentum. The band structure of the tight binding model (2.35-2.36) is depicted in the Figure 8 where the *Dirac-like* cones at $k = n\frac{\pi}{2}$ with $n \in \mathbb{Z}^*$ are drawn in dashed lines.

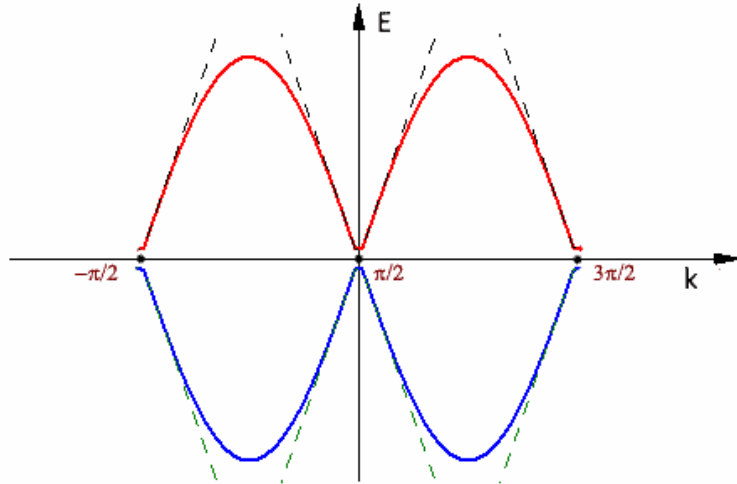


Figure 8: Band structure of the toy model (2.35). It gives the variation of $E_{\pm} = \pm \sqrt{tt^* \cos^2 k}$ (solid line). In dashed line, we draw the behaviour around the Dirac-like points given by the zeros of $\pm |t(k - n\frac{\pi}{2})|$.

3 Extension to SU(3) Lattices

Construction A of code based NCFTs is deeply connected to the lattice structures of SU(2) and SO(4) Lie algebras. This naturally raises the question of whether similar constructions can be extended to lattices associated with other Lie algebras like for instance the rank two SU(3), SO(5) and G₂ [59]-[61]. In this section, we focus on the SU(3) case and apply the algorithm introduced in section 2 to develop a new realisation of NCFTs with central charge $c_{L/R} = 2r$ ($r \geq 1$) thus generalising the previous $(\Lambda_k^{\text{su}_2}, \Lambda_{k\mathcal{C}}^{\text{su}_3}, \Lambda_k^{\text{su}_2^*})$. We denote the new lattice triplet like

$$(\Lambda_k^{\text{su}_3}, \Lambda_{k\mathcal{C}}^{\text{su}_3}, \Lambda_k^{\text{su}_3^*}) \quad (3.1)$$

with the embedding sequence $\Lambda_k^{\text{su}_3} \subset \Lambda_{k\mathcal{C}}^{\text{su}_3} \subset \Lambda_k^{\text{su}_3^*} \subset \mathbb{R}^{2r,2r}$. For $r=1$, the lattices $\Lambda_k^{\text{su}_3}$ and $\Lambda_k^{\text{su}_3^*}$ are 4D, factorising respectively as follows

$$\Lambda_k^{\text{su}_3} = \mathbf{R}_k^{\text{su}_3} \times \mathbf{R}_k^{\text{su}_3'} \quad , \quad \Lambda_k^{\text{su}_3^*} = \mathbf{W}_k^{\text{su}_3} \times \mathbf{W}_k^{\text{su}_3'} \quad (3.2)$$

where $\mathbf{R}_k^{\text{su}_3}$ and $\mathbf{W}_k^{\text{su}_3}$ are the 2D root and weight lattices of SU(3). By using the isomorphism

$$\mathbf{W}_3^{\text{su}_3} / \mathbf{R}_3^{\text{su}_3} \simeq \mathbb{Z}_3 \quad (3.3)$$

it results that the discriminant $\Lambda_k^{\text{su}_3^*} / \Lambda_k^{\text{su}_3}$ is isomorphic to $\mathbb{Z}_3 \times \mathbb{Z}_3$. To build the realisation (3.1), we consider the case $k=3$, supported by the \mathbb{Z}_3 centre of SU(3) and report the more general cases $k>3$ and $k<3$ to appendix C.

3.1 Realisation at level $k=3$

In light of the factorisation (3.2), our focus narrows to the two dimensional lattices $\mathbf{R}_3^{\text{su}_3}$ and $\mathbf{W}_3^{\text{su}_3}$ along with their key properties. The root lattice $\mathbf{R}_3^{\text{su}_3}$ is generated by the two simple roots α_1 and α_2 of SU(3) and takes the form $\mathbf{R}_3^{\text{su}_3} = \mathbb{Z}\alpha_1 \oplus \mathbb{Z}\alpha_2$. In the standard Cartesian basis, the simple roots are as follows⁴

$$\alpha_1 = \sqrt{2}(1, 0), \quad \alpha_2 = \frac{\sqrt{2}}{2}(-1, \sqrt{3}), \quad \alpha_1 + \alpha_2 = \frac{1}{\sqrt{2}}(1, \sqrt{3}) \quad (3.4)$$

They satisfy the Euclidean inner product $\alpha_i \cdot \alpha_j = K_{ij}$ where K_{ij} is the Cartan matrix. The resulting $\mathbf{R}_3^{\text{su}_3}$ is an hexagonal lattice with angle $(\widehat{\alpha_1}, \widehat{\alpha_2}) = 2\pi/3$ as depicted by the Figure 9 where the unit cell is given by the pistachio colored hexagon. The site

⁴ An equivalent basis is given by $\alpha_1 = \frac{\sqrt{2}}{2}(1, -\sqrt{3})$ and $\alpha_2 = \frac{\sqrt{2}}{2}(1, \sqrt{3})$ as well as $\alpha_1 + \alpha_2 = \sqrt{2}(0, 1)$. We also have

$$A = \frac{\sqrt{2}}{2} \begin{pmatrix} 1 & 1 \\ -\sqrt{3} & \sqrt{3} \end{pmatrix}, \quad B = \frac{\sqrt{2}}{2} \begin{pmatrix} 1 & -\frac{1}{3}\sqrt{3} \\ 1 & \frac{1}{3}\sqrt{3} \end{pmatrix}$$

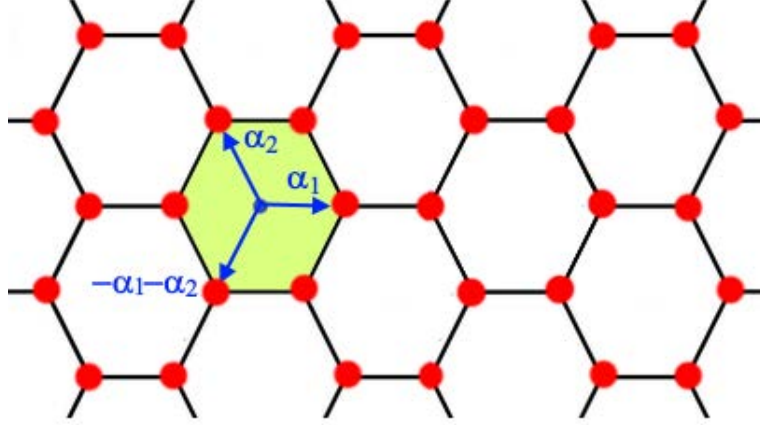


Figure 9: Hexagonal lattice $\mathbb{Z}\alpha_1 \oplus \mathbb{Z}\alpha_2$ generated by the simple roots α_1 and α_2 of $\text{SL}(3)$ with $(\widehat{\alpha_1, \alpha_2}) = 2\pi/3$. It is the root lattice $\text{R}_3^{\text{sl}_3}$ of $\text{sl}(3)$. The unit cell is in grey color.

vectors $\mathbf{x} \in \text{R}_3^{\text{su}_3}$ have the form $A\mathbf{n}$ with integer $\mathbf{n} = (n_1, n_2)$; their discrete components $x_{\mathbf{n}}^i$ are given by the linear combinations $\sum A_j^i n^j$ where A_j^i is a characteristic matrix whose entries can be identified with the components $A_j^i = (\alpha_j^i)$ of the standard vector expansion $\mathbf{x}_{\mathbf{n}} = \sum \alpha_j n^j$. Using (3.4), it reads explicitly as follows

$$A_j^i = \begin{pmatrix} \alpha_1^1 & \alpha_2^1 \\ \alpha_1^2 & \alpha_2^2 \end{pmatrix} = \begin{pmatrix} \sqrt{2} & -\frac{\sqrt{2}}{2} \\ 0 & \frac{\sqrt{6}}{2} \end{pmatrix} \quad (3.5)$$

with $\det A = \sqrt{3} > 1$. With the help of these relationships, the euclidian length $\mathbf{x}_{\mathbf{n}}^2$ of the site vectors in the root lattice compute as $\sum n^i K_{ij} n^j$ with matrix $K = A^T A$ coinciding with the Cartan matrix given in (3.10).

The weight lattice $\text{W}_3^{\text{su}_3}$

Just as with the root lattice $\text{R}_3^{\text{su}_3}$, the weight lattice $\text{W}_3^{\text{su}_3}$ is generated by the two fundamental weight vectors of $\text{SU}(3)$ denoted λ_1 and λ_2 , that is $\text{W}_3^{\text{su}_3} = \mathbb{Z}\lambda^1 \oplus \mathbb{Z}\lambda^2$ with

$$\lambda^1 = \frac{1}{\sqrt{6}} (\sqrt{3}, 1), \quad \lambda^2 = \frac{1}{\sqrt{6}} (0, 2), \quad \lambda^1 + \lambda^2 = \frac{1}{\sqrt{2}} (1, \sqrt{3}) \quad (3.6)$$

and euclidian intersection $\lambda_i \cdot \lambda_j = \tilde{K}_{ij}$ where \tilde{K}_{ij} is the inverse of the Cartan matrix. These weight vectors are related to the simple roots via the duality relation $\alpha_i \cdot \lambda^j = \delta_i^j$ which is solved explicitly as

$$\lambda_1 = \frac{1}{3} (2\alpha_1 + \alpha_2), \quad \lambda_2 = \frac{1}{3} (\alpha_1 + 2\alpha_2) \quad (3.7)$$

The lattice $\text{W}_3^{\text{su}_3}$ has a triangular structure with angle $(\widehat{\lambda_1, \lambda_2}) = \pi/3$; it is depicted in Figure 10 where the unit cell is given by the pistachio colored triangle. The site vectors

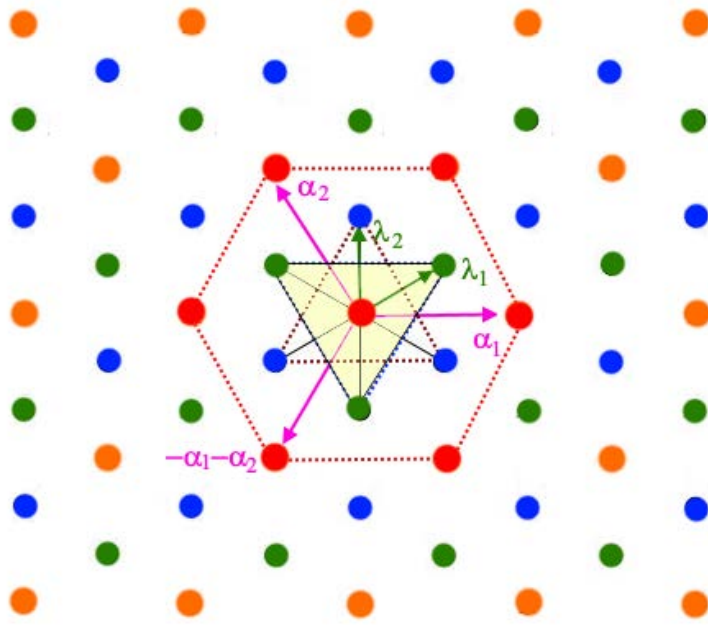


Figure 10: Triangular lattice $\mathbb{Z}\lambda_1 \oplus \mathbb{Z}\lambda_2$ with $(\widehat{\lambda_1, \lambda_2}) = \pi/3$. It is the weight lattice $W_3^{\text{su}_3}$ of $\text{su}(3)$. The unit cell is a triangle as in pistachio color. Sites in $W_3^{\text{su}_3}$ are painted in three colors: red, blue and green as an illustration of the splitting (3.16).

$\mathbf{k}_n \in W_3^{\text{su}_3}$ can be written as $B\mathbf{m}$ with integer vector $\mathbf{m} = (m_1, m_2)$ and components $(k_{\mathbf{m}})_i$ expressed as $\sum m_j B_i^j$ where $B_i^j = (\lambda_i^j)$ defines the characteristic matrix of $W_3^{\text{su}_3}$ reading explicitly as follows

$$B_i^j = \begin{pmatrix} \lambda_1^1 & \lambda_2^1 \\ \lambda_1^2 & \lambda_2^2 \end{pmatrix} = \begin{pmatrix} \frac{\sqrt{2}}{2} & \frac{\sqrt{6}}{6} \\ 0 & \frac{\sqrt{6}}{3} \end{pmatrix} \quad (3.8)$$

with $\det B = 1/\sqrt{3} < 1$. Due to the duality, B is the inverse of the root matrix A . The euclidian length $\mathbf{k}_{\mathbf{m}}^2$ of a site vector is computed as $\sum m_i \tilde{K}^{ij} m_j$ with matrix $\tilde{K} = BB^T$ coinciding with the inverse of the Cartan matrix. By replacing into (3.5, 3.8), we get

$$\begin{aligned} (x_{\mathbf{n}})_1 &= \sqrt{2}n_1 - \frac{\sqrt{2}}{2}n_2 & (k_{\mathbf{m}})_1 &= \frac{\sqrt{2}}{2}m_1 \\ (x_{\mathbf{n}})_2 &= \frac{\sqrt{6}}{2}n_2 & (k_{\mathbf{m}})_2 &= \frac{\sqrt{6}}{6}m_1 + \frac{\sqrt{6}}{3}m_2 \end{aligned} \quad (3.9)$$

and in $K = A^T A$ as well as $\tilde{K} = BB^T$:

$$K = \begin{pmatrix} 2 & -1 \\ -1 & 2 \end{pmatrix}, \quad \tilde{K} = \frac{1}{3} \begin{pmatrix} 2 & 1 \\ 1 & 2 \end{pmatrix} \quad (3.10)$$

with

$$\begin{aligned} \mathbf{x}_{\mathbf{n}}^T \cdot \mathbf{x}_{\mathbf{n}} &= 2[(n_1)^2 + (n_2)^2 - n_1 n_2] & \in & 2\mathbb{Z} \\ \mathbf{k}_{\mathbf{m}}^T \cdot \mathbf{k}_{\mathbf{m}} &= \frac{2}{3}[(m_1)^2 + (m_2)^2 + m_1 m_2] & \in & \frac{2}{3}\mathbb{Z} \\ \mathbf{x}_{\mathbf{n}}^T \cdot \mathbf{k}_{\mathbf{m}} &= n_1 m_1 + n_2 m_2 & \in & \mathbb{Z} \end{aligned} \quad (3.11)$$

Notice also that substituting $\lambda_1 = (2\alpha_1 + \alpha_2)/3$ and $\lambda_2 = (\alpha_1 + 2\alpha_2)/3$ into the linear combination $\mathbf{k}_m = \sum m_j \lambda^j$, yields the following

$$\mathbf{k}_m = \frac{1}{3} (2m_1 + m_2) \alpha_1 + \frac{1}{3} (m_1 + 2m_2) \alpha_2 \quad (3.12)$$

Introducing new integers p,q and congruence classes $\xi, \zeta \in \{0, 1, 2\} \bmod 3$ via $2m_1 + m_2 = 3p + \xi$ and $m_1 + 2m_2 = 3q + \zeta$, we rewrite \mathbf{k}_m as

$$\begin{aligned} \mathbf{k}_m &= \mathbf{k}_m^0 + \frac{1}{3} (2\xi - \zeta) \lambda_1 + \frac{1}{3} (2\zeta - \xi) \lambda_2 \\ \mathbf{k}_m^0 &= p\alpha_1 + q\alpha_2 \end{aligned} \quad (3.13)$$

where $\mathbf{k}_m^0 \in R_3^{\text{su}_3}$. The extra term $\frac{1}{3} (2\xi - \zeta) \lambda_1 + \frac{1}{3} (2\zeta - \xi) \lambda_2$ introduces global shifts to the sites of $R_3^{\text{su}_3}$. Setting $\zeta = 2\xi$ and $\xi = \varepsilon$ with $\varepsilon = 0, 1, 2 \bmod 3$, $\mathbf{k}_m(\varepsilon)$ simplifies to

$$\mathbf{k}_m(\varepsilon) = \mathbf{k}_m^0 + \varepsilon \lambda_2 \quad , \quad \varepsilon = 0, 1, 2 \quad (3.14)$$

Thus, the weight lattice $W_3^{\text{su}_3}$ decomposes into three superposed sheets (equivalent classes) indexed by ε :

m_1	m_2	sites \mathbf{k}_m^0	sites \mathbf{k}_m	weight lattice $W_3^{\text{su}_3}$
$2p - q$	$2q - p + \varepsilon$	$p\alpha_1 + q\alpha_2$	$\mathbf{k}_m^0 + \varepsilon \lambda_2$	$R_3^{\text{su}_3}[\varepsilon] = R_3^{\text{su}_3} + \varepsilon \lambda_2$

(3.15)

with

$$W_3^{\text{su}_3} = \bigcup_{\varepsilon=0}^2 R_3^{\text{su}_3}[\varepsilon] = R_3^{\text{su}_3} \cup \{R_3^{\text{su}_3} + \lambda_2\} \cup \{R_3^{\text{su}_3} + 2\lambda_2\} \quad (3.16)$$

This reflects the quotient $W_3^{\text{su}_3}/R_3^{\text{su}_3} \simeq \mathbb{Z}_3$ where the cyclic action permutes the three sheets.

3.2 The triplet $(\Lambda^{\text{su}_3}, \Lambda_C^{\text{su}_3}, \Lambda^{*\text{su}_3})$

Using the above results and the construction (3.2), we find that in addition to the root lattice $\Lambda_3^{\text{su}_3} = R_3^{\text{su}_3} \times R_3^{\text{su}_3'}$, we have the four dimensional dual weight given by $\Lambda_3^{*\text{su}_3} = W_3^{\text{su}_3} \times W_3^{\text{su}_3'}$ which splits into nine sheets as follows

$$\Lambda_3^{*\text{su}_3} = \bigcup_{\varepsilon, \varepsilon'=0}^2 R_3^{\text{su}_3}[\varepsilon] \times R_3^{\text{su}_3}[\varepsilon'] \quad (3.17)$$

Each sheet is isomorphic to $\Lambda_3^{\text{su}_3}$ of $SU_3 \times SU_3$ with metric η . Explicitly, we have

$$\begin{aligned} \Lambda_3^{*\text{su}_3} &= \{\Lambda_3^{\text{su}_3}\} \cup \{\Lambda_3^{\text{su}_3} + \lambda_2 + \lambda_2'\} \cup \{\Lambda_3^{\text{su}_3} + (2\lambda_2 + 2\lambda_2')\} \cup \\ &\quad \{\Lambda_3^{\text{su}_3} + \lambda_2\} \cup \{\Lambda_3^{\text{su}_3} + 2\lambda_2\} \cup \\ &\quad \{\Lambda_3^{\text{su}_3} + \lambda_2'\} \cup \{\Lambda_3^{\text{su}_3} + 2\lambda_2'\} \cup \\ &\quad \{\Lambda_3^{\text{su}_3} + 2\lambda_2 + \lambda_2'\} \cup \{\Lambda_3^{\text{su}_3} + \lambda_2 + 2\lambda_2'\} \end{aligned} \quad (3.18)$$

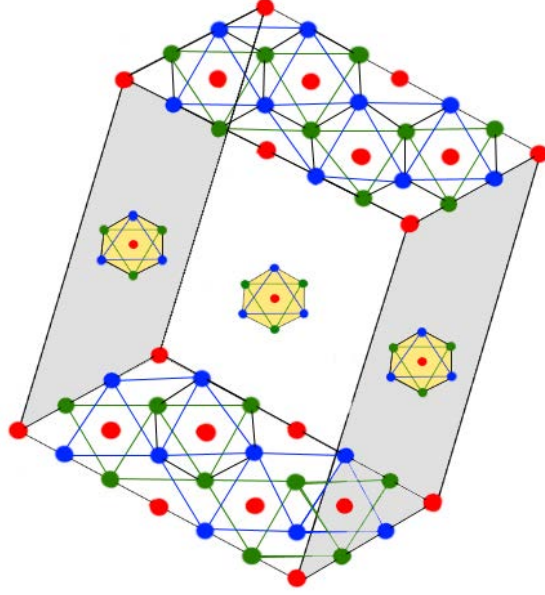


Figure 11: Schematic representation of the 4D lattice $\Lambda_3^{sl_3^*}$ in 3D space by stacking sheets of weight lattices in the direction normal to the plane of $W_3^{sl_3}$. The 2D base is given by the weight lattice $\mathbb{Z}\lambda_1 \oplus \mathbb{Z}\lambda_2$.

A schematic illustration of the 4D lattice $\Lambda_3^{su_3} = W_3^{su_3} \times W_3^{su_3}$ embedded in 3D space is shown in Figure 11 where the base plane is spanned by $W_3^{su_3}$ given by $\mathbb{Z}\lambda_1 \oplus \mathbb{Z}\lambda_2$. The even self dual lattice $\Lambda_{3C}^{su_3}$ is constructed as

$$\Lambda_{3C}^{su_3} = \Lambda_3^{su_3} \cup [\Lambda_3^{su_3} + \lambda_2] \cup [\Lambda_3^{su_3} + 2\lambda_2] \quad (3.19)$$

corresponding to a three sheet structure, each isomorphic to $\Lambda_3^{su_3}$. The characteristic 4×4 matrices of the three lattices ($\Lambda_3^{su_3}, \Lambda_{3C}^{su_3}, \Lambda_3^{*su_3}$) are as follows

$$\Lambda_3^{su_3} = \begin{pmatrix} A & 0 \\ 0 & A \end{pmatrix}, \quad \Lambda_3^{*su_3} = \begin{pmatrix} B & 0 \\ 0 & B \end{pmatrix}, \quad \Lambda_{3C}^{su_3} = \begin{pmatrix} A & 0 \\ 0 & B \end{pmatrix} \quad (3.20)$$

with determinants $\det \Lambda_3^{su_3} = 3$, $\det \Lambda_3^{*su_3} = 1/3$ and $\det \Lambda_{3C}^{su_3} = 1$. The induced metrics for the various lattices are defined like $g_{\Lambda_3} = (\Lambda_3^{su_3})^T \boldsymbol{\eta} \Lambda_3^{su_3}$ and $g_{\Lambda_3^*} = (\Lambda_3^{*su_3})^T \boldsymbol{\eta} \Lambda_3^{*su_3}$ as well as $g_{\Lambda_{3C}} = (\Lambda_{3C}^{su_3})^T \boldsymbol{\eta} \Lambda_{3C}^{su_3}$, they are given by

$$g_{\Lambda_3} = \begin{pmatrix} 0 & K \\ K & 0 \end{pmatrix}, \quad g_{\Lambda_3^*} = \begin{pmatrix} 0 & K^{-1} \\ K^{-1} & 0 \end{pmatrix}, \quad g_{\Lambda_{3C}} = \begin{pmatrix} 0 & I_2 \\ I_2 & 0 \end{pmatrix} \quad (3.21)$$

with $\det g_{\Lambda_3^{su_3}} = 3^2$, $\det g_{\Lambda_3^{*su_3}} = 1/3^2$ and $\det (g_{\Lambda_{3C}}) = 1$. Based on (3.20), and using the construction (B.14) of code-CFTs with $c_{L/R} = 2r \geq 2$, the code \mathcal{C} is contained into

$(\mathbb{Z}_3 \times \mathbb{Z}_3)^r$ and maps to a $4r$ dimensional lattice $\Lambda_{3\mathcal{C}}^{r,r}$ satisfying the inclusions

$$\underbrace{\Lambda_3^{\text{su}_3} \oplus \dots \oplus \Lambda_3^{\text{su}_3}}_{r \text{ times}} \subset \Lambda_{3\mathcal{C}}^{r,r} \subset \underbrace{\Lambda_3^{*\text{su}_3} \oplus \dots \oplus \Lambda_3^{*\text{su}_3}}_{2r \text{ times}} \subset \mathbb{R}^{2r,2r} \quad (3.22)$$

This lattice $\Lambda_{3\mathcal{C}}^{r,r}$ is even and self dual, characterized by the matrices:

$$\Lambda_{3\mathcal{C}}^{r,r} = \begin{pmatrix} \oplus_{i=1}^r A & 0 \\ 0 & \oplus_{i=1}^r B \end{pmatrix}, \quad g_{\Lambda_{3\mathcal{C}}}^{[2r]} = \begin{pmatrix} 0 & I_{2r} \\ I_{2r} & 0 \end{pmatrix} \quad (3.23)$$

with determinants $\det \Lambda_{3\mathcal{C}}^{r,r} = 1$ and $\det \Lambda_{3\mathcal{C}}^{*,r,r} = 1$. Thus, $\Lambda_{3\mathcal{C}}^{r,r}$ defines a Narain theory with central charge $2r$.

4 Particles in NCFTs and path to topological matter

The present and following section lay out a proposal to extend the holographic ensemble framework to discrete lattice QFT with applications to topological phases of matter featuring Dirac points with fermionic zero modes [41]-[66]. In this context, Code and Narain CFTs are imagined as sitting at critical points of quantum fields $\phi(\mathbf{r}_m)$ populating the sites of the lattice $\Lambda_{\mathcal{C}}$ with position vectors $\mathbf{r}_m = x_m^a \epsilon_a$ and Fourier expansions

$$\phi(\mathbf{r}_m) \simeq \sum_{\mathbf{k}} e^{i\mathbf{k} \cdot \mathbf{r}_m} \tilde{\phi}_{\mathbf{k}} \quad , \quad \tilde{\phi}_{\mathbf{k}} \simeq \sum_{\mathbf{r}_m} e^{-i\mathbf{k} \cdot \mathbf{r}_m} \phi(\mathbf{r}_m) \quad (4.1)$$

Here the waves $\phi(\mathbf{r}_m)$ will be interpreted as KK particles $|KK_m\rangle$ and winding states $|W_m\rangle$ sitting in $\Lambda_{\mathcal{C}}$ as illustrated in Figure 12. Our proposal borrows ideas from tight

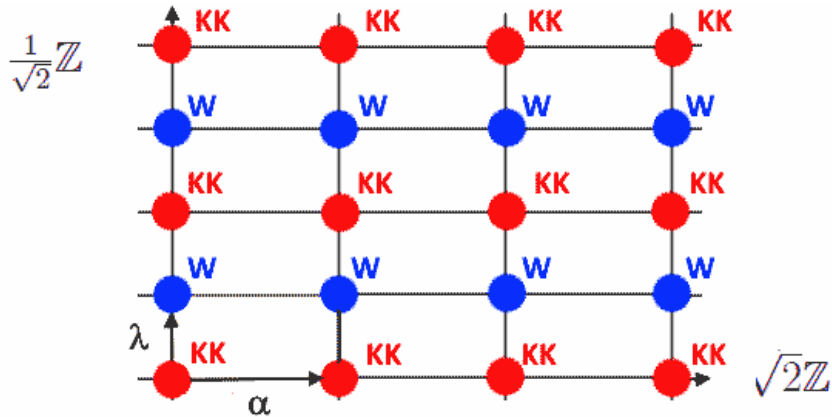


Figure 12: The 2D even self dual lattice $\Lambda_{2\mathcal{C}}^{1,1} \simeq (\sqrt{2}\mathbb{Z}) \times (\frac{1}{\sqrt{2}}\mathbb{Z})$ with red sites occupied by KKs and blue sites by windings. A red (blue) site has two first closed neighbors of blue (red) color; this is because $\alpha = 2\lambda$. The area of the unit cell is equal to 1.

binding constructions of particles on lattices to describe critical properties of KKs and winding states. A more detailed treatment of this tight binding will be developed in section 5 with explicit computations. Meanwhile, we lay here the groundwork by studying first the energy and the momentum properties of particle states in code-CFTs characterised by the triplet $(\mathbf{\Lambda}_k, \mathbf{\Lambda}_{kC}, \mathbf{\Lambda}_k^*)$ realised in terms of the lattices of SU(2). After that, we extend this construction to the SU(3) based CFT.

4.1 Particles in SU(2) based model

We now investigate the quantum particles in the code CFT description of the model with central anomaly $c_{L/R}=1$, corresponding to an SU(2) CS theory in the bulk. It consists of left and right moving particle states $|P_L, P_R\rangle$ having quantized left/right moving momenta given by (A.3) namely [67]

$$\begin{aligned} P_L &= \frac{1}{\sqrt{2k}} \left(\frac{1}{R\sqrt{2}} [a + kn] + \sqrt{2R} [b + km] \right) \\ P_R &= \frac{1}{\sqrt{2k}} \left(\frac{1}{R\sqrt{2}} [a + kn] - \sqrt{2R} [b + km] \right) \end{aligned} \quad (4.2)$$

These momenta are labeled by two pairs of quantum numbers namely: **(i)** the pair (a, b) with $a, b = 0, \dots, k-1$ defining the ground configurations; and **(ii)** the pair $(n, m) \in \mathbb{Z} \times \mathbb{Z}$ encoding the degrees of KK and winding mode excitations. For convenience, we rewrite these momenta like

$$\begin{aligned} (P_L)_{\bar{a}\bar{b}} &= \frac{1}{\sqrt{2k}} \left(\frac{1}{R\sqrt{2}} \bar{a} + \sqrt{2R} \bar{b} \right) \\ (P_R)_{\bar{a}\bar{b}} &= \frac{1}{\sqrt{2k}} \left(\frac{1}{R\sqrt{2}} \bar{a} - \sqrt{2R} \bar{b} \right) \end{aligned} \quad (4.3)$$

where we have set $\bar{a} = a + kn$ and $\bar{b} = b + km$ (i.e: $\bar{a}, \bar{b} \in \mathbb{Z}_k$). From the above expressions, several interesting features emerge. In particular, we highlight the following four:

(i) Hilbert space of zero modes:

By setting $n = m = 0$ in (4.3), we find k^2 left and k^2 right moving ground states with momenta $(\mathring{p}_{L/R})_{ab}$. They are given by

$$\begin{aligned} (\mathring{p}_L)_{ab} &= \frac{1}{\sqrt{2k}} \left(\frac{1}{R\sqrt{2}} a + \sqrt{2R} b \right) \\ (\mathring{p}_R)_{ab} &= \frac{1}{\sqrt{2k}} \left(\frac{1}{R\sqrt{2}} a - \sqrt{2R} b \right) \end{aligned} \quad (4.4)$$

These can be interpreted as classical charges defining distinct vacuum states.

(ii) Excitations:

The full momenta in eq(4.2) split into two sectors: the ground sector defining ground configurations with $(\mathring{p}_{L/R})_{ab}$ and a second sector for the excitations having

momenta $(p_{L/R})_{nm}$ as follows

$$\begin{aligned} P_L &= \dot{p}_L + p_L & (p_L)_{nm} &= \frac{k}{\sqrt{2k}} \left(\frac{1}{R\sqrt{2}} n + \sqrt{2} R m \right) \\ P_R &= \dot{p}_R + p_R & (p_R)_{nm} &= \frac{k}{\sqrt{2k}} \left(\frac{1}{R\sqrt{2}} n - \sqrt{2} R m \right) \end{aligned} \quad (4.5)$$

(iii) Energy and momentum:

Because the left and the right $P_{L/R}$ are linear combinations, the KK and the windings can be decoupled via a change of variables

$$\begin{aligned} H &= \frac{1}{\sqrt{2}} (P_L + P_R) \\ P &= \frac{1}{\sqrt{2}} (P_L - P_R) \end{aligned} \quad (4.6)$$

with

$$\begin{aligned} H &= \dot{h} + h \\ P &= \dot{p} + p \end{aligned} \quad (4.7)$$

and

$$\begin{aligned} \dot{h} &= \frac{a}{\sqrt{2k}} \frac{1}{R\sqrt{2}} & h &= \frac{kn}{\sqrt{2k}} \frac{1}{R\sqrt{2}} \\ \dot{p} &= \frac{b}{\sqrt{2k}} \sqrt{2} R & p &= \frac{km}{\sqrt{2k}} \sqrt{2} R \end{aligned} \quad (4.8)$$

(iv) Topological index:

Using eqs(4.2-4.3), we introduce a "topological index" $(I_k)_{LR}$ given by $P_L^2 - P_R^2$ which is globally defined on the moduli space of the NCFT. It factorises like $(P_L - P_R)(P_L + P_R)$ and evaluates to

$$\begin{aligned} (I_k)_{LR} &= \frac{2}{k} \bar{a} \bar{b} \\ &= \frac{2}{k} (a + kn) (b + km) \end{aligned} \quad (4.9)$$

Remarkably, this index is independent of the parameter R coordinating the moduli space of NCFT. By substituting $\bar{a} = a + kn$ and $\bar{b} = b + km$, this index expands in terms of the CS level as follows

$$(I_k)_{LR} = \frac{2}{k} ab + 2(am + bn) + (2k) nm \quad (4.10)$$

Notice that for $k = 1$, it reduces to the usual $(I_1)_{LR} = 2nm \in 2\mathbb{Z}$ and for $k = 2$, we have $(I_2)_{LR} = ab + 2(am + bn) + 4nm$. And because $(I_k)_{LR}$ is a globally defined feature, we may fix the parameter R for convenience and set for example $R = \frac{1}{\sqrt{2k}}$.

4.1.1 Exhibiting the SU(2) symmetry

The above relations characterising the left/right momenta $P_{L/R}$ admit a natural lattice description in terms of the SU(2) root and weight systems. They can be imagined as vectors $\mathbf{P}_{L/R}$ valued in the root $R_k^{\text{su}2}$ and weight $W_k^{\text{su}2}$ lattices of SU(2) as follows

$$\mathbf{P}_{L/R} \sim n\boldsymbol{\alpha} \pm m\boldsymbol{\lambda} \quad \sim \quad z_{\pm}\boldsymbol{\lambda} \quad , \quad z_{\pm} = 2n \pm m \quad \in \quad \mathbb{Z} \quad (4.11)$$

Recall that $R_k^{\text{su}_2}$ and $W_k^{\text{su}_2}$ are respectively generated by the simple root α and the fundamental λ satisfying the duality relation $\alpha \cdot \lambda = 1$ with norms $\alpha^2 = 2$ and $\lambda^2 = 1/2$. For simplicity, we may identify these vectors like $\alpha = \sqrt{2}$ and $\lambda = 1/\sqrt{2}$ in which case the momenta (4.2) take the form:

$$\begin{aligned} \mathbf{P}_L &= \frac{1}{\sqrt{2k}} \left(\frac{1}{2R} [a + kn] \alpha + 2R [b + km] \lambda \right) \\ \mathbf{P}_R &= \frac{1}{\sqrt{2k}} \left(\frac{1}{2R} [a + kn] \alpha - 2R [b + km] \lambda \right) \end{aligned} \quad (4.12)$$

Moreover, by setting $\tilde{\alpha} = \frac{1}{2R} \alpha$ and $\tilde{\lambda} = 2R \lambda$, the momenta written as

$$\begin{aligned} \mathbf{P}_L &= \frac{1}{\sqrt{2k}} \left([a + kn] \tilde{\alpha} + [b + km] \tilde{\lambda} \right) \\ \mathbf{P}_R &= \frac{1}{\sqrt{2k}} \left([a + kn] \tilde{\alpha} - [b + km] \tilde{\lambda} \right) \end{aligned} \quad (4.13)$$

with $\tilde{\alpha} \cdot \tilde{\lambda} = 1$ and $\tilde{\alpha}^2 = \frac{1}{2R^2}$ as well as $\tilde{\lambda}^2 = 2R^2$. Using $R = \frac{1}{\sqrt{2k}}$, we get

$$\tilde{\alpha} = \sqrt{\frac{k}{2}} \alpha \quad , \quad \tilde{\lambda} = \sqrt{\frac{2}{k}} \lambda \quad , \quad \tilde{\alpha} \cdot \tilde{\lambda} = 1 \quad (4.14)$$

showing that for $k=2$, we have $\tilde{\alpha} = \alpha$ and $\tilde{\lambda} = \lambda$. Putting these changes into the above relationship, we end up with

$$\begin{aligned} \dot{\mathbf{h}} &= \frac{a}{\sqrt{2k}} \tilde{\alpha} & \mathbf{h} &= \frac{kn}{\sqrt{2k}} \tilde{\alpha} \\ \dot{\mathbf{p}} &= \frac{b}{\sqrt{2k}} \tilde{\lambda} & \mathbf{p} &= \frac{km}{\sqrt{2k}} \tilde{\lambda} \end{aligned} \quad , \quad (4.15)$$

and

$$\begin{aligned} \mathbf{H} &= \frac{1}{\sqrt{2k}} \bar{a} \tilde{\alpha} = \frac{1}{\sqrt{2k}} (a + kn) \tilde{\alpha} \\ \mathbf{P} &= \frac{b}{\sqrt{2k}} \bar{b} \tilde{\lambda} = \frac{b}{\sqrt{2k}} (b + km) \tilde{\lambda} \end{aligned} \quad (4.16)$$

and subsequently

$$\begin{aligned} \mathbf{P}_L &= \frac{1}{\sqrt{2k}} \left(\bar{a} \tilde{\alpha} + \bar{b} \tilde{\lambda} \right) \\ &= \frac{1}{\sqrt{2k}} \left([a + kn] \tilde{\alpha} + [b + km] \tilde{\lambda} \right) \\ \mathbf{P}_R &= \frac{1}{\sqrt{2k}} \left(\bar{a} \tilde{\alpha} - \bar{b} \tilde{\lambda} \right) \\ &= \frac{1}{\sqrt{2k}} \left([a + kn] \tilde{\alpha} - [b + km] \tilde{\lambda} \right) \end{aligned} \quad (4.17)$$

In this relation, T-duality acts through the change $(a, n, \tilde{\alpha}) \leftrightarrow (b, m, \tilde{\lambda})$; it leaves invariant the spectrum of the left momenta \mathbf{P}_L while flipping the sign of \mathbf{P}_R . Here are some noteworthy features that arise:

- **Ground configurations:** The charge momenta $(\dot{\mathbf{h}})_a$ and $(\dot{\mathbf{p}})_b$ of the ground configurations span a k - dimensional space. The associated Hilbert space can be generated by classical ground plane waves $\psi_a = e^{i\dot{\mathbf{h}}_a \cdot \hat{\mathbf{x}}}$ and $\tilde{\psi}_b = e^{i\dot{\mathbf{p}}_b \cdot \hat{\mathbf{y}}}$ with position

variables $\hat{\mathbf{x}} = \hat{x}\tilde{\boldsymbol{\lambda}}$ and $\hat{\mathbf{y}} = \hat{y}\tilde{\boldsymbol{\alpha}}$. These waves combine into $2j+1$ components with label $-j \leq a \leq j$ forming an $SU(2)$ representation of isospin

$$j = \frac{k-1}{2} \quad (4.18)$$

which for $k=1$ gives an isosinglet with $j=0$ and for $k=2$, a doublet with $j=1/2$.

- **Interpolating vacua** $\psi_a \pm \tilde{\psi}_b$: these describe correlated ground configurations corresponding to the states with $n = m = 0$. For these values, the eqs(4.13) reduce to

$$\begin{aligned} \hat{\mathbf{p}}_L &= \frac{1}{\sqrt{2k}} \left(a\tilde{\boldsymbol{\alpha}} + b\tilde{\boldsymbol{\lambda}} \right) \\ \hat{\mathbf{p}}_R &= \frac{1}{\sqrt{2k}} \left(a\tilde{\boldsymbol{\alpha}} - b\tilde{\boldsymbol{\lambda}} \right) \end{aligned} \quad (4.19)$$

They yield the momenta of the k^2 ground configurations $\Psi_{a,b}^\pm \sim \psi_a \pm \tilde{\psi}_b$ which are characterised by the topological index:

$$\hat{\mathbf{p}}_L^2 - \hat{\mathbf{p}}_R^2 = 2\hat{\mathbf{h}}\hat{\mathbf{p}} \quad , \quad 2\hat{\mathbf{h}}\hat{\mathbf{p}} = \frac{2}{k}ab \in 2\mathbb{Z}_k \quad (4.20)$$

- **Excitations:** For non vanishing n and m , one obtains excited states $\Psi_{a,b}^{(n,m)} \sim \psi_a^{(n)} \pm \tilde{\psi}_b^{(m)}$ with relative momenta as follows

$$\begin{aligned} \mathbf{p}_L &= \sqrt{\frac{k}{2}} \left(n\tilde{\boldsymbol{\alpha}} + m\tilde{\boldsymbol{\lambda}} \right) \\ \mathbf{p}_R &= \sqrt{\frac{k}{2}} \left(n\tilde{\boldsymbol{\alpha}} - m\tilde{\boldsymbol{\lambda}} \right) \end{aligned} \quad (4.21)$$

and associated topological index

$$\mathbf{p}_L^2 - \mathbf{p}_R^2 = (2k)nm \in 2k\mathbb{Z} \quad (4.22)$$

For future reference, it is useful to express the difference $\mathbf{P}_L^2 - \mathbf{P}_R^2$ in terms of the variable $\mathbf{H} = (\mathbf{P}_L + \mathbf{P}_R)/\sqrt{2}$ and $\mathbf{P} = (\mathbf{P}_L - \mathbf{P}_R)/\sqrt{2}$ like

$$\mathbf{P}_L^2 - \mathbf{P}_R^2 = 2\mathbf{H}\mathbf{P} \quad (4.23)$$

By substituting $\mathbf{H} = \hat{\mathbf{h}} + \mathbf{h}$ and $\mathbf{P} = \hat{\mathbf{p}} + \mathbf{p}$, the topological index splits into three contributions:

$$\mathbf{P}_L^2 - \mathbf{P}_R^2 = 2\hat{\mathbf{h}}\hat{\mathbf{p}} + 2(\hat{\mathbf{h}}\mathbf{p} + \mathbf{h}\hat{\mathbf{p}}) + 2\mathbf{h}\mathbf{p} \quad (4.24)$$

4.1.2 About the even integer condition

Here, we revisit the even integer condition defining the lattices $\Lambda_k^{r,r}$ and $\Lambda_{kC}^{r,r}$ of the discriminant group $\mathbb{Z}_k \times \mathbb{Z}_k$. Our formulation involves *three constraint relations* stemming from the decomposition (4.24) which also reads

$$\mathbf{P}_L^2 - \mathbf{P}_R^2 = (\hat{\mathbf{p}}_L^2 - \hat{\mathbf{p}}_R^2) + (\mathbf{p}_L^2 - \mathbf{p}_R^2) + [(\hat{\mathbf{p}}_L^2 - \mathbf{p}_R^2) + (\mathbf{p}_L^2 - \hat{\mathbf{p}}_R^2)] \quad (4.25)$$

It reduces to the familiar even integer condition in the case of a trivial code with $k=1$ where $\mathring{\mathbf{p}}_{L/R} = 0$. The final result we seek to retain are given by the conditions (4.29).

To that purpose, we start from the standard even integer condition of Narain lattices namely

$$\mathbf{p}_L^2 - \mathbf{p}_R^2 \in 2\mathbb{Z} \quad , \quad \mathbf{p}_L, \mathbf{p}_R \in \Lambda_{1C}^{r,r} \quad (4.26)$$

This corresponds to the case where $a = b = 0$ for which the momenta $\mathbf{p}_L, \mathbf{p}_R$ are given by (4.21) with CS level $k=1$ in the action (B.1). Using (4.21), one finds $\mathbf{p}_L^2 - \mathbf{p}_R^2 = 2knm$ which indeed belongs to $2\mathbb{Z}$ for $k=1$. For higher values of the CS level, this generalises to $2k\mathbb{Z}$; i.e:

$$\mathbf{p}_L^2 - \mathbf{p}_R^2 \in 2k\mathbb{Z} \quad \text{for} \quad k \geq 1 \quad (4.27)$$

To derive the conditions for non trivial values of the labels (a,b) , we compute $\mathbf{P}_L^2 - \mathbf{P}_R^2$ by using (4.17) which yields $\frac{2}{k}(a+kn)(b+km)$. This expression decomposes as in (4.10) namely $\frac{2}{k}ab + 2(am+bn) + 2knm$. Given that $(a,b) \in \mathbb{Z}_k \times \mathbb{Z}_k$ and $(n,m) \in \mathbb{Z} \times \mathbb{Z}$, it follows that

$$\begin{aligned} \frac{2}{k}ab &\in \frac{2}{k}\mathbb{Z} & 2am &\in 2\mathbb{Z} \\ 2knm &\in 2k\mathbb{Z} & 2bn &\in 2\mathbb{Z} \end{aligned} \quad , \quad (4.28)$$

However, equating with (4.24), indicates that $\mathbf{P}_L^2 - \mathbf{P}_R^2 = 2\mathring{\mathbf{h}}\mathring{\mathbf{p}} + 2(\mathring{\mathbf{h}}\mathbf{p} + \mathbf{h}\mathring{\mathbf{p}}) + 2\mathbf{h}\mathbf{p}$ as in eq(4.24). Accordingly, we deduce the three constraint relations that characterise the code CFT

$$\begin{aligned} 2\mathring{\mathbf{h}}\mathring{\mathbf{p}} &\in \frac{2}{k}\mathbb{Z} & 2\mathring{\mathbf{h}}\mathbf{p} &\in 2\mathbb{Z} \\ 2\mathbf{h}\mathring{\mathbf{p}} &\in 2k\mathbb{Z} & 2\mathbf{h}\mathbf{p} &\in 2\mathbb{Z} \end{aligned} \quad , \quad (4.29)$$

Moreover, using the identifications $\mathring{\mathbf{h}}\mathring{\mathbf{p}} = \frac{1}{k}ab$ and $\mathbf{h}\mathbf{p} = knm$, it also results the two following: (i) the structure of the lattices hosting the ground momenta $(\mathring{\mathbf{h}}, \mathring{\mathbf{p}})$ which are given by

$$\begin{aligned} \mathring{\mathbf{h}} &= x\mathbf{a}\tilde{\boldsymbol{\alpha}} \in x\mathbf{R}_k^{\text{su}_2} & \Rightarrow & \mathring{\mathbf{h}} &= \frac{1}{k}a\tilde{\boldsymbol{\alpha}} \in \frac{1}{k}\mathbf{R}_k^{\text{su}_2} \\ \mathring{\mathbf{p}} &= y\mathbf{b}\tilde{\boldsymbol{\lambda}} \in y\mathbf{W}_k^{\text{su}_2} & & \mathring{\mathbf{p}} &= \frac{1}{k}b\tilde{\boldsymbol{\alpha}} \in \frac{1}{k}\mathbf{R}_k^{\text{su}_2} \end{aligned} \quad (4.30)$$

with the property $xy = \frac{1}{k}$. This condition can be satisfied in multiple ways such as $x = y = \frac{1}{\sqrt{k}}$ or $x = \frac{1}{k}$ and $y = 1$. For the second case, we have $\mathring{\mathbf{h}} = \frac{1}{k}a\tilde{\boldsymbol{\alpha}} \in \mathbf{R}_k^{\text{su}_2}$ and $\mathring{\mathbf{p}} = b\tilde{\boldsymbol{\lambda}} \in \mathbf{W}_k^{\text{su}_2}$ with $\tilde{\boldsymbol{\lambda}} = \frac{1}{k}\tilde{\boldsymbol{\alpha}}$. (ii) Regarding the excited momenta (\mathbf{h}, \mathbf{p}) , we obtain

$$\begin{aligned} \mathbf{h} &= zn\tilde{\boldsymbol{\alpha}} \in z\mathbf{R}_k^{\text{su}_2} & \Rightarrow & \mathbf{h} &= n\tilde{\boldsymbol{\alpha}} \in \mathbf{R}_k^{\text{su}_2} \\ \mathbf{p} &= tm\tilde{\boldsymbol{\lambda}} \in t\mathbf{W}_k^{\text{su}_2} & & \mathbf{p} &= km\tilde{\boldsymbol{\lambda}} \in k\mathbf{W}_k^{\text{su}_2} \end{aligned} \quad (4.31)$$

with $zt = k$ which can be solved for $z = t = \sqrt{k}$ or equivalently $z = 1$ and $t = k$. For the CS level $k = 2$, eq(4.30) reduces to

$$\begin{aligned} \mathring{\mathbf{h}} &= \frac{a}{2}\boldsymbol{\alpha} = \frac{a}{2}\boldsymbol{\alpha} & \mathbf{h} &= n\boldsymbol{\alpha} = n\boldsymbol{\alpha} \\ \mathring{\mathbf{p}} &= b\boldsymbol{\lambda} = \frac{b}{2}\boldsymbol{\alpha} & \mathbf{p} &= 2m\boldsymbol{\lambda} = m\boldsymbol{\alpha} \end{aligned} \quad , \quad (4.32)$$

The graphic representation of $(\mathring{\mathbf{h}}, \mathring{\mathbf{p}})$ within the unit cell of the 2D lattice $\Lambda_2^{1,1}$ is depicted in Figure 13. The ground states are given by the 4 left moving $(\psi_a + \tilde{\psi}_b)/\sqrt{2}$ and the 4 right moving $(\psi_a - \tilde{\psi}_b)/\sqrt{2}$.

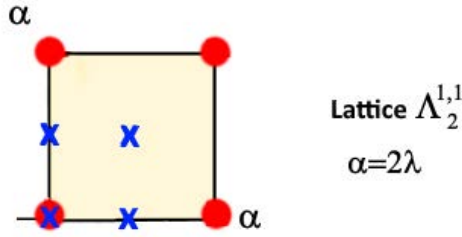


Figure 13: The values of the points $(\mathring{\mathbf{h}}, \mathring{\mathbf{p}})$ in root lattice of $\text{SO}(4)$. These points are given by $(\mathring{\mathbf{h}}, \mathring{\mathbf{p}}) = (0, 0), (\frac{1}{2}, 0), (0, \frac{1}{2}), (\frac{1}{2}, \frac{1}{2})$. Here, we have $k=2$ and $r=1$. In general, there are k^2 points sitting in the unit cell of $\Lambda_k^{1,1}$.

4.2 Particles in the $\text{SU}(3)$ based model

The properties of particle states in the code CFT based on $\text{SU}(3)$, with discriminant group $\mathbb{Z}_k \times \mathbb{Z}_k$ and lattices $(\Lambda_k^{\text{su}_3}, \Lambda_{k\mathbb{C}}^{\text{su}_3}, \Lambda_k^{*\text{su}_3})$ realised in terms of the root $\mathbf{R}_k^{\text{su}_3}$ and weight $\mathbf{W}_k^{\text{su}_3}$ systems, follow an analogous structure to that of the $\text{SU}(2)$ theory. Here, the momenta of the particle states

$$P_{L/R} := (P_{L/R})_{\mathbf{a}, \mathbf{b}}^{\mathbf{n}, \mathbf{m}} \quad (4.33)$$

are labeled by two pairs of integer vectors: (i) a pair (\mathbf{a}, \mathbf{b}) with $\mathbf{a} = (a_1, a_2)$ and $\mathbf{b} = (b_1, b_2)$ ranging in $a_i, b_i = 0, \dots, k-1$; they label the ground configurations. (ii) A pair $(\mathbf{n}, \mathbf{m}) \in \mathbb{Z}^2 \times \mathbb{Z}^2$ with $\mathbf{n} = (n_1, n_2)$ and $\mathbf{m} = (m_1, m_2)$ determining the degrees of excitations of the KK and the windings modes.

4.2.1 Momenta $P_{L/R}$ and $\text{SU}(3)$ symmetry

To derive the left/right momenta $P_{L/R}$ for the $\text{SU}(3)$ based model, we extend the relation (4.17) from the $\text{SU}(2)$ theory. For that, we start by $\mathbf{P}_{L/R} = \frac{1}{\sqrt{2}}(\mathbf{H} \pm \mathbf{P})$ where

$$\mathbf{H} = \frac{1}{\sqrt{2}}(\mathbf{P}_L + \mathbf{P}_R) \quad , \quad \mathbf{P} = \frac{1}{\sqrt{2}}(\mathbf{P}_L - \mathbf{P}_R) \quad (4.34)$$

and

$$\mathbf{H} = \mathring{\mathbf{h}} + \mathbf{h} \quad , \quad \mathbf{P} = \mathring{\mathbf{p}} + \mathbf{p} \quad (4.35)$$

here $(\mathring{\mathbf{h}}, \mathring{\mathbf{p}})$ encode the ground configurations while (\mathbf{h}, \mathbf{p}) are used to describe the KK and winding excitations. Then, we require the SU(2) conditions (4.29) to remain valid for the SU(3) model. These constraints generalise as follows

$$\begin{aligned} \mathring{\mathbf{h}} \cdot \mathring{\mathbf{p}} &= \frac{1}{k} \mathbf{a} \cdot \mathbf{b} \in \frac{1}{k} \mathbb{Z} & \mathring{\mathbf{h}} \cdot \mathbf{p} &= \mathbf{a} \cdot \mathbf{m} \in \mathbb{Z} \\ \mathbf{h} \cdot \mathbf{p} &= k \mathbf{n} \cdot \mathbf{m} \in k \mathbb{Z} & \mathbf{h} \cdot \mathring{\mathbf{p}} &= \mathbf{b} \cdot \mathbf{n} \in \mathbb{Z} \end{aligned} \quad (4.36)$$

where each pairing, like $\mathbf{a} \cdot \mathbf{b}$, stands for the scalar products, $a_1 b_1 + a_2 b_2$. A solution to these constraints (4.36) is given as follows:

(i) values of $(\mathring{\mathbf{h}}, \mathring{\mathbf{p}})$:

$$\begin{aligned} \mathring{\mathbf{h}} &= \frac{1}{k} (a_1 \tilde{\alpha}_1 + a_2 \tilde{\alpha}_2) \in \frac{1}{k} \mathbf{R}_k^{\text{su}_3} \\ \mathring{\mathbf{p}} &= b \tilde{\lambda}_1 + b_2 \tilde{\lambda}_2 \in \mathbf{W}_k^{\text{su}_3} \end{aligned} \quad (4.37)$$

with

$$\tilde{\alpha}_i = \sqrt{\frac{k}{3}} \alpha_i \quad , \quad \tilde{\lambda}^i = \sqrt{\frac{3}{k}} \lambda^i \quad , \quad \tilde{\alpha}_i \cdot \tilde{\lambda}^j = \delta_i^j \quad (4.38)$$

Using the relations $\tilde{\lambda}_1 = \frac{1}{k} (2\tilde{\alpha}_1 + \tilde{\alpha}_2)$ and $\tilde{\lambda}_2 = \frac{1}{k} (\tilde{\alpha}_1 + 2\tilde{\alpha}_2)$, we also have

$$\begin{aligned} \mathring{\mathbf{h}} &= \frac{1}{k} (a_1 \tilde{\alpha}_1 + a_2 \tilde{\alpha}_2) \in \frac{1}{k} \mathbf{R}_k^{\text{su}_3} \\ \mathring{\mathbf{p}} &= \frac{1}{k} (b'_1 \tilde{\alpha}_1 + b'_2 \tilde{\alpha}_2) \in \frac{1}{k} \mathbf{R}_k^{\text{su}_3} \end{aligned} \quad (4.39)$$

where we have set $b'_1 = 2b_1 + b_2$ and $b'_2 = b_1 + 2b_2$.

(ii) values of (\mathbf{h}, \mathbf{p}) :

$$\begin{aligned} \mathbf{h} &= n_1 \tilde{\alpha}_1 + n_2 \tilde{\alpha}_2 \in \mathbf{R}_k^{\text{su}_3} \\ \mathbf{p} &= k (m_1 \tilde{\lambda}_1 + m_2 \tilde{\lambda}_2) \in k \mathbf{W}_k^{\text{su}_3} \end{aligned} \quad (4.40)$$

reading also like

$$\begin{aligned} \mathbf{h} &= n_1 \tilde{\alpha}_1 + n_2 \tilde{\alpha}_2 \in \mathbf{R}_k^{\text{su}_3} \\ \mathbf{p} &= m'_1 \tilde{\alpha}_1 + m'_2 \tilde{\alpha}_2 \in \mathbf{R}_k^{\text{su}_3} \end{aligned} \quad (4.41)$$

with $m'_1 = 2m_1 + m_2$ and $m'_2 = m_1 + 2m_2$.

By substituting these expressions into (4.34), we get

$$\begin{aligned} \mathbf{H} &= \frac{1}{\sqrt{2k}} (a^i + kn^i) \tilde{\alpha}_i & \Leftrightarrow & \quad \mathbf{H} = \frac{1}{\sqrt{2k}} \bar{a}^i \tilde{\alpha}_i \\ \mathbf{P} &= \frac{1}{\sqrt{2k}} (b_i + km_i) \tilde{\lambda}^i & & \quad \mathbf{P} = \frac{1}{\sqrt{2k}} \bar{b}_i \tilde{\lambda}^i \end{aligned} \quad (4.42)$$

and subsequently

$$\begin{aligned}
\mathbf{P}_L &= \frac{1}{\sqrt{2k}} \left(\bar{a}^i \tilde{\alpha}_i + \bar{b}_i \tilde{\lambda}^i \right) \\
&= \frac{1}{\sqrt{2k}} \left[(a^i + kn^i) \tilde{\alpha}_i + (b_i + km_i) \tilde{\lambda}^i \right] \\
\mathbf{P}_R &= \frac{1}{\sqrt{2k}} \left(\bar{a}^i \tilde{\alpha}_i - \bar{b}_i \tilde{\lambda}^i \right) \\
&= \frac{1}{\sqrt{2k}} \left[(a^i + kn^i) \tilde{\alpha}_i - (b_i + km_i) \tilde{\lambda}^i \right]
\end{aligned} \tag{4.43}$$

We conclude by giving the locii of the ground states characterised by the pair $(\mathring{\mathbf{h}}, \mathring{\mathbf{p}})$ written in terms of the $\tilde{\alpha}_i$ as in eq(4.38). Focussing on $\mathring{\mathbf{h}}$, the loci for the cases $k=2$ and $k=3$ are depicted in the Figure 14.

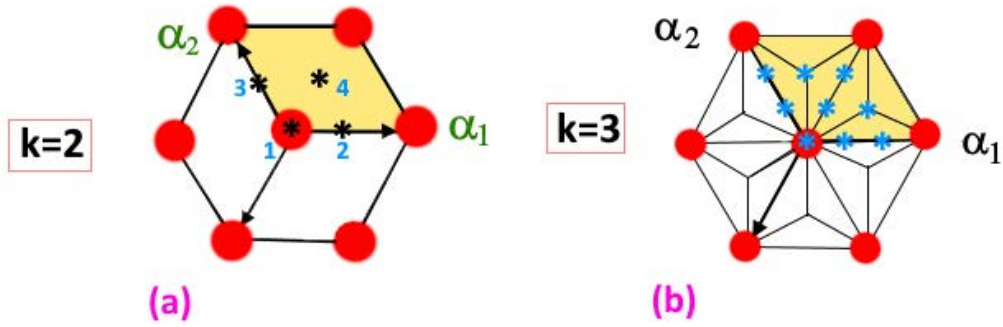


Figure 14: The values of the points $\mathring{\mathbf{h}}$ in root lattices $R_k^{\text{su}_3}$. On left we have 4 ground points. On right there are 9 points in unit cell.

4.2.2 Ground configurations and SU(3) representations

We begin by recalling that, for SU(2) based model, the ground state configurations for a CS level k transform in the representation with isospin $j = (k-1)/2$ as in (4.18). In the case of code CFTs based on SU(3), a similar structure emerges. By using $\tilde{\alpha}_1 = \frac{k}{3}(2\tilde{\lambda}_1 - \tilde{\lambda}_2)$ and $\tilde{\alpha}_2 = \frac{k}{3}(2\tilde{\lambda}_2 - \tilde{\lambda}_1)$, the scaled quantum numbers $(\mathring{\mathbf{h}}', \mathring{\mathbf{p}}') = (\sqrt{3k}\mathring{\mathbf{h}}, \sqrt{k/3}\mathring{\mathbf{p}})$ characterising the ground configurations are given by the weight vectors

$$\begin{aligned}
\mathring{\mathbf{h}}' &= r_1 \lambda_1 + r_2 \lambda_2 \\
\mathring{\mathbf{p}}' &= b_1 \lambda_1 + b_2 \lambda_2
\end{aligned} \tag{4.44}$$

where the integers $r_1 = 2a_1 - a_2$ and $r_2 = 2a_2 - a_1$ (modulo k) take values in the range $[0, k-1]$. These quantum numbers correspond to the highest weight vectors of SU(3). Recall that highest weight representations $\mathcal{D}^{(s_1, s_2)}$ of the symmetry SU(3) are defined by the highest weight vector $\boldsymbol{\omega} = s_1 \tilde{\lambda}_1 + s_2 \tilde{\lambda}_2$ parameterised by two positive integers (s_1, s_2) . Their dimensions are given by

$$d_{s_1, s_2} = \frac{1}{2} (s_1 + 1) (s_2 + 1) (s_1 + s_2 + 2) \tag{4.45}$$

For the particular situation $s_2 = 0$ where the $SU(3)$ is broken down to $SU(2) \times U(1)$, the dimension reduces to $d_{s,0} = \frac{1}{2}(s+1)(s+2)$. As for the case $s = 2j$, we have $d_{2j,0} = (2j+1)(j+1)$ that splits into $j+1$ multiplets like

$$d_{2j,0} = \underbrace{(2j+1) + \dots + (2j+1)}_{j+1 \text{ iso-multiplets}} \quad (4.46)$$

5 Lattice fermions and topological phases

This section builds on the previous and further develops the connection between Narain CFT and topological matter with Dirac cones formulated in terms of fermionic lattices. To establish this link explicitly, we present three *guiding arguments* (**A1**, **A2** and **A3**) while focussing on the CS level $k=2$ to illustrate the basic ideas using the associated 2D lattices $R_2^{\text{su}_3}$ and $W_2^{\text{su}_3}$:

- **A1**: lattice $W_2^{\text{su}_3} = \text{honeycomb } \mathbb{A}_2 + \mathbb{B}_2$.

The weight lattice $W_2^{\text{su}_3}$ contains the root lattice $R_2^{\text{su}_3} \subset W_2^{\text{su}_3}$ leading to the discriminant $W_2^{\text{su}_3}/R_2^{\text{su}_3} \simeq \mathbb{Z}_2$, this allows to split the weight lattice as follows

$$W_2^{\text{su}_3} = \mathbb{A}_2 \cup \mathbb{B}_2, \quad \begin{aligned} \mathbb{A}_2 &= R_2^{\text{su}_3} \\ \mathbb{B}_2 &= W_2^{\text{su}_3} \setminus R_2^{\text{su}_3} \end{aligned} \quad (5.1)$$

To distinguish the two sublattices of $W_2^{\text{su}_3}$, we introduce a physical hypothesis: we interpret the lattices \mathbb{A}_2 and \mathbb{B}_2 as being occupied by different (*colored*) particles, each localized on one sublattice as described in **A2**.

- **A2**: the *KK/W* correspondence

Leveraging the root/weight duality and the $\text{KK} \leftrightarrow \text{Winding}$ correspondence, we propose that quantum excitations $|KK_{\mathbf{m}}\rangle$ sit in \mathbb{A}_2 while the winding modes $|W_{\mathbf{m}}\rangle$ live in \mathbb{B}_2 ; see Figure 15 for illustration.

This assumption implies that both type of states $|KK_{\mathbf{m}}\rangle$ and $|W_{\mathbf{m}}\rangle$ are hosted by the honeycomb $W_2^{\text{su}_3}$ where each unit cell is occupied by a \mathbb{Z}_2 doublet as also depicted in Figure 19),

$$\begin{pmatrix} |KK\rangle \\ |W\rangle \end{pmatrix} \quad (5.2)$$

Observe that the NCFT based on $W_2^{\text{su}_3}$ has a central anomaly $c_{L/R} = 2$ which suggests that the theory has two bosonic conformal fields $X^1(\tau, \sigma)$ and $X^2(\tau, \sigma)$

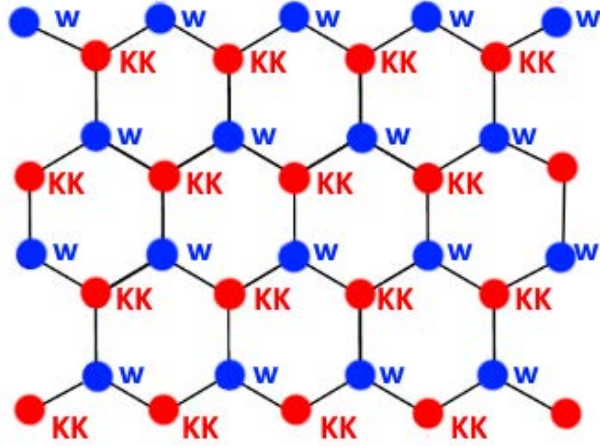


Figure 15: Lattice of KK and winding particles. Each unit cell contains a pair KK/W in agreement with \mathbb{Z}_2 symmetry of code CFT at CS level $k=2$.

splitting into left $X_L^i(\tau + \sigma)$ and right $X_R^i(\tau - \sigma)$ moving fields. In complex coordinates $z = \tau + i\sigma$, these become the holomorphic $X_L^i = X_L^i(z)$ and the anti-holomorphic $X_R^i = X_R^i(\bar{z})$.

- **A3:** *fermionisation*

We apply fermionisation techniques⁵ in two dimensions [62, 63] as in the table Eq(5.4) to reinterpret the bosonic theory as a fermionic one with a tight binding model having Dirac cones, enabling thus the modeling of critical points in topological phases of matter. The main lines of this proposal can be formally schematised in the following algorithm

$$\begin{array}{c}
 \text{Code-CFT} \\
 \downarrow \\
 \text{Narain CFT} \\
 \downarrow \\
 \text{bosonic CFT} \\
 \downarrow \uparrow \\
 \boxed{
 \begin{array}{ccc}
 \text{fermionic CFT} & \rightarrow & \text{Dirac cones} \\
 \uparrow & \circlearrowleft & \downarrow \\
 \text{gapless states} & \leftarrow & \text{lattice model}
 \end{array}
 }
 \end{array} \tag{5.3}$$

⁵ Free conformal fermions $\psi_{L/R}$ can be expressed in terms of bosons $\phi_{L/R}$ by using vertex operators $e^{\pm i\phi_{L/R}}$. For constructions using bosonisation and tight binding models, see [30–32]

Using the arguments ([A1](#), [A2](#), [A3](#)), we show throughout this section how known results from 2D Lattice matter such as 2D graphene [[27](#), [28](#)] can be recast in terms of a NCFT. These particular insulators feature gapless states protected by discrete symmetry and carry non trivial Chern invariant [[34](#), [36](#)] similarly to topological Haldane theory of the anomalous quantum Hall effect.

5.1 KK/W system on the lattice

We begin by recalling that the Narain CFT with $c_{L/R}=2$ can be realised using two free real bosonic fields $X^i(\tau, \sigma)$ splitting like $X_L^i(\tau + \sigma) + X_R^i(\tau - \sigma)$. The Narain compactification imposes the periodicity condition $X_{L/R}(\sigma + 2\pi) = X_{L/R}(\sigma) + 2\pi Rm$ and the KK constraint $e^{i2\pi R P_{L/R}} = 1$ which captures the single valuedness of $X_{L/R}$ and $X_{L/R} + 2\pi R$. The allowed values of the momenta $P_{L/R}$ are quantized and described in detail in section 4.

5.1.1 Fermionisation

In the fermionic representation, we reinterpret the central charge value $c_{L/R} = 2$ by expressing the two real free conformal bosons (X^1, X^2) in terms of four free real Fermi fields as shown in the table below

2 real bosons	4 real fermions \rightarrow 2 complex	$c_{L/R}$
X^1	$\begin{pmatrix} \psi^1 \\ \psi^2 \end{pmatrix} \rightarrow \psi = \psi^1 + i\psi^2$	1
X^2	$\begin{pmatrix} \chi^1 \\ \chi^2 \end{pmatrix} \rightarrow \chi = \chi^1 + i\chi^2$	1

(5.4)

By using the complex field $X = X_1 + iX_2$, the left J_z^L and the right J_z^R conformal currents are respectively given by $\partial_z X_L$ and $\partial_{\bar{z}} X_R$. In terms of the two complex Fermi fields $\psi = \psi_1 + i\psi_2$ and $\chi = \chi_1 + i\chi_2$, these conformal currents read as $J_z^L \sim : \psi_L \psi_L^\dagger + \chi_L \chi_L^\dagger :$ and $J_z^R \sim : \psi_R \psi_R^\dagger + \chi_R \chi_R^\dagger :$. Notice that the two Fermi fields may be also thought of as the two Weyls of a Dirac spinor: $f_\uparrow = \psi$ and $f_\downarrow = \chi$. With the compact notation $(\psi, \chi) := \varphi^a$, the left and right currents can be written more concisely as: $\varphi_L^a \varphi_{La}^\dagger$: and $\varphi_R^a \varphi_{Ra}^\dagger$:

Moreover, the classical dynamics of these free conformal fermions is governed by the massless 2D Dirac equation $i\gamma^\mu \partial_\mu \varphi = \mathbf{0}$. After performing a Fourier transform, it reads as follows $(\gamma^\mu q_\mu) \tilde{\varphi} = \mathbf{0}$ with $\tilde{\varphi} = \tilde{\varphi}(q)$ and γ^μ defining Dirac matrices in 2D. The above Dirac equation describes gapless states in continuum; however it also appears in lattice

field theory in the vicinity of the so-called Dirac points where the Dirac Hamiltonian satisfies [33]

$$H_{Dirac}|\tilde{\varphi}\rangle = 0 \quad , \quad E_g = E_+ - E_- = 0 \quad (5.5)$$

In lattice modeling, the fermionic fields $\varphi_{\mathbf{r}_n} = (\psi_{\mathbf{r}_n}, \chi_{\mathbf{r}_n})$ are defined on a honeycomb (5.1) with position sites $\mathbf{r}_n^A \in \mathbb{A}_2$ and $\mathbf{r}_n^B \in \mathbb{B}_2$. The local fermionic fields $\psi_{\mathbf{r}_n}$ and $\chi_{\mathbf{r}_n}$ sit respectively at the two superposed lattices as

$$\begin{aligned} \psi_{\mathbf{r}_n} &= \varphi(\mathbf{r}_n^A) & \mathbf{r}_n^A &= n_1\alpha_1 + n_2\alpha_2 \\ \chi_{\mathbf{r}_n} &= \varphi(\mathbf{r}_n^B) & \mathbf{r}_n^B &= \mathbf{r}_n^A + \omega \end{aligned} \quad , \quad (5.6)$$

where the highest weight vector ω is a fundamental weight of SU(3); say $\omega = \lambda_1$. They expand like

$$\psi_{\mathbf{r}_n} = \sum_{\mathbf{k}} e^{i\mathbf{k}\cdot\mathbf{r}_n} \tilde{\psi}_{\mathbf{k}} \quad , \quad \chi_{\mathbf{r}_n} = \sum_{\mathbf{k}} \sum_{l=1}^3 e^{i\mathbf{k}\cdot(\mathbf{r}_n+\omega_l)} \tilde{\chi}_{\mathbf{k}} \quad (5.7)$$

with the three $\omega_1, \omega_2, \omega_3$ as in eq(5.13). In this description, the lattice Hamiltonian H_{lat} of the KK/W system is given by the sum over the quadratic interactions $\varphi_{\mathbf{r}_n}^\dagger t_{nm} \varphi_{\mathbf{r}_m} + hc$ expanding as

$$\begin{aligned} \varphi_{\mathbf{r}_n}^\dagger t_{nm} \varphi_{\mathbf{r}_m} &= \psi_{\mathbf{r}_n^A}^\dagger t_{\mathbf{r}_n^A \mathbf{r}_m^A} \psi_{\mathbf{r}_m^A} + \chi_{\mathbf{r}_n^B}^\dagger t_{\mathbf{r}_n^B \mathbf{r}_m^B} \chi_{\mathbf{r}_m^B} + \\ &\psi_{\mathbf{r}_n^A}^\dagger t_{\mathbf{r}_n^A \mathbf{r}_m^B} \chi_{\mathbf{r}_m^B} + \chi_{\mathbf{r}_n^B}^\dagger t_{\mathbf{r}_n^B \mathbf{r}_m^A} \psi_{\mathbf{r}_m^A} \end{aligned} \quad (5.8)$$

with coupling tensors t_{nm} function of the positions $(\mathbf{r}_n^A, \mathbf{r}_m^B)$. In models such as the Haldane theory, these couplings are subject to the Peierls substitution $t_{nm} \rightarrow t_{nm} \exp(-i \int_{\mathbf{r}_n}^{\mathbf{r}_m} \vec{A} \cdot \vec{dl})$ generating Aharonov-Bohm phases during hoppings. In practice, one typically includes only the first and the second coupling orders when calculating the spectrum of lattice hamiltonians H_{lat} involving the first and the second closest neighbouring as given below

$$H_{lat} \simeq H_{lat}^{(0)} + \sum_{\langle \mathbf{r}_n, \mathbf{r}_m \rangle} \psi_{\mathbf{r}_n}^\dagger t_{nm}^{(1)} \chi_{\mathbf{r}_m} + \sum_{\langle \langle \mathbf{r}_n, \mathbf{r}_m \rangle \rangle} t_{nm}^{(2)} (\psi_{\mathbf{r}_n}^\dagger \psi_{\mathbf{r}_m} + \chi_{\mathbf{r}_n}^\dagger \chi_{\mathbf{r}_m}) + hc \quad (5.9)$$

which we refer to as $H_{lat}^{(0)} + H_{lat}^{(1)} + H_{lat}^{(2)}$ where we have added the on site energy $H_{lat}^{(0)}$ having the form $M(\psi_{\mathbf{r}_n}^\dagger \psi_{\mathbf{r}_n} - \chi_{\mathbf{r}_n}^\dagger \chi_{\mathbf{r}_n})$ breaking the inversion symmetry. This tight binding model mirrors the structure of the Haldane theory for the anomalous quantum Hall effect [33, 34]. In this regard, we recall that the Haldane theory has non trivial topological phases for the filled band in 2D graphene. Consequently, the Haldane results apply to the KK/W system imagined in terms of the ψ/χ fermions. As such, the eq(5.9) has a non vanishing first Chern number ($C_1 \neq 0$) given by the integral of the curvature of the Berry connection $A = \langle \mathbf{k} | \frac{1}{i} \nabla_{\mathbf{k}} | \mathbf{k} \rangle$ [33–35],

$$C_1 = \int_{BZ} F \quad (5.10)$$

where the Berry curvature $F = dA$ (intrinsic magnetic field) is induced by the second closest neighbors ($M, t_{nm}^{(2)} \neq 0$) which open the gap E_g in (5.5) therefore breaking inversion and time reversal symmetries due to the non vanishing Berry curvature.

5.1.2 Hamiltonian Eq(5.9) in reciprocal space

Here, we consider the lattice hamiltonian (5.9) and draw the path leading to Dirac cones, which are essential for the gapless states (massless Dirac modes) and 2D topological matter. Starting from the lattice H_{lat} , the analysis ultimately yields the 2-dimensional massless Dirac equation

$$\mathcal{D}_{\mathbf{q}}\tilde{\varphi} = (\sigma^x q_x + \sigma^y q_y)\tilde{\varphi} = 0 \quad (5.11)$$

A) Expression of $H_{lat}^{(1)}$: We first consider the bloc hamiltonian

$$H_{lat}^{(1)} = \sum_{\mathbf{r}_n \in \mathbb{A}} \sum_{l=1}^3 t_l \psi_{\mathbf{r}_n}^\dagger \chi_{\mathbf{r}_n + \boldsymbol{\omega}_l} + hc \quad (5.12)$$

with coupling parameters t_l (in general complex) and where the vectors $(\boldsymbol{\omega}_1, \boldsymbol{\omega}_2, \boldsymbol{\omega}_3)$ represent the displacements to the three nearest neighbors of the site \mathbf{r}_n^A given by $\mathbf{r}_n^B = \mathbf{r}_n^A + \boldsymbol{\omega}_l$; these neighbours generate the fundamental dimensional representation of SU(3) and can be expressed in terms of the highest weight vector $\boldsymbol{\lambda}_1$ as follows

$$\begin{pmatrix} \boldsymbol{\omega}_1 \\ \boldsymbol{\omega}_2 \\ \boldsymbol{\omega}_3 \end{pmatrix} = \begin{pmatrix} \boldsymbol{\lambda}_1 \\ \boldsymbol{\lambda}_1 - \boldsymbol{\alpha}_1 \\ \boldsymbol{\lambda}_1 - \boldsymbol{\alpha}_1 - \boldsymbol{\alpha}_2 \end{pmatrix} = \frac{1}{3} \begin{pmatrix} 2\boldsymbol{\alpha}_1 + \boldsymbol{\alpha}_2 \\ -\boldsymbol{\alpha}_1 + \boldsymbol{\alpha}_2 \\ -\boldsymbol{\alpha}_1 - 2\boldsymbol{\alpha}_2 \end{pmatrix} \quad (5.13)$$

Notice that these weight vectors satisfy $\boldsymbol{\omega}_1 + \boldsymbol{\omega}_2 + \boldsymbol{\omega}_3 = 0$ reflecting the tracelessness condition of SU(3) matrices. Furthermore, the weight vectors satisfy some useful relations such as $\boldsymbol{\omega}_1 - \boldsymbol{\omega}_2 = \boldsymbol{\alpha}_1$ and $\boldsymbol{\omega}_1 - \boldsymbol{\omega}_3 = \boldsymbol{\alpha}_3$ where we set $\boldsymbol{\alpha}_3 = \boldsymbol{\alpha}_1 + \boldsymbol{\alpha}_2$. Substituting the Fourier transform of the lattice fields ($\varphi_{\mathbf{r}_n} = \sum_{\mathbf{k}} e^{i\mathbf{k} \cdot \mathbf{r}_n} \tilde{\varphi}_{\mathbf{k}}$) in the hamiltonian (5.12), we can bring the $H_{lat}^{(1)}$ into the quadratic form

$$H_{lat}^{(1)} = \sum_{\mathbf{k} \in \mathbb{R}^2} \begin{pmatrix} \tilde{\psi}_{\mathbf{k}}^\dagger & \tilde{\chi}_{\mathbf{k}}^\dagger \end{pmatrix} \mathbb{H}_{lat}^{(1)} \begin{pmatrix} \tilde{\psi}_{\mathbf{k}} \\ \tilde{\chi}_{\mathbf{k}} \end{pmatrix} \quad (5.14)$$

with the 2×2 matrix $\mathbb{H}_{lat}^{(1)}$ given by

$$\mathbb{H}_{lat}^{(1)} = \begin{pmatrix} 0 & f_{\mathbf{k}} \\ f_{\mathbf{k}}^* & 0 \end{pmatrix}, \quad \begin{aligned} f_{\mathbf{k}} &= t_1 e^{i\mathbf{k} \cdot \boldsymbol{\omega}_1} + t_2 e^{i\mathbf{k} \cdot \boldsymbol{\omega}_2} + t_3 e^{i\mathbf{k} \cdot \boldsymbol{\omega}_3} \\ &= t e^{i\mathbf{k} \cdot \boldsymbol{\omega}_1} (1 + e^{-i\mathbf{k} \cdot \boldsymbol{\alpha}_1} + e^{-i\mathbf{k} \cdot \boldsymbol{\alpha}_3}) \end{aligned} \quad (5.15)$$

where we have assumed real $t_i = t$. By decomposing the function $f_{\mathbf{k}}$ like $h_{\mathbf{k}}^{(x)} + i h_{\mathbf{k}}^{(y)}$ with $h_{\mathbf{k}}^{(x)} = t \sum_{l=1}^3 \cos \mathbf{k} \cdot \boldsymbol{\omega}_l$ and $h_{\mathbf{k}}^{(y)} = -t \sum_{l=1}^3 \sin \mathbf{k} \cdot \boldsymbol{\omega}_l$, we finally obtain

$$\mathbb{H}_{lat}^{(1)} = h_{\mathbf{k}}^x \sigma^x + h_{\mathbf{k}}^y \sigma^y \quad (5.16)$$

B) Expression of $\mathbf{H}_{lat}^{(2)}$: We now consider the block hamiltonian $\mathbf{H}_{lat}^{(2)}$ describing the couplings between second closest neighbours on the lattice

$$\mathbf{H}_{lat}^{(2)} = \sum_{\mathbf{r}_n} \sum_{a=1}^6 \left(\psi_{\mathbf{r}_n}^\dagger t_{\mathbf{r}_n, \mathbf{r}_n + \varpi_a}^{\psi\psi} \psi_{\mathbf{r}_n + \varpi_a} + \chi_{\mathbf{r}_n}^\dagger t_{\mathbf{r}_n, \mathbf{r}_n + \varpi_a}^{\chi\chi} \chi_{\mathbf{r}_n + \varpi_a} \right) + hc \quad (5.17)$$

here, $t_{\mathbf{r}_n, \mathbf{r}_n + \varpi_a}^{\psi\psi}$ and $t_{\mathbf{r}_n, \mathbf{r}_n + \varpi_a}^{\chi\chi}$ are complex coupling functions of $(\mathbf{r}_n, \mathbf{r}_m)$. The six ϖ_a s label the second nearest neighbours of a given site \mathbf{r}_n with $\mathbf{r}_n - \mathbf{r}_m = \varpi_a$. They read in terms of the simple roots of SU(3) as follows,

$$\begin{aligned} \varpi_1 &= +\alpha_1 & \varpi_2 &= +\alpha_2 & \varpi_3 &= +\alpha_3 \\ \varpi_4 &= -\alpha_1 & \varpi_5 &= -\alpha_2 & \varpi_6 &= -\alpha_3 \end{aligned} \quad (5.18)$$

where we have set $\alpha_3 = \alpha_1 + \alpha_2$. Due to the homogeneity of the honeycomb lattice, the coupling parameters can be assumed to depend only on the difference $\mathbf{r}_n - \mathbf{r}_m$ leading to constant $t_a^{\psi\psi}$ and $t_a^{\chi\chi}$. Being complex, these couplings can be moreover parameterised like $t_a^{\psi\psi} = t_a^{\psi\psi} e^{i\Phi_a}$ and $t_a^{\chi\chi} = t_a^{\chi\chi} e^{i\Phi_a}$. And by using the Fourier transforms, we can put $\mathbf{H}_{lat}^{(2)}$ in the form

$$\mathbf{H}_{lat}^{(2)} = \sum_{\mathbf{k} \in \mathbb{R}^2} \left(\tilde{\psi}_{\mathbf{k}}^\dagger, \tilde{\chi}_{\mathbf{k}}^\dagger \right) \mathbb{H}_{lat}^{(2)} \begin{pmatrix} \tilde{\psi}_{\mathbf{k}} \\ \tilde{\chi}_{\mathbf{k}} \end{pmatrix} \quad (5.19)$$

with

$$\mathbb{H}_{lat}^{(2)} = \begin{pmatrix} \text{Re } g_{\mathbf{k}}^{\psi\psi} + M & 0 \\ 0 & \text{Re } g_{\mathbf{k}}^{\chi\chi} - M \end{pmatrix} \quad (5.20)$$

and

$$g_{\mathbf{k}}^{\psi\psi} = \sum_{a=1}^6 t_a^{\psi\psi} e^{i\mathbf{k} \cdot \boldsymbol{\omega}_a} \quad , \quad g_{\mathbf{k}}^{\chi\chi} = \sum_{a=1}^6 t_a^{\chi\chi} e^{i\mathbf{k} \cdot \boldsymbol{\omega}_a} \quad (5.21)$$

Adding (5.14,5.21), we get

$$\mathbb{H}_{lat} = \begin{pmatrix} \text{Re } g_{\mathbf{k}}^{\psi\psi} + M & f_{\mathbf{k}} \\ f_{\mathbf{k}}^* & \text{Re } g_{\mathbf{k}}^{\chi\chi} - M \end{pmatrix} \quad (5.22)$$

with eigenvalues

$$E_{\pm} = \text{Re}[g_{\mathbf{k}}^{\psi\psi} + g_{\mathbf{k}}^{\chi\chi}] \pm \sqrt{\left(\text{Re}[g_{\mathbf{k}}^{\psi\psi} - g_{\mathbf{k}}^{\chi\chi}] - M \right)^2 + f_{\mathbf{k}} f_{\mathbf{k}}^*} \quad (5.23)$$

and gap energy $E_g = 2[(\text{Re}[g_{\mathbf{k}}^{\psi\psi} - g_{\mathbf{k}}^{\chi\chi}] - M)^2 + f_{\mathbf{k}} f_{\mathbf{k}}^*]^{1/2}$.

5.2 Dirac cones and gapless states

In this subsection, we consider the gapless regime by setting the mass and diagonal couplings to $M = t_a^{\psi\psi} = t_a^{\chi\chi} = 0$ in order to derive the location of the Dirac cones by

computing the zero modes of $\mathbb{H}_{lat}^{(1)}$. To that purpose, observe first that $f_{\mathbf{k}}$ is invariant under cyclic permutation $(\boldsymbol{\omega}_1, \boldsymbol{\omega}_2, \boldsymbol{\omega}_3)$ generating \mathbb{Z}_3 ; and as such, $f_{\mathbf{k}}$ can be also factorised in two equivalent ways as follows:

$$f_{\mathbf{k}} = te^{i\mathbf{k}\cdot\boldsymbol{\omega}_2} (1 + e^{i\mathbf{k}\cdot\boldsymbol{\alpha}_1} + e^{-i\mathbf{k}\cdot\boldsymbol{\alpha}_2}), \quad f_{\mathbf{k}} = te^{i\mathbf{k}\cdot\boldsymbol{\omega}_3} (1 + e^{-i\mathbf{k}\cdot\boldsymbol{\alpha}_2} + e^{-i\mathbf{k}\cdot\boldsymbol{\alpha}_3}) \quad (5.24)$$

The two energy eigenvalues E_{\pm} of the matrix \mathbb{H}_{lat} are given by $\pm\sqrt{f_{\mathbf{k}}f_{\mathbf{k}}^*}$ from which we deduce the expression of the gap energy which is equal to $E_g = 2\sqrt{f_{\mathbf{k}}f_{\mathbf{k}}^*}$. Hence, the condition for a vanishing gap is given by $f_{\mathbf{k}} = 0$; its solution can be inspired from the well known identity $1 + e^{i\frac{2\pi}{3}} + e^{i\frac{4\pi}{3}} = 0$ concerning the three roots of $z^3 = 1$. It leads to two different solutions (mod \mathbb{Z}_3 transformations), one at $\mathbf{k} = \boldsymbol{\kappa}_0$ and the other at $\mathbf{k} = \boldsymbol{\kappa}_0^*$. They are often termed as the Dirac points and are given by the particular momenta

Dirac point $\boldsymbol{\kappa}_0$		
$\boldsymbol{\kappa}_0 \cdot \boldsymbol{\alpha}_1$	=	$\frac{2\pi}{3} \text{ mod } 2\pi$
$\boldsymbol{\kappa}_0 \cdot \boldsymbol{\alpha}_3$	=	$\frac{4\pi}{3} \text{ mod } 2\pi$

 \Rightarrow

$$\begin{aligned} \boldsymbol{\kappa}_0 &= \frac{2\pi}{3} (\boldsymbol{\lambda}_1 + \boldsymbol{\lambda}_2) \\ &= \frac{2\pi}{3} (\boldsymbol{\alpha}_1 + \boldsymbol{\alpha}_2) \end{aligned} \quad (5.25)$$

or equivalently $\boldsymbol{\kappa}_{\mathbf{m}} = \boldsymbol{\kappa}_0 + 2\pi (m_1\boldsymbol{\lambda}_1 + m_2\boldsymbol{\lambda}_2)$ with integers m_i . Additionally, we have

Dirac point $\boldsymbol{\kappa}_0^*$		
$\boldsymbol{\kappa}_0^* \cdot \boldsymbol{\alpha}_1$	=	$\frac{4\pi}{3} \text{ mod } 2\pi$
$\boldsymbol{\kappa}_0^* \cdot \boldsymbol{\alpha}_3$	=	$\frac{2\pi}{3} \text{ mod } 2\pi$

 \Rightarrow

$$\begin{aligned} \boldsymbol{\kappa}_0^* &= \frac{2\pi}{3} (2\boldsymbol{\lambda}_1 - \boldsymbol{\lambda}_2) \\ &= \frac{2\pi}{3} \boldsymbol{\alpha}_1 \end{aligned} \quad (5.26)$$

or equivalently $\boldsymbol{\kappa}_{\mathbf{m}}^* = \boldsymbol{\kappa}_0^* + 2\pi (m_1\boldsymbol{\alpha}_1 + m_2\boldsymbol{\alpha}_2)$ giving the Brillouin zone. The Dirac points together with \mathbb{Z}_3 symmetry are depicted by the Figure 16. Near these Dirac points; say

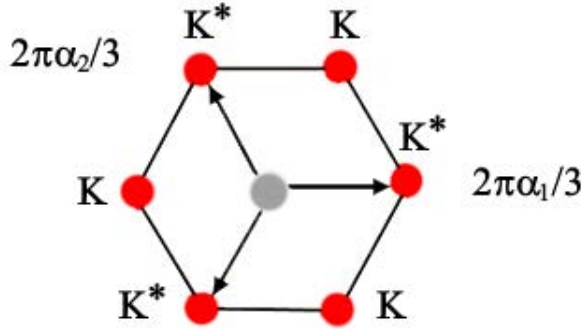


Figure 16: Dirac points $\boldsymbol{\kappa}_0$ and $\boldsymbol{\kappa}_0^*$ as well as the action do the \mathbb{Z}_3 transformations.

$\mathbf{k} = \boldsymbol{\kappa}_0 + \mathbf{q}$ with small \mathbf{q} , the function f approximates at leading order like $3te^{i\frac{\pi}{6}}\mathbf{q}\cdot\boldsymbol{\lambda}_1$. Putting into $f_{\mathbf{k}} = te^{i\mathbf{k}\cdot\boldsymbol{\omega}_2} (1 + e^{i\mathbf{k}\cdot\boldsymbol{\alpha}_1} + e^{-i\mathbf{k}\cdot\boldsymbol{\alpha}_2})$ with $\boldsymbol{\kappa}_0 = \frac{2\pi}{3} (\boldsymbol{\lambda}_1 + \boldsymbol{\lambda}_2)$ and $\boldsymbol{\kappa}_0 \cdot \boldsymbol{\omega}_2 = 2\pi$, then using $\boldsymbol{\kappa}_0 \cdot \boldsymbol{\alpha}_1 = \frac{2\pi}{3}$ and $\boldsymbol{\kappa}_0 \cdot \boldsymbol{\alpha}_2 = \frac{2\pi}{3}$, we get

$$\begin{aligned} f_{\mathbf{q}} &\simeq te^{i\boldsymbol{\kappa}_0 \cdot \boldsymbol{\alpha}_1} (\mathbf{q} \cdot \boldsymbol{\alpha}_1) + te^{-i\boldsymbol{\kappa}_0 \cdot \boldsymbol{\alpha}_2} (\mathbf{q} \cdot \boldsymbol{\alpha}_2) + O(\mathbf{q}^2) \\ &\simeq -\frac{t}{2}\mathbf{q} \cdot (\boldsymbol{\alpha}_1 + \boldsymbol{\alpha}_2) + i\frac{t\sqrt{3}}{2}\mathbf{q} \cdot (\boldsymbol{\alpha}_1 - \boldsymbol{\alpha}_2) + O(\mathbf{q}^2) \end{aligned} \quad (5.27)$$

Substituting in the hamiltonian (5.15) while setting $f_{\mathbf{q}} := q_x - iq_y + O(q^2)$ with $q_x = -\frac{t}{2}\mathbf{q} \cdot (\boldsymbol{\alpha}_2 + \boldsymbol{\alpha}_1)$ and $q_y = \frac{t\sqrt{3}}{2}\mathbf{q} \cdot (\boldsymbol{\alpha}_2 - \boldsymbol{\alpha}_1)$, we end up with

$$\mathbb{H}_{loc} = \begin{pmatrix} 0 & q_x - iq_y \\ q_x + iq_y & 0 \end{pmatrix} + O(\mathbf{q}^2) \quad (5.28)$$

where the leading linear term is the Dirac operator $\mathcal{D}_{\mathbf{q}}$.

6 Conclusion and discussion

In this study, we began by revisiting the so-called construction A of code CFTs realising Narain CFTs with an initial emphasis on the lattices $(\Lambda_{\mathbf{k}}^{1,1}, \Lambda_{\mathbf{k}C}^{1,1}, \Lambda_{\mathbf{k}}^{*1,1})$ sitting in $\mathbb{R}^{1,1}$ and then extended the analysis to their higher dimensional generalisations $(\Lambda_{\mathbf{k}}^{r,r}, \Lambda_{\mathbf{k}C}^{r,r}, \Lambda_{\mathbf{k}}^{*r,r})$. These lattices are characterised by the central charges of the 2D NCFT ($c_L = c_R = r$) and the CS level k of the 3D holographic dual. Then, in section 2, we showed that the lattice $\Lambda_{\mathbf{k}}^{1,1}$ and its dual $\Lambda_{\mathbf{k}}^{*1,1}$ as well as the even self dual $\Lambda_{\mathbf{k}C}^{1,1}$ exhibit remarkable properties; in particular the following:

- (1) They can be imagined via the nested structure:

$$\Lambda_{\mathbf{k}}^{\text{su}2} \subset \Lambda_{\mathbf{k}C}^{\text{su}2} \subset \Lambda_{\mathbf{k}}^{*\text{su}2} \subset \mathbb{R}^{1,1} \quad (6.1)$$

with components provided by fibrations of root-like $R_{\mathbf{k}}^{\text{su}2}$ and weight-like $W_{\mathbf{k}}^{\text{su}2}$ lattices of the $\text{su}(2)$ algebra, given explicitly by:

$$\Lambda_{\mathbf{k}}^{\text{su}2} = R_{\mathbf{k}}^{\text{su}2} \times R_{\mathbf{k}}^{\text{su}2}, \quad \Lambda_{\mathbf{k}C} = R_{\mathbf{k}}^{\text{su}2} \times W_{\mathbf{k}}^{\text{su}2}, \quad \Lambda_{\mathbf{k}}^* = W_{\mathbf{k}}^{\text{su}2} \times W_{\mathbf{k}}^{\text{su}2} \quad (6.2)$$

We refer to them as root-like and weight-like because only for $k=2$, the lattices coincide exactly with the standard root and weight lattices of $\text{su}(2)$. Generally speaking, $R_{\mathbf{k}}^{\text{su}2}$ consists of points of the form $\{n\tilde{\boldsymbol{\alpha}}, n \in \mathbb{Z}\}$ while $W_{\mathbf{k}}^{\text{su}2}$ is defined by $\{m\tilde{\boldsymbol{\lambda}}, m \in \mathbb{Z}\}$ with dilated root $\tilde{\boldsymbol{\alpha}}$ and compressed fundamental weight $\tilde{\boldsymbol{\lambda}}$ related to their standard counterparts $\boldsymbol{\alpha}$ and $\boldsymbol{\lambda}$ as

$$\tilde{\boldsymbol{\alpha}} = \sqrt{\frac{k}{2}}\boldsymbol{\alpha} \quad , \quad \tilde{\boldsymbol{\lambda}} = \sqrt{\frac{2}{k}}\boldsymbol{\lambda}$$

For physical applications, we interpreted the sites $\mathbf{x}_n \in R_{\mathbf{k}}^{\text{su}2}$ as hosts of Kaluza-Klein excitations $|KK_n\rangle$ and the sites $\mathbf{k}_m \in W_{\mathbf{k}}^{\text{su}2} \setminus R_{\mathbf{k}}^{\text{su}2}$ as carriers of winding modes $|W_n\rangle$. A detailed discussion of this description was given in section 5.

- (2) The one dimensional lattices $R_{\mathbf{k}} = \sqrt{k}\mathbb{Z}$ and $W_{\mathbf{k}} = \frac{1}{\sqrt{k}}\mathbb{Z}$ defined for a generic CS level k , exhibit several notable properties: First, for $k=1$, they coincide $R_1^{\text{su}2} = W_1^{\text{su}2}$.

In this case, the lattice is integral and self dual with generators obeying $\tilde{\alpha}^2 = \tilde{\lambda}^2 = 1$. Second, for $k=2$, $R_2^{\text{su}2} = \sqrt{2}\mathbb{Z}$ correspond to the root lattice of $SU(2)$ and $W_2^{\text{su}2} = \frac{1}{\sqrt{2}}\mathbb{Z}$ is its weight lattice. The former is even integer valued whereas the latter is half integer. Third, these discrete lattices $R_2^{\text{su}2}$ and $W_2^{\text{su}2}$ can be identified geometrically as the (anti)-diagonal 1D sublattices of the ambient $\mathbb{Z} \times \mathbb{Z}$ and the $\frac{1}{2}\mathbb{Z} \times \frac{1}{2}\mathbb{Z}$ square lattices respectively.

(3) A detailed inspection of these properties leads to the key identification: $R_k^{\text{su}2} = \sqrt{\frac{k}{2}}\mathbb{Z}\alpha$ and $W_k^{\text{su}2} = \sqrt{\frac{2}{k}}\mathbb{Z}\lambda$ where α and λ are the usual simple root and the fundamental weight λ vectors of $SU(2)$ which satisfy $\alpha^2 = 2$, $\lambda^2 = 1/2$ as well as $\alpha \cdot \lambda = 1$. For generic CS levels $k > 2$, the inner products scale like

$$\tilde{\alpha}^2 = k, \quad \tilde{\lambda}^2 = \frac{1}{k}, \quad \tilde{\alpha} \cdot \tilde{\lambda} = 1$$

From the above description, several important consequences follow:

- (i) there is an embedding hierarchy $R_k^{\text{su}2} \subseteq W_k^{\text{su}2}$ for all $k \geq 1$. The discriminant group $W_k^{\text{su}2}/R_k^{\text{su}2}$ is isomorphic to $\mathbb{Z}_k = \mathbb{Z}/(k\mathbb{Z})$, in agreement with the well known property regarding the group centre of $SU(2)$ implying $W_2^{\text{su}2}/R_2^{\text{su}2} \simeq \mathbb{Z}_2$.
- (ii) For $k > 2$, $W_k^{\text{su}2}$ can be decomposed as a union of k isomorphic sublattices $\{R_k^{\text{su}2} + \varepsilon\lambda\}$ labeled as

$$W_k^{\text{su}2} = R_k^{\text{su}2} + \varepsilon\lambda \quad , \quad \varepsilon = 0, \dots, k-1 \pmod{k} \quad (6.3)$$

- (iii) Given these $R_k^{\text{su}2}$ and $W_k^{\text{su}2}$, one can then build the triplet $\Lambda_k^{\text{su}2}, \Lambda_{k\mathcal{C}}^{\text{su}2}, \Lambda_k^{*\text{su}2}$ following the fibration prescription. For example, the even self dual lattice $\Lambda_{k\mathcal{C}}^{\text{su}2}$ is realised as the product $R_k^{\text{su}2} \times W_k^{\text{su}2}$. Vector sites $\mathbf{u}_{n,m} \in \Lambda_{k\mathcal{C}}^{\text{su}2}$ are labeled by two integers with components $n\tilde{\alpha} \oplus m\tilde{\lambda}$; its Euclidian pairing $\mathbf{u}_{n,m}^T \mathbf{u}_{n,m}$ is given by $kn^2 + \frac{1}{k}m^2$ while its Lorentzian product reads as follows

$$\mathbf{u}_{n,m}^T \boldsymbol{\eta} \mathbf{u}_{n,m} = 2nm \in 2\mathbb{Z} \quad (6.4)$$

The self duality feature of $\Lambda_{k\mathcal{C}}$ is captured by the unimodular property of the matrix $\tilde{A}_i^j \oplus \tilde{B}_i^j$ which is manifestly ensured by the duality relation $\tilde{\alpha} \cdot \tilde{\lambda} = 1$. For graphic illustrations of the discrete structures of the various lattices, see the Figures 2, 3, 4, 5 and 7.

Moreover, building on the $SU(2)$ results, we constructed new realisations of Narain CFTs

based on the root-like $R_k^{\text{su}_3}$ and the weight-like $W_k^{\text{su}_3}$ lattices. Several structural features established for $\text{su}(2)$ carry over naturally to the $\text{SU}(3)$ - based CFT. Particularly, for generic CS levels k , the inclusion $R_k^{\text{su}_3} \subset W_k^{\text{su}_3}$ holds and the discriminant $W_k^{\text{su}_3}/R_k^{\text{su}_3}$ group is isomorphic to \mathbb{Z}_k . As with $\text{SU}(2)$, the case of $k=3$, the symmetry \mathbb{Z}_3 emerging from the discriminant corresponds to the centre of $\text{SU}(3)$ generated by the 3-cycle $(1, 2, 3)$ acting on the fundamental 3D representations of $\text{SU}(3)$ as given by (5.13).

This $\text{SU}(3)$ based construction was initially developed for central charges $c_{L/R} = 2$ but it generalizes directly to $c_{L/R} = 2d$ by using higher dimensional self dual lattices $\Lambda_{kC}^{\text{su}_3(d,d)} \subset \mathbb{R}^{2d,2d}$ with nested structure as:

$$\Lambda_k^{\text{su}_3(d,d)} \subset \Lambda_{kC}^{\text{su}_3(d,d)} \subset \Lambda_k^{*\text{su}_3(d,d)} \subset \mathbb{R}^{2d,2d} \quad (6.5)$$

For $d=1$, the three lattices in the above sequence (6.5) correspond respectively to the fibrations $R_k^{\text{su}_3} \times R_k^{\text{su}_3}$ and $R_k^{\text{su}_3} \times W_k^{\text{su}_3}$ as well as $W_k^{\text{su}_3} \times W_k^{\text{su}_3}$. To illustrate this construction, we gave several explicit realisations as depicted by the Figures 9, 10, 11 and 20. The generalisation to $d>1$ follows straightforwardly.

After establishing this new framework in terms of algebraic data of code based Narain CFT, we exploited the new setting to develop a pathway towards topological phases of matter by linking Narain CFT to critical lattice QFT. We set out by describing the particle content of the model by studying the lattice fields excitations that manifest as KK and winding modes. We then proposed three guiding arguments based on: (i) the structure of the weight lattice, (ii) the duality with the root grid and the correspondence with the KK/winding system in addition to (iii) the possibility of fermionising the bosonic excitations to introduce a tight binding model with Dirac cones. By deriving the particle states populating the critical lattice points, we were thus able to capture key features of gapless topological systems akin to that of the Haldane theory of quantum anomalous Hall effect. This unlocked several promising research directions among which is the embedding of these lattice dualities into holographic ones with a one to one correspondence between the bulk duals. It will be interesting to investigate whether one can construct a bulk theory to the 2D lattice QFT describing the topological matter as a realisation of the AB Chern-Simons theory dual to the code based Narain CFT.

Appendices:

The following three appendices provide technical details omitted from the main text in order to alleviate and streamline the presentation. In appendix A, we give a review on the

link between code CFTs and Narain ensembles. In appendix B, we describe construction A of code Narain CFT with explicit realisations. In appendix C, we complete the analysis of section 3 by discussing the cases of $k > 3$ and $k < 3$.

A From code-CFT to Narain ensemble

In this appendix, we review the construction of two-dimensional Narain theories from the perspective of code-based CFTs. We begin by outlining the key elements of code-CFT constructions and establishing their correspondence with Narain CFTs through the associated partition functions. We then examine the sequence of lattices these constructions generate and revisit their interpretation.

A.1 Overview on code-CFT

Over the past decade, an increasing interest has been devoted to the connection between additive codes and a class of Narain conformal field theories (NCFT) with $U(1)^{c_L} \times U(1)^{c_R}$ where $c_L = c_R = r$ [4]-[16]. Starting from an even self dual code \mathcal{C} defined as a discrete set of codewords $\{C = (\mathbf{a}, \mathbf{b}) \in G_k^{r,r}\}$ subject to additional conditions to be specified later, one can build realisations of both the NCFT and its holographic dual given by the AB Chern-Simons (CS) theory with coupling constant $k \in \mathbb{N}^*$ (CS level) [21]. These constructions also allow to perform explicit calculations of generalised Narain partition functions using code based algorithms. The structure of the even self dual codes \mathcal{C} enables to build discrete sets $\Lambda_{k\mathcal{C}}^{r,r}$ sitting in $\mathbb{R}^{r,r}$ which in turn realise $2r$ dimensional Narain lattices Λ_{NARAIN} . For a given code \mathcal{C} over the abelian group $G_k^{r,r}$, with codewords satisfying the algebraic relations $c^T \eta C \in 2\mathbb{Z}$ and $c^T \eta C' \in \mathbb{Z}$ [22, 23], the associated even self dual lattice $\Lambda_{k\mathcal{C}}^{r,r}$ is imagined as embedded between a pair of lattices like $\Lambda_k^{r,r} \subset \Lambda_{k\mathcal{C}}^{r,r} \subset (\Lambda_k^{r,r})^*$. In this setting, the discrete group $G_k^{r,r}$ is identified with the discriminant $\Lambda_k^{r,r*} / \Lambda_k^{r,r}$ taken in this study to be $\mathbb{Z}_k^r \times \mathbb{Z}_k^r$. Moreover, one can represent the usual genus- one partition function of the NCFT namely [24, 68]-[71]

$$Z_{\text{NCFT}}[\tau, \xi, \zeta] = Tr[q^{L_0 - c_L/24} \bar{q}^{\bar{L}_0 - c_R/24} e^{2\pi i(\xi Q - \bar{\zeta} \bar{Q})}], \quad q = e^{2\pi i\tau} \quad (\text{A.1})$$

in term of Mac-Williams functionals $W_{\mathcal{C}}$ that are characteristic functions of coding theory with particular realisations as in the eq(A.2); see also [68] for other examples. In this representation of Z_{NCFT} , the above partition function has been found to exhibit intrinsic features amongst which we cite:

The Z_{NCFT} is generally labeled by a pair of integer vectors $(\mathbf{a}, \mathbf{b}) \in \mathbb{Z}_k^r \times \mathbb{Z}_k^r$ versus the familiar situation where it behaves as a scalar under the discrete group \mathbb{Z}_k as it

corresponds to the special value $k=1$ (for which $\{\mathbb{Z}_1 = I_{id}\}$) and roughly speaking to the neutral element $I_{id} \in \mathbb{Z}_k$. And as such, the above partition (A.1) should be imagined in general as a *matrix* function $(Z_{\text{NCFT}})_{\mathbf{a},\mathbf{b}}$ often denoted like $\Psi_{\mathbf{a},\mathbf{b}}$. This tensorial quantity has been found to describe wave functions in the holographic dual [69, 70] that capture interesting information. For instance, in the case $r=1$, the $\Psi_{a,b}$ indexed by $a, b = 0, \dots, k-1$ generate a Hilbert space with k^2 dimensions. For $k=1$, it reduces to the one dimensional $\Psi_{0,0}$ which is associated with the trivial code word $c=(0,0)$ and which describes the familiar torus partition function of Narain CFTs. The $\Psi_{\mathbf{a},\mathbf{b}}$ has been also found to describe multi-holomorphic wave functions $\Psi_{\mathbf{a},\mathbf{b}}(\tau, \xi_i, \tilde{\zeta}_i)$ where the complex variables $\xi_i, \tilde{\zeta}_i$ can be imagined in terms of boundary values of r gauge potential pairs $(\mathcal{A}_i, \mathcal{B}_i)_{1 \leq i \leq r}$ with action as in eq(B.1) describing the 3D holographic dual of the Narain theory [21, 71].

From the view of code theory, the Z_{NCFT} has been represented by the code enumerator polynomials $W_C(X)$ shown to play an important role in code CFTs. These polynomials have the typical structure [54]

$$W_C(X) = \sum_{(\mathbf{a},\mathbf{b}) \in \mathcal{C}} \prod_{i=1}^r X_{a_i, b_i} \sim \sum_{a_i, b_i \in \mathbb{Z}_k} X_{a_1, b_1} \dots X_{a_r, b_r} \quad (\text{A.2})$$

where $\mathbf{a} = (a_1, \dots, a_r)$ and $\mathbf{b} = (b_1, \dots, b_r)$ are integer vectors with components $a_i, b_i \in \mathbb{Z}_k$. The complex $X_{a,b} := X_{a,b}(\tau, \xi)$ are formal variables; they are functions of the complex parameter τ of the 2-torus and the fugacities $\xi_i, \tilde{\zeta}_i$. In NCFT, they are realised in terms of the generalized Siegel theta $\Theta_{a,b}^{r,r}$ and the Dedekind $\eta(\tau)$ functions like $\frac{1}{|\eta(\tau)|^{2r}} \Theta_{a,b}^{r,r}(\tau)$. For the conformal model with $c_{L/R} = r = 1$, these thetas have the structure $e^{i\pi\tau p_L^2 - i\pi\tilde{\tau} p_R^2}$ with quantized left/right momenta $p_{L/R}$ reading in terms of the codewords $c=(a,b)$, the Kaluza-Klein (KK) mode n and the winding integer m as follows

$$(p_{L/R})_{(a,n)}^{(b,m)} = \frac{1}{\sqrt{2k}} \left[\frac{1}{R\sqrt{2}}(a + kn) \pm R\sqrt{2}(b + km) \right] \quad (\text{A.3})$$

with $a, b \in \mathbb{Z}_k$ and $p_L^2 - p_R^2 \in 2\mathbb{Z}$. Here, the real number R is the radius of the Narain circle; it plays an important role in Ensemble averaging [17, 71, 72]; but in the present study it is fixed to (eg $R=1/\sqrt{2}$). For $n = m = 0$ and CS level $k=2$, there are several *ground* (un-excited) configurations with left/right momenta $(p_{L/R})_{a,b}$ given by $\frac{a}{2}\epsilon_x \pm \frac{b}{2}\epsilon_y$. As we will see throughout this study, these *fundamental* momenta define $2k^2$ ground states [k^2 for $p_{La,b}$ and k^2 for $p_{Ra,b}$] within the unit cell $\epsilon_x \times \epsilon_y$ of the rectangular lattice

$$(\epsilon_x \mathbb{Z}) \times (\epsilon_y \mathbb{Z}) \quad (\text{A.4})$$

with parameters $\epsilon_x = \frac{1}{R\sqrt{2}}$ and $\epsilon_y = R\sqrt{2}$. For $R = 1/\sqrt{2}$, this lattice reduces to the square lattice $\mathbb{Z} \times \mathbb{Z}$. Moreover, the usual modular symmetry of the Narain CFT translates into the invariance $W_C(X) = W_C(X')$ with X' referring to the two following transformations (translation and inversion of $\text{SL}(2, \mathbb{Z})$) [17, 21]

$$\begin{aligned} (i) & : X_{a,b}(\tau + 1) = e^{2\pi i ab/k} X_{a,b}(\tau) \\ (ii) & : X_{a,b}(-1/\tau) = X'_{a,b} = U_{ab}^{a'b'} X_{a',b'}(\tau) \end{aligned} \quad (\text{A.5})$$

where the phase $U_{ab}^{a'b'}$ is given by $e^{2\pi i(ab' + ba')/k}$.

A.2 Lattice sequence: $\Lambda_k^{r,r} \subset \Lambda_{k\mathcal{C}}^{r,r} \subset \Lambda_k^{*,r}$

As we revisit the so-called *construction A* of code-CFT (see also appendix B), focusing on the lattice suite $\Lambda_k^{r,r} \subset \Lambda_{k\mathcal{C}}^{r,r} \subset \Lambda_k^{*,r}$, in terms of the root and weight lattices of Lie algebras \mathfrak{g} , we then present new realisations of this construction, in which the discrete groups $G_k^{r,r}$ are interpreted in terms of the symmetries of unit cells of the real lattice $\Lambda_k^{r,r}$, its dual $\Lambda_k^{*,r}$ and the even self dual $\Lambda_{k\mathcal{C}}^{r,r}$. We begin by showing that the construction A of the $c_{L/R} = 1$ Narain theory has a natural interpretation in terms of the root $\mathbb{R}^{\text{su}_2} := \mathbb{R}_k^{\text{su}_2}|_{k=2}$ and the weight $\mathbb{W}^{\text{su}_2} = \mathbb{W}_k^{\text{su}_2}|_{k=2}$ lattices of $\text{SU}(2)$ and their fibrations as given by eq(A.6) valid for generic values of k (including the special value $k=2$). Recall that the group $\text{SU}(2)$ has rank $r=1$, and for $k=2$ the associated discriminant $\mathbb{W}^{\text{su}_2}/\mathbb{R}^{\text{su}_2}$ is isomorphic to \mathbb{Z}_2 . This discriminant shows that the unit cell of \mathbb{W}^{su_2} has two different types of sites (two colored sites) versus one site-type for \mathbb{R}^{su_2} as shown on the Figure 17. In this illustrative image, we used 4 types of colored sites (red, blue, green, black) to draw graphic representations of the particular $k=2$ suite $\Lambda_2^{1,1} \subset \Lambda_{2\mathcal{C}}^{1,1} \subset \Lambda_2^{*,1,1}$ where we used: (i) four colors for the bigger $\Lambda_2^{*,1,1} = \mathbb{W}_2^{\text{su}_2} \times \mathbb{W}_2^{\text{su}_2}$, (ii) two colors for $\Lambda_{2\mathcal{C}}^{1,1} = \mathbb{R}_2^{\text{su}_2} \times \mathbb{W}_2^{\text{su}_2}$; and (iii) one color for $\Lambda_2^{1,1} = \mathbb{R}_2^{\text{su}_2} \times \mathbb{W}_2^{\text{su}_2}$. For generic values of the CS level k , we need k^2 colored sites to draw graphs for the triplet in the suite $\Lambda_k^{1,1} \subset \Lambda_{k\mathcal{C}}^{1,1} \subset \Lambda_k^{1,1*}$ sitting in $\mathbb{R}^{1,1}$, they are remarkably realized by the fibrations

$$\begin{aligned} \Lambda_k^{1,1} &= \mathbb{R}_k^{\text{su}_2} \times \mathbb{R}_k^{\text{su}_2} & \Lambda_k^{\text{su}_2} &= \mathbb{R}_k^{\text{su}_2} \times \mathbb{R}_k^{\text{su}_2} \\ \Lambda_{k\mathcal{C}}^{1,1} &= \mathbb{R}_k^{\text{su}_2} \times \mathbb{W}_k^{\text{su}_2} & \Leftrightarrow & \Lambda_{k\mathcal{C}}^{\text{su}_2} &= \mathbb{R}_k^{\text{su}_2} \times \mathbb{W}_k^{\text{su}_2} \\ \Lambda_k^{*,1,1} &= \mathbb{W}_k^{\text{su}_2} \times \mathbb{W}_k^{\text{su}_2} & \Lambda_k^{*\text{su}_2} &= \mathbb{W}_k^{\text{su}_2} \times \mathbb{W}_k^{\text{su}_2} \end{aligned} \quad (\text{A.6})$$

In these fibrations, the $\mathbb{R}_k^{\text{su}_2}$ is isomorphic to the 1D lattice $\sqrt{k}\mathbb{Z}$ while the $\mathbb{W}_k^{\text{su}_2}$ is isomorphic to its dual $\frac{1}{\sqrt{k}}\mathbb{Z}$ with coset $\mathbb{W}_k^{\text{su}_2}/\mathbb{R}_k^{\text{su}_2} \simeq \mathbb{Z}_k$. From this discriminant, one can imagine $\mathbb{W}_k^{\text{su}_2}$ like the product $\mathbb{Z}_k \times \mathbb{R}_k^{\text{su}_2}$ letting understand that $\mathbb{W}_k^{\text{su}_2}$ is made of the superposition of k sublattices $\mathbb{R}_k^{\text{su}_2}$ distant by some weight vector as explicitly shown

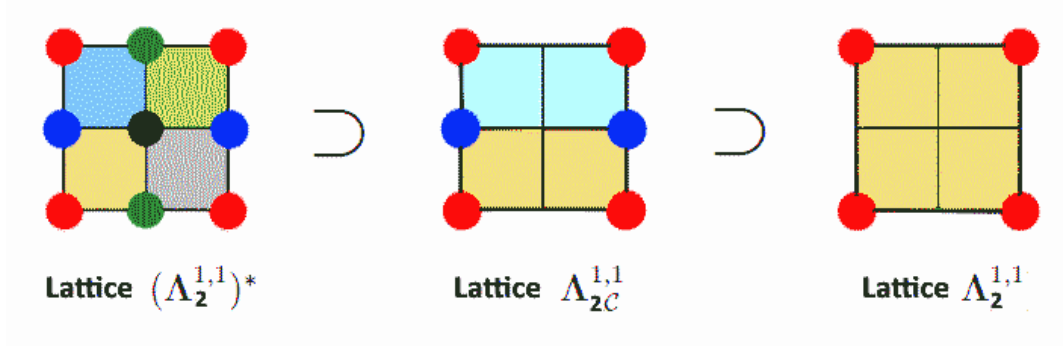


Figure 17: The unit cells of the 2D lattices of construction A of the $c_{L/R} = 1$ theory. Sites in these lattices are colored, the number of colors is variable: k^2 colors for $\Lambda_k^{1,1*}$, k colors for $\Lambda_{kC}^{1,1}$ and one color for $\Lambda_k^{1,1}$. The areas of the unit cells are exhibited in increasing order. On left, $\Lambda_2^{1,1*}$ with 4 unit cells. In middle, the $\Lambda_{2C}^{1,1}$ with 2 unit cells. On right, the unit cell of $\Lambda_2^{1,1}$.

in the core of paper (*sections 3 and 4*). Sites in the above lattices Λ describe quantum particle states $|\psi_{a,n}^{b,m}\rangle$ labeled, in addition to the indices (a,b) of the ground configurations, by Kaluza modes $|n\rangle$ and windings $|m\rangle$.

a) Constraints using unit cells

Notice that in the language of colored sites and unit cells, which for the 1D lattices $a_\rho\mathbb{Z}$ are given by the parameter a_ρ [below $uc(a_\rho\mathbb{Z}) := a_\rho$], a set of interesting features follow: First, we have the condition $ucW_k^{\text{su}_2} < ucR_k^{\text{su}_2}$ because the number of sites \mathbf{k}_m in $W_k^{\text{su}_2}$ is bigger than that those \mathbf{x}_n in $R_k^{\text{su}_2}$. Consequently the suite of the construction A gets mapped into the inequalities

$$uc\Lambda_k^{*\text{su}_2} < uc\Lambda_{kC}^{\text{su}_2} < uc\Lambda_k^{\text{su}_2} \quad (\text{A.7})$$

Second, by using the relations $ucW_k^{\text{su}_2} = \frac{1}{\sqrt{k}}$ and $ucR_k^{\text{su}_2} = \sqrt{k}$ and subsequently $ucR_k^{\text{su}_2} = k(ucW_k^{\text{su}_2})$, we end up with the characteristic properties $uc\Lambda_k^{*\text{su}_2} = \frac{1}{k}$ and $uc\Lambda_{kC}^{\text{su}_2} = 1$ as well as $uc\Lambda_k^{\text{su}_2} = k$. We also have the following result:

$$uc\Lambda_k^{\text{su}_2} = k(uc\Lambda_{kC}^{\text{su}_2}) = k^2(uc\Lambda_k^{*\text{su}_2}) \quad (\text{A.8})$$

Regarding new realisations of construction A of code CFT going beyond the SU(2) buildings briefly presented above, we extend the SU(2) realisation (A.6) to higher dimensional lattices of Lie algebras especially those symmetries with rank 2 such as SU(3), SO(5) and G2. Focussing on the interesting case of SU(3), we get for the 4D lattices involved

in the basis sequence $\Lambda_k^{\text{su}_3} \subset \Lambda_{k\mathbb{C}}^{\text{su}_3} \subset \Lambda_k^{*\text{su}_3}$ hosted by $\mathbb{R}^{2,2}$ the following representation

$$\begin{aligned} \Lambda_k^{\text{su}_3} &= R_k^{\text{su}_3} \times R_k^{\text{su}_3} \\ \Lambda_{k\mathbb{C}}^{\text{su}_3} &= R_k^{\text{su}_3} \times W_k^{\text{su}_3} \quad , \quad uc\Lambda_k^{*\text{su}_3} < uc\Lambda_{k\mathbb{C}}^{\text{su}_3} < uc\Lambda_k^{\text{su}_3} \\ \Lambda_k^{*\text{su}_3} &= W_k^{\text{su}_3} \times W_k^{\text{su}_3} \end{aligned} \quad (\text{A.9})$$

where for $k=3$, the 2D discrete sets $R_k^{\text{su}_3}$ and $W_k^{\text{su}_3}$ sitting in \mathbb{R}^2 are nothing but the root and the weight lattices of $\text{SU}(3)$. For this generalisation, we distinguish three cases according to the values of the Chern-Simons level k of the holographic dual of the Narain CFT.

b) Three sectors

These cases concern the following intervals:

- (i) **Case $k=3$:** this is the canonical CS level for which the discriminant group is equal to $\mathbb{Z}_3 \times \mathbb{Z}_3$. Here, the abelian set \mathbb{Z}_3 is just the group centre of $\text{SU}(3)$. For this value, we find that the 4D lattice $\Lambda_3^{\text{su}_3}$ is made of the fibration of two hexagonal lattices like $R_3^{\text{su}_3} \times R_3^{\text{su}_3}$ while the dual $\Lambda_3^{*\text{su}_3}$ is constructed out of the fibration of two triangular lattices as $W_3^{\text{su}_3} \times W_3^{\text{su}_3}$. The areas of the unit cells of these lattices are depicted by the Figure 18 in yellow color where for convenience we have also exhibited the triangulation of the underlying surfaces. In this Figure, we have

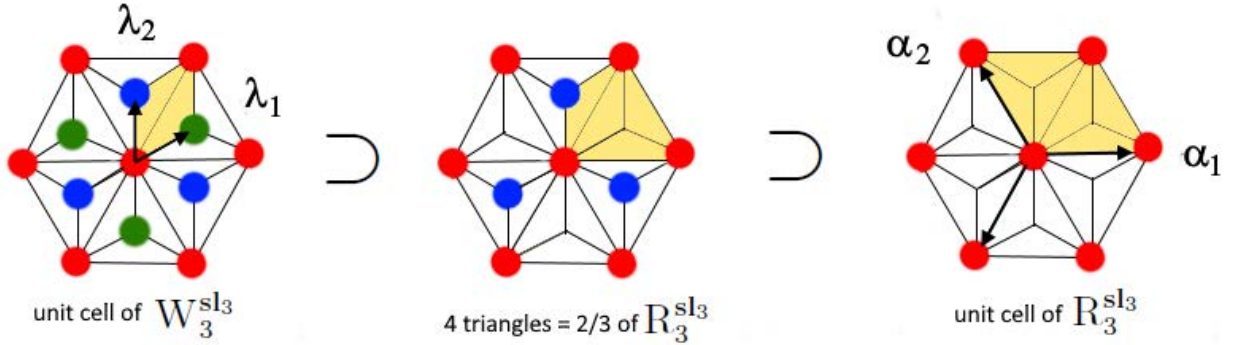


Figure 18: The areas of unit cells of the weight $W_3^{\text{sl}_3}$ and the root $R_3^{\text{sl}_3}$ lattices of $\text{SU}(3)$. The unit cell of $R_3^{\text{sl}_3}$ is three times the unit cell of $W_3^{\text{sl}_3}$. In the middle we also give the configuration with 2 times $ucW_3^{\text{sl}_3}$.

used three different colors (red, blue, green) to distinguish the three superposed sublattices $\mathbb{A} + \mathbb{B} + \mathbb{C}$ making $W_3^{\text{su}_3}$ with red color for sublattice \mathbb{A} ; blue color for \mathbb{B} and green color for \mathbb{C} . The unit cells of $W_3^{\text{su}_3}$ and $R_3^{\text{su}_3}$ in the Figure 18 are

respectively given by

$$\begin{aligned} ucR_3^{\text{su}_3} &= \sqrt{3} & \Rightarrow & & uc\Lambda_3^{\text{su}_3} &= 3 \\ ucW_3^{\text{su}_3} &= \frac{1}{\sqrt{3}} & & & uc\Lambda_3^{*\text{su}_3} &= \frac{1}{3} \end{aligned} \quad (\text{A.10})$$

showing that $ucR_3^{\text{su}_3} = 3 \times ucW_3^{\text{su}_3}$ and then $uc\Lambda_3^{\text{su}_3} = 9 \times uc\Lambda_3^{*\text{su}_3}$. In these relations the λ_i 's are the two fundamental weight vectors of $SU(3)$ with angle $(\widehat{\lambda_1, \lambda_2}) = \frac{2\pi}{6}$ and the α_i 's are the associated simple roots with $(\widehat{\alpha_1, \alpha_2}) = \frac{2\pi}{3}$. In the Figure 18, the representative graphs have 18 fundamental elementary triangles forming 9 unit cells of $W_3^{\text{su}_3}$ ($18 = 2 \times 9$) and 3 unit cells of $R_3^{\text{su}_3}$ ($18 = 6 \times 3$).

- (ii) **Case $k > 3$:** the results obtained for $k=3$ extends also to $k > 3$ for which we have the discriminants $W_k^{\text{su}_3}/R_k^{\text{su}_3} \simeq \mathbb{Z}_k$ and $\Lambda_k^{*\text{su}_3}/\Lambda_k^{\text{su}_3} \simeq \mathbb{Z}_k \times \mathbb{Z}_k$. For instance, the group \mathbb{Z}_k indicates that $W_k^{\text{su}_3}$ is made of the superposition of k sublattices

$$\mathbb{A}_0 \cup \mathbb{A}_1 \cup \dots \cup \mathbb{A}_{k-2} \cup \mathbb{A}_{k-1} \quad (\text{A.11})$$

each one of them is isomorphic to $R_k^{\text{su}_3}$ but distant by the weight vectors $\varepsilon \boldsymbol{\lambda}$ with $\varepsilon = 0, \dots, k-1$. We also have the following relationships between the values of the areas of the unit cells of the real $R_k^{\text{su}_3}$ and the dual $W_k^{\text{su}_3}$ lattices namely

$$ucR_k^{\text{su}_3} = \frac{k^2}{3} \times ucW_k^{\text{su}_3} \quad \Rightarrow \quad uc\Lambda_k^{\text{su}_3} = \frac{k^4}{9} \times uc\Lambda_k^{*\text{su}_3} \quad (\text{A.12})$$

They can be checked by using the results

$$\begin{aligned} ucR_k^{\text{su}_3} &= \frac{k}{\sqrt{3}} & \Rightarrow & & uc\Lambda_3^{\text{su}_3} &= \frac{k^2}{3} \\ ucW_k^{\text{su}_3} &= \frac{\sqrt{3}}{k} & & & uc\Lambda_3^{*\text{su}_3} &= \frac{3}{k^2} \end{aligned} \quad (\text{A.13})$$

from which we also learn $uc\Lambda_{3C}^{\text{su}_3} = 1$ independently of the value of the CS level.

- (iii) **Case $k < 3$:** for those integer values of the CS level k less than 3, we distinguish two possibilities namely $k = 1, 2$. While the CS level $k=1$ is somehow "exotic" because the condition $ucW_1^{\text{su}_3} < ucR_1^{\text{su}_3}$ is violated since $ucW_1^{\text{su}_3} = \sqrt{3}$ while $ucR_1^{\text{su}_3} = 1/\sqrt{3}$. This condition holds only for $k \geq \sqrt{3}$ coming from solving $\frac{\sqrt{3}}{k} < \frac{k}{\sqrt{3}}$. This bound rules out $k=1$ but includes $k=2$ for which the weight lattice $W_2^{\text{su}_3}$ is given by the 2D honeycomb while the $R_2^{\text{su}_3}$ is an hexagonal lattice. For illustration, see the pictures depicted by the Figure 19. For this CS level, the discriminant $W_2^{\text{su}_3}/R_2^{\text{su}_3}$ is equal to \mathbb{Z}_2 indicating in turn that $W_2^{\text{su}_3}$ is made of the superposition $\mathbb{A} + \mathbb{B}$ of two isomorphic sublattices (red and blue in the Figure 19) distant by a weight vector. The areas of the unit cell $ucR_2^{\text{su}_3}$ is equal to $\frac{4}{3}$ times $ucW_k^{\text{su}_3}$.

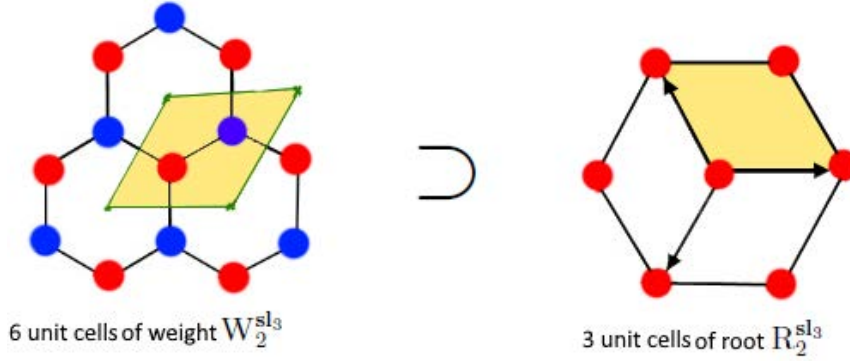


Figure 19: Unit cells of weight $W_2^{\text{sl}_3}$ (honeycomb) and root $R_2^{\text{sl}_3}$ (hexagonal) lattices. $W_2^{\text{sl}_3}$ is given by the superposition of two isomorphic sublattices (red and blue)

B Construction A of code Narain CFT

Following [17, 21], the construction A of code based NCFT establishes a correspondence between algebraic coding theory on the finite abelian group $G_k^{r,r} \sim \mathbb{Z}_k^r \times \mathbb{Z}_k^r$ and CFTs defined on toroidal backgrounds. This framework provides a systematic method to build Narain CFTs, describing strings on torii, by using code theory based on the Mac-Williams functional $W_{\mathcal{C}}(X)$ [18, 19]. The structure of linear codes $\mathcal{C} \subset G_k^{r,r}$ determine the fundamental features of the associated NCFTs. In the holographic dual of these NCFTs [20], the positive integer k corresponds to the Chern-Simons (CS) level of the so-called AB theory which consists of two gauge blocks of abelian potentials $\mathcal{A} := \sum_{i=1}^r \mathcal{A}^i Q_i$ and $\mathcal{B} := \sum_{i=1}^r \mathcal{B}_i \tilde{Q}^i$ valued in $[U(1)_A \times U(1)_B]^r$ and coupled as follows

$$\mathcal{S}_{\text{CS}} + \mathcal{S}_{\text{BND}} = \frac{ik}{4\pi} \int_{\mathcal{M}} \text{Tr}(\mathcal{A} \wedge d\mathcal{B} + \mathcal{B} \wedge d\mathcal{A}) + \int_{\partial\mathcal{M}} \text{Tr}(\mathcal{A}_z \mathcal{A}_{\bar{z}} + \mathcal{B}_z \mathcal{B}_{\bar{z}}) \quad (\text{B.1})$$

with trace relations as $\text{Tr}(Q_i \tilde{Q}^j) = \delta_i^j$ and $\text{Tr}(Q_i Q_j) = K_{ij}$ as well as $\text{Tr}(\tilde{Q}^i \tilde{Q}^j) = \tilde{K}^{ij}$. In the eq(B.1), \mathcal{M} is generally a 3D handlebody (e.g. a solid torus) with boundary $\partial\mathcal{M}$ given by a Riemann surface Σ_g such as the 2-torus for genus $g = 1$. For the leading value of the integral central charge $c_{L/R} = 1$, corresponding to the model $r=1$, the code-CFT constructed over $G_k^{1,1} := G_k$ maps codes \mathcal{C} into even self dual lattices $\Lambda_{k\mathcal{C}}^{1,1}$ constrained like

$$\Lambda_k^{1,1} \subset \Lambda_{k\mathcal{C}}^{1,1} \subset \Lambda_k^{*,1,1} \subset \mathbb{R}^{1,1} \quad (\text{B.2})$$

In this hierarchy, the discrete set $\Lambda_k^{1,1} := \Lambda$ is a 2D even integral lattice embedded in the Lorentzian plane $\mathbb{R}^{1,1}$ endowed with the metric:

$$\eta = \begin{pmatrix} 0 & 1 \\ 1 & 0 \end{pmatrix} \quad \leftrightarrow \quad \eta_{ij} \equiv \begin{pmatrix} 0_{AA} & 1_{AB} \\ 1_{BA} & 0_{BB} \end{pmatrix} \quad (\text{B.3})$$

and scalar product $\langle \mathbf{v}, \mathbf{v} \rangle_\eta = \mathbf{v}^T \eta \mathbf{v}$ evaluating to $2v_1 v_2$. The metric η couples the two gauge sectors \mathcal{A} and \mathcal{B} in eq(B.1). The dual lattice Λ^* is defined as the set

$$\Lambda^* = \{ \mathbf{w} \mid \mathbf{v}^T \eta \mathbf{w} \in \mathbb{Z}, \forall \mathbf{v} \in \Lambda \} \quad (\text{B.4})$$

where $\Lambda = \{ \mathbf{v} \mid \mathbf{v}^T \eta \mathbf{v} \in 2\mathbb{Z} \}$ is an even integer lattice satisfying the usual inclusion property $\Lambda \subset \Lambda^*$. The intermediate lattice Λ_C is both even and self dual, that is $\Lambda_C \sim \Lambda_C^*$, and is nested between Λ and Λ^* ; see Figure 17 for illustration.

B.1 An explicit realisation

Here, we give an explicit realisation of the triplet $(\Lambda, \Lambda_C, \Lambda^*)$ which has been exploited in our analysis, sections 2 & 3, where it has been given a natural interpretation in terms of the root and the weight lattices of SU(2) and SU(3). To gain further insight into the embedding chain $\Lambda \subset \Lambda_C \subset \Lambda^*$, we start by describing the sites \mathbf{v} populating the abelian lattice Λ . They are represented by discrete 2D vectors $\mathbf{v}_\mathbf{n} = v_\mathbf{n}^i \mathbf{e}_i$ labeled by: (i) the integer vector $\mathbf{n} = (n_1, n_2)$ parameterising the square lattice $\mathbb{Z} \times \mathbb{Z}$ with unit spacing $\mathbf{a}=1$; in addition to (ii) the usual canonical basis vectors $\mathbf{e}_1 = (\mathbf{a}, 0)$ and $\mathbf{e}_2 = (0, \mathbf{a})$ with Euclidian $\mathbf{e}_1 \cdot \mathbf{e}_2 = 0$ but Lorentzian $\mathbf{e}_1 \eta \mathbf{e}_2 = \mathbf{a}^2 = 1$. For convenience, we express the vector $\mathbf{v}_\mathbf{n}$ as a linear combination of the integer vector \mathbf{n} like

$$v_\mathbf{n}^i = \sum_{j=1}^2 \Lambda_j^i n^j \quad , \quad \Lambda_j^i = \frac{\partial v_\mathbf{n}^i}{\partial n^j} \quad , \quad \Lambda := \begin{pmatrix} a & b \\ c & d \end{pmatrix} \quad (\text{B.5})$$

where Λ_j^i is a characteristic matrix of the real lattice Λ , acting as a linear map between \mathbb{Z}^2 and Λ with $\det \Lambda_{ij} \neq 0$ (i.e: $\Lambda_{ij} : \mathbf{n} \in \mathbb{Z}^2 \rightarrow \mathbf{v}_\mathbf{n} \in \Lambda$). For any lattice vector $\mathbf{v}_\mathbf{n} \in \Lambda$, the Lorentzian scalar product $\mathbf{v}_\mathbf{n}^T \eta \mathbf{v}_\mathbf{n}$ must be an even integer (i.e. belonging to $2\mathbb{Z}$) thus imposing a strong constraint on the form of the generating matrix Λ_j^i . Indeed, substituting $\mathbf{v}_\mathbf{n} = \Lambda \cdot \mathbf{n}$ into the Lorentzian scalar yields the conditions

$$\mathbf{n}^T (g_\Lambda) \mathbf{n} \in 2\mathbb{Z} \quad \text{with} \quad g_\Lambda = \Lambda^T \eta \Lambda \quad (\text{B.6})$$

where (i) the induced metric g_Λ is a quadratic function of Λ , with (ii) diagonal entries taking even integer values

$$g_\Lambda = \begin{pmatrix} 2m & l \\ l & 2n \end{pmatrix}, \quad m, n, l \in \mathbb{Z} \quad (\text{B.7})$$

this implies that $\det g_\Lambda = -\det \Lambda^2$. Additionally, the characteristic matrix Λ is not unique; it is defined up to $\mathcal{O}(1,1, \mathbb{R})$ orthogonal transformations namely $\Lambda' = \mathcal{O} \Lambda$ with

$\mathcal{O}^T \eta \mathcal{O} = \eta$. A simple example of such transformation is given by $\mathcal{O} = \eta$ leading to $\Lambda' = \eta \Lambda$. Moreover, using (B.5), we obtain the relations $ac = m$, $bd = n$ and $ad + bc = l$ along with the identity $4mn - l^2 = -(ad - bc)^2$ that factorises like

$$\det g_\Lambda = \left(m + n + \sqrt{l^2 + (m - n)^2} \right) \left(m + n - \sqrt{l^2 + (m - n)^2} \right) \quad (\text{B.8})$$

In what follows, we exhibit the dependence on the CS level k by labeling the above 2D lattice triplet like $(\Lambda_k, \Lambda_{k\mathcal{C}}, \Lambda_k^*)$ with (prime) integer $k \geq 2$. These lattices can be realised in terms of scaled cubic lattices with spacings $a = \sqrt{k}$ and $a_* = \frac{1}{\sqrt{k}}$ as follows

$$\begin{aligned} \Lambda_k &\sim \sqrt{k} \mathbb{Z} \times \sqrt{k} \mathbb{Z} \\ \Lambda_k^* &\sim \frac{1}{\sqrt{k}} \mathbb{Z} \times \frac{1}{\sqrt{k}} \mathbb{Z} \\ \Lambda_{k\mathcal{C}} &\sim \sqrt{k} \mathbb{Z} \times \frac{1}{\sqrt{k}} \mathbb{Z} \end{aligned} \quad (\text{B.9})$$

Formally, the intermediate lattice $\Lambda_{k\mathcal{C}}$ may be imagined as the product $\mathbf{R}_k \times \mathbf{W}_k^*$ where \mathbf{R}_k and \mathbf{W}_k correspond, respectively, to the root and weight lattices as defined in section 2. The realisation (9) satisfies the following features: (1) each site $v_{\mathbf{n}}^i$ generating the real lattice Λ_k can be written as $\sqrt{k} X_j^i n^j$ with invertible

$$\Lambda_j^i = \sqrt{k} X_j^i \quad (\text{B.10})$$

and induced $g_\Lambda = k X^T \eta X$ which must have the typical form (B.7). A particular solution for X is given by the identity matrix $X = I_{2 \times 2}$. For this special solution, the induced metric becomes $g_\Lambda = k\eta$ which corresponds to setting $m = n = 0$ and $l = k$ in (B.7). Substituting into the product $\mathbf{v}_{\mathbf{n}}^T \eta \mathbf{v}_{\mathbf{n}}$, we obtain $n^i (g_\Lambda)_{ij} n^j = 2kn^1 n^2$ which is indeed an even integer. (2) The sites $\mathbf{w}_{\mathbf{m}}$ in the dual Λ_k^* have components $w_{\mathbf{m}}^i = \frac{1}{\sqrt{k}} Y_j^i m^j$ with

$$(\Lambda^*)^i_j = \frac{1}{\sqrt{k}} Y_j^i \quad (\text{B.11})$$

Inserting this into the form $\mathbf{v}_{\mathbf{n}}^T \eta \mathbf{w}_{\mathbf{m}}$, while requiring the duality constraint, we end up with the condition $X^T \eta Y = n \in \mathbb{Z}$; this is easily satisfied by choosing $Y = (X^T \eta)^{-1} = \eta$. Therefore, for the particular solution $X = I_{2 \times 2}$ and $Y = \eta$, we have the characteristic matrices (Λ, Λ^*) and the associated induced metrics $(g_\Lambda, g_{\Lambda^*})$ explicitly given by

$$\begin{aligned} \Lambda &= \sqrt{k} I_{2 \times 2} & \Lambda^* &= \frac{1}{\sqrt{k}} \eta \\ g_\Lambda &= k\eta & g_{\Lambda^*} &= \frac{1}{k} \eta \end{aligned} \quad (\text{B.12})$$

with determinants $\det \Lambda = k$, $\det \Lambda^* = -\frac{1}{k}$ and $\det g_\Lambda = -k^2$ as well as $\det g_{\Lambda^*} = -\frac{1}{k^2}$. For this specific solution, one notes that $\Lambda^{-1} = \eta \Lambda^*$ highlighting the fact that Λ^* is

closely related to the inverse Λ^{-1} . Based on these results, we deduce the explicit forms of the intermediate lattice $\Lambda_{k\mathcal{C}}$, its dual $\Lambda_{k\mathcal{C}}^* \sim \Lambda_{k\mathcal{C}}$ and the corresponding induced metrics $g_{\Lambda_{k\mathcal{C}}}$ and $g_{\Lambda_{k\mathcal{C}}^*}$ as follows

$$\Lambda_{k\mathcal{C}} = \begin{pmatrix} \sqrt{k} & 0 \\ 0 & \frac{1}{\sqrt{k}} \end{pmatrix}, \quad \Lambda_{k\mathcal{C}}^* = \begin{pmatrix} 0 & \sqrt{k} \\ \frac{1}{\sqrt{k}} & 0 \end{pmatrix}, \quad g_{\Lambda_{k\mathcal{C}}} = \begin{pmatrix} 0 & 1 \\ 1 & 0 \end{pmatrix} \quad (\text{B.13})$$

They verify the property $\Lambda_{k\mathcal{C}} \eta \Lambda_{k\mathcal{C}}^* = I_{2 \times 2}$ and are unimodular in the sense that $\det \Lambda_{k\mathcal{C}} = 1$, $\det \Lambda_{k\mathcal{C}}^* = -1$ and $\det g_{\Lambda_{k\mathcal{C}}} = -1$. This unimodularity captures the self duality property of the intermediate lattice $\Lambda_{k\mathcal{C}}$.

B.2 Higher dimensions

Using the results obtained for the case $r=1$, the construction A for code-CFTs with higher central charges $c_{L/R} = r \geq 2$ extends straightforwardly by the help of tensor sums and products. In this generalisation, the codes \mathcal{C} are embedded in the abelian group $\mathbb{Z}_k^r \times \mathbb{Z}_k^r$ and are associated with a $2r$ dimensional lattice $\Lambda_{k\mathcal{C}}^{r,r}$ constrained as follows

$$\underbrace{\Lambda_k^{1,1} \oplus \dots \oplus \Lambda_k^{1,1}}_{r \text{ times}} \subset \Lambda_{k\mathcal{C}}^{r,r} \subset \underbrace{\Lambda_k^{*,1,1} \oplus \dots \oplus \Lambda_k^{*,1,1}}_{r \text{ times}} \subset \mathbb{R}^{r,r} \quad (\text{B.14})$$

When the codes \mathcal{C} satisfy additional constraints, namely evenness and self duality conditions, the associated lattices $\Lambda_{k\mathcal{C}}^{r,r}$ are in turn even and self dual, thus defining a Narain theory with central charge r . For the particular solution introduced earlier, the relevant matrices take the form

$$\Lambda_{k\mathcal{C}}^{r,r} = \begin{pmatrix} \sqrt{k} I_r & 0 \\ 0 & \frac{1}{\sqrt{k}} I_r \end{pmatrix}, \quad \Lambda_{k\mathcal{C}}^{*,r,r} = \begin{pmatrix} 0 & \sqrt{k} I_r \\ \frac{1}{\sqrt{k}} I_r & 0 \end{pmatrix}, \quad g_{\Lambda_{k\mathcal{C}}}^{r,r} = \begin{pmatrix} 0 & I_r \\ I_r & 0 \end{pmatrix} \quad (\text{B.15})$$

with I_r referring to the $r \times r$ identity matrix. These matrices satisfy $\Lambda_{k\mathcal{C}}^{r,r} \eta \Lambda_{k\mathcal{C}}^{*,r,r} = I_{2r,2r}$, $\det \Lambda_{k\mathcal{C}}^{r,r} = 1$ as well as $\det \Lambda_{k\mathcal{C}}^{*,r,r} = (-)^r$.

C Lattices Λ^{su_3} , $\Lambda_{\mathcal{C}}^{\text{su}_3}$, $\Lambda^{*\text{su}_3}$ for $k < 3$ and $k > 3$

In this appendix, we complete the study of section 3 by giving realisations of the triplet $(\Lambda^{\text{su}_3}, \Lambda_{\mathcal{C}}^{\text{su}_3}, \Lambda^{*\text{su}_3})$ for values of the CS level k distinct than $k=3$. Particularly, we construct models with $k > 3$ and then discuss cases having $k < 3$.

C.1 Lattice triplet for $k > 3$

The extension of the root $R_3^{\text{su}_3}$ and the weight $W_3^{\text{su}_3}$ towards $R_k^{\text{su}_3}$ and $W_k^{\text{su}_3}$ are constructed using dilated roots as $\tilde{\alpha}_i = \sqrt{\frac{k}{3}}\alpha_i$ and compressed weight vectors $\tilde{\lambda}_i = \sqrt{\frac{3}{k}}\lambda_i$, leading to

$$\begin{aligned} R_k^{\text{su}_3} &= \mathbb{Z}\tilde{\alpha}_1 \oplus \mathbb{Z}\tilde{\alpha}_2 & L_{ij} &:= \tilde{\alpha}_i \cdot \tilde{\alpha}_j \\ W_k^{\text{su}_3} &= \mathbb{Z}\tilde{\lambda}_1 \oplus \mathbb{Z}\tilde{\lambda}_2 & \tilde{L}^{ij} &:= \tilde{\lambda}^i \cdot \tilde{\lambda}^j \end{aligned} \quad (\text{C.1})$$

with intersections $L_{ij} = \frac{k}{3}K_{ij}$ and $\tilde{L}^{ij} = \frac{3}{k}\tilde{K}^{ij}$ as well as $\tilde{\alpha}_i \cdot \tilde{\lambda}^j = \delta_i^j$. These scaled vectors can be solved as $\tilde{\lambda}_1 = \frac{1}{k}(2\tilde{\alpha}_1 + \tilde{\alpha}_2)$ and $\tilde{\lambda}_2 = \frac{1}{k}(\tilde{\alpha}_1 + 2\tilde{\alpha}_2)$ as well as $\tilde{\lambda}_1 + \tilde{\lambda}_2 = \frac{3}{k}(\tilde{\alpha}_1 + \tilde{\alpha}_2)$. This realisation yields the two matrices A_k and B_k that read as follows

$$(A_k)_j^i = \sqrt{\frac{k}{3}} \begin{pmatrix} \sqrt{2} & -\frac{\sqrt{2}}{2} \\ 0 & \frac{\sqrt{6}}{2} \end{pmatrix}, \quad (B_k)_i^j = \sqrt{\frac{3}{k}} \begin{pmatrix} \frac{\sqrt{2}}{2} & \frac{\sqrt{6}}{6} \\ 0 & \frac{\sqrt{6}}{3} \end{pmatrix} \quad (\text{C.2})$$

with $\det A_k = \frac{k}{\sqrt{3}}$ and $\det B_k = \frac{\sqrt{3}}{k}$. We then have

$$\Lambda_k^{\text{su}_3} = \begin{pmatrix} A_k & 0 \\ 0 & A_k \end{pmatrix}, \quad \Lambda_k^{\text{su}_3^*} = \begin{pmatrix} B_k & 0 \\ 0 & B_k \end{pmatrix}, \quad \Lambda_{k\mathcal{C}}^{\text{su}_3} = \begin{pmatrix} A_k & 0 \\ 0 & B_k \end{pmatrix} \quad (\text{C.3})$$

Site vectors \mathbf{x}_n in $R_k^{\text{su}_3}$ are given by the expansion $\sum n^i \tilde{\alpha}_i$ while the grid vectors \mathbf{k}_m in $W_k^{\text{su}_3}$ develop like $\sum m_i \tilde{\lambda}^i$. By substituting the $\tilde{\lambda}^i$'s in terms of the $\tilde{\alpha}_i$'s, we get

$$\mathbf{k}_m = \frac{1}{k}(2m_1 + m_2)\tilde{\alpha}_1 + \frac{1}{k}(m_1 + 2m_2)\tilde{\alpha}_2 \quad (\text{C.4})$$

Defining $2m_1 + m_2 = kp + \xi$ and $m_1 + 2m_2 = kq + \zeta$ with p, q arbitrary integers and $\xi, \zeta = 0, \dots, k-1, \text{ mod } k$ gives the vector \mathbf{k}_m as follows

$$\begin{aligned} \mathbf{k}_m &= \mathbf{k}_m^0 + \frac{1}{3}(2\xi - \zeta)\tilde{\lambda}_1 + \frac{1}{3}(2\zeta - \xi)\tilde{\lambda}_2 \\ \mathbf{k}_m^0 &= p\tilde{\alpha}_1 + q\tilde{\alpha}_2 \end{aligned} \quad (\text{C.5})$$

By choosing $\zeta = 2\xi$ and $\xi = \varepsilon$ with $\varepsilon = 0, \dots, k-1, \text{ mod } k$, we get

$$\mathbf{k}_m(\varepsilon) = \mathbf{k}_m^0 + \varepsilon\tilde{\lambda}_2, \quad \varepsilon = 0, \dots, k-1 \quad (\text{C.6})$$

This shows that $W_k^{\text{su}_3}$ consists of k superposed sheets (k equivalent classes) given by the values of ε . These sheets can be presented in a compact form by using the spectral parameter ε as follows

$2m_1 + m_2$	$m_1 + 2m_2$	sites \mathbf{k}_m^0	sites \mathbf{k}_m	weight lattice $W_k^{\text{su}_3}$
$kp + \varepsilon$	$kq + 2\varepsilon$	$p\tilde{\alpha}_1 + q\tilde{\alpha}_2$	$\mathbf{k}_m^0 + \varepsilon\tilde{\lambda}_2$	$R_k^{\text{su}_3}[\varepsilon] = R_k^{\text{su}_3} + \varepsilon\tilde{\lambda}_2$

(C.7)

Similarly to the previous case, $W_k^{\text{su}_3}$ can be imagined as the superposition of k sheets of 2D sublattices like

$$W_k^{\text{su}_3} = R_k^{\text{su}_3} \cup \{R_k^{\text{su}_3} + \lambda_2\} \cup \dots \cup \{R_k^{\text{su}_3} + (k-1)\lambda_2\} \quad (\text{C.8})$$

Where each sheet is isomorphic to the hexagonal $R_k^{\text{su}_3}$ generated by $\tilde{\alpha}_i$ with $(\tilde{\alpha}_1, \tilde{\alpha}_2) = 2\pi/3$. For the CS levels $k > 3$, the discriminant $W_k^{\text{su}_3}/R_k^{\text{su}_3}$ is isomorphic to the abelian group \mathbb{Z}_k generated by the cyclic permutation $(1, 2, \dots, k)$ modulo k .

C.2 Lattice triplet for $k < 3$

An intriguing case arises when considering CS levels $k < 3$, particularly for $k = 1$ and $k = 2$. Recall that for generic k , the scaled root and weight lattice generators $\tilde{\alpha}_i$ and $\tilde{\lambda}^i$ obey the relations: $\tilde{\alpha}_i \cdot \tilde{\alpha}_j = \frac{k}{3} K_{ij}$ and $\tilde{\lambda}^i \cdot \tilde{\lambda}^j = \frac{3}{k} \tilde{K}^{ij}$ as well as $\tilde{\alpha}_i \cdot \tilde{\lambda}^j = \delta_i^j$. These imply the squared lengths $\tilde{\alpha}_i^2 = \frac{2k}{3}$ and $\tilde{\lambda}_i^2 = \frac{2}{k}$ that lead to the ratios $\tilde{\alpha}_i^2/\tilde{\lambda}_i^2$ that exceed one only for $k \geq \sqrt{3}$ as illustrated in the table below:

k	$\tilde{\alpha}_i^2$	$\tilde{\lambda}_i^2$	$\tilde{\alpha}_i^2/\tilde{\lambda}_i^2$
1	$\frac{2}{3}$	2	$\frac{1}{3} < 1$
$\frac{3}{2}$	1	$\frac{4}{3}$	$\frac{3}{4} < 1$
2	$\frac{4}{3}$	1	$\frac{4}{3} > 1$
3	2	$\frac{2}{3}$	$\frac{16}{9} > 1$

(C.9)

a) Cases $k=1$ and $k=\sqrt{3}$

Using the relations (3.15) and (C.8), the matrices A_k and B_k for $k=1$ and $k=\sqrt{3}$ read like⁶

$$\begin{aligned} A_1 &= \sqrt{\frac{2}{3}} \begin{pmatrix} 1 & -\frac{1}{2} \\ 0 & \frac{\sqrt{3}}{2} \end{pmatrix}, & A_{\sqrt{3}} &= \frac{\sqrt{2}}{3^{1/4}} \begin{pmatrix} 1 & -\frac{1}{2} \\ 0 & \frac{\sqrt{3}}{2} \end{pmatrix} \\ B_1 &= \sqrt{\frac{3}{2}} \begin{pmatrix} 1 & \frac{\sqrt{3}}{3} \\ 0 & \frac{2\sqrt{3}}{3} \end{pmatrix}, & B_{\sqrt{3}} &= \frac{\sqrt{2}}{3^{1/4}} \begin{pmatrix} \frac{1}{2} & \frac{\sqrt{3}}{6} \\ 0 & \frac{\sqrt{3}}{3} \end{pmatrix} \end{aligned} \quad (\text{C.10})$$

with $\det A_1 = \frac{1}{\sqrt{3}} < 1$ and $\det B_1 = \sqrt{3} > 1$ while $\det A_{\sqrt{3}} = \det B_{\sqrt{3}} = 1$. The inequality $\det A_1 < \det B_1$ contradicts the desired condition $\det A_k \geq \det B_k$ expected for the inclusion $R_k^{\text{su}_3} \subseteq W_k^{\text{su}_3}$. This makes the case $k=1$ anomalous and worthy of closer scrutiny. To reconcile this, we interpret $k=1$ as the integer part of $\sqrt{3}$ that is $k = [\sqrt{3}] = 1$ which allows us to retain the property $\det A_k \geq \det B_k$ within the regime $k \geq \sqrt{3}$. Moreover, for $k > [\sqrt{3}]$ the set $W_k^{\text{su}_3}$ splits into a union of k sheets. Specifically, when

⁶ Matrices of type $A_{\sqrt{3}}$ and $B_{\sqrt{3}}$ appeared in [54]; see eqs(4.5, 4.19, 4.26) there.

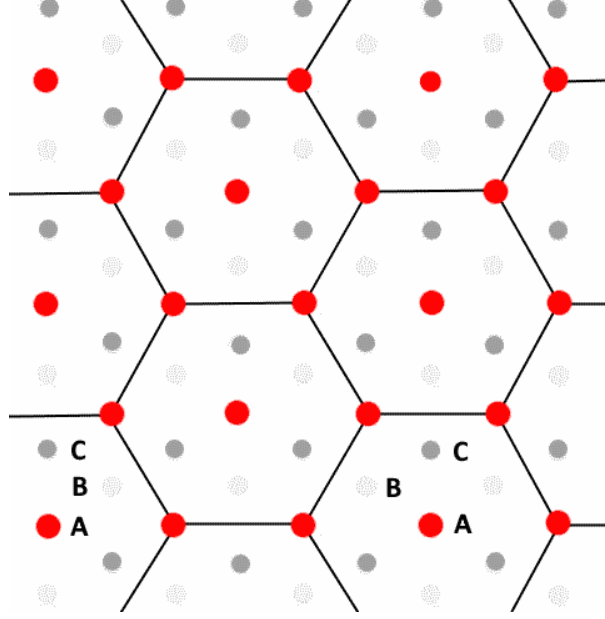


Figure 20: the $W_k^{\text{su}_3}$ for $k=\sqrt{3}$ is isomorphic to the sheet $R_3^{\text{su}_3}(\varepsilon)|_{\varepsilon=0}$ with red sites of Figure 11. Sublattices with light and bold grey refer to $R_3^{\text{su}_3}(\varepsilon)|_{\varepsilon=1,2}$.

$k=\sqrt{3}$ the lattice W , depicted in Figure 20, is generated by site vectors \mathbf{k}_m labeled as $(2m_1 + m_2)\tilde{\alpha}_1 + (m_1 + 2m_2)\tilde{\alpha}_2$ with $\mathbf{m} = (m_1, m_2)$ and $\tilde{\alpha}_i = \frac{1}{3^{1/4}}\alpha_i$ where the two α_i 's are the simple roots of SL_3 . The graphic of $W_{\sqrt{3}}^{\text{su}_3}$ in the Figure 20 is isomorphic to the red sublattice (A-sites) in the three sheet lattice $W_3^{\text{su}_3}$ shown in Figure 11.

b) Case $k=2$

For the CS level $k=2$, which lies above $\sqrt{3}$, the following hold: (i) the inclusion $R_2^{\text{su}_3} \subset W_2^{\text{su}_3}$ with $R_2^{\text{su}_3}$ being the hexagonal lattice generated by the dilated $\tilde{\alpha}_i = \sqrt{\frac{2}{3}}\alpha_i$. (ii) the weight lattice $W_2^{\text{su}_3}$ is generated by the compressed $\tilde{\lambda}_i = \sqrt{\frac{3}{2}}\lambda_i$ and comprises two superposed sheets $R_2^{\text{su}_3}(\varepsilon)$ with $\varepsilon = 0, 1$. Each sheet $R_2^{\text{su}_3}(\varepsilon)$ is isomorphic to the hexagonal root lattice $R_2^{\text{su}_3}$ which can be directly inferred from eq(C.8). Analogously, for $k=3$, the $W_3^{\text{su}_3}$ consists of three superposed sheets as depicted by the Figure 11. Notice also that the coordinates \mathbf{k}_m^0 of $R_2^{\text{su}_3}|_{\varepsilon=0}$ and \mathbf{k}_m of $R_2^{\text{su}_3}|_{\varepsilon=1}$ in $W_2^{\text{su}_3}$ are given by

$$\begin{aligned} \mathbf{k}_m^0 &= (2m_1 + m_2)\tilde{\alpha}_1 + (m_1 + 2m_2)\tilde{\alpha}_2 \\ \mathbf{k}_m &= \mathbf{k}_m^0 + \tilde{\lambda}_2 \end{aligned} \tag{C.11}$$

Here, A-sites in $R_2^{\text{su}_3}|_{\varepsilon=0}$ are colored red, while B-sites in $R_2^{\text{su}_3}|_{\varepsilon=1}$ are blue, giving rise to the two layer honeycomb structure depicted by the Figure 21. The corresponding

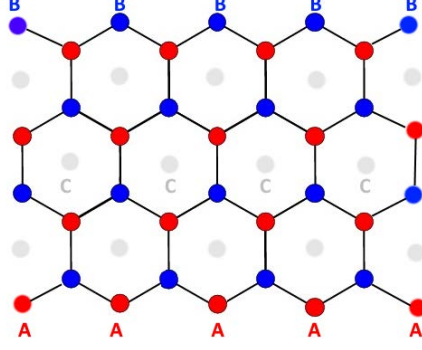


Figure 21: The two sheets $R_2^{sl_3} [0] \cup R_2^{sl_3} [1]$ of $W_3^{sl_3}$. The sites A in $R_2^{sl_3} [0]$ are in red color while the site B in $R_2^{sl_3} [1]$ are in blue. The sites C of the omitted sheet are in grey.

matrices A_2 and B_2 are given by

$$A_2 = \frac{2}{\sqrt{3}} \begin{pmatrix} 1 & -\frac{1}{2} \\ 0 & \frac{\sqrt{3}}{2} \end{pmatrix}, \quad B_2 = \sqrt{3} \begin{pmatrix} \frac{1}{2} & \frac{\sqrt{3}}{6} \\ 0 & \frac{\sqrt{3}}{3} \end{pmatrix} \quad (\text{C.12})$$

and finally the triplet $(\Lambda_2^{\text{su}_3}, \Lambda_2^{\text{su}_3^*}, \Lambda_{2C}^{\text{su}_3})$ read as follows

$$\Lambda_2^{\text{su}_3} = \begin{pmatrix} A_2 & 0 \\ 0 & A_2 \end{pmatrix}, \quad \Lambda_2^{\text{su}_3^*} = \begin{pmatrix} B_2 & 0 \\ 0 & B_2 \end{pmatrix}, \quad \Lambda_{2C}^{\text{su}_3} = \begin{pmatrix} A_2 & 0 \\ 0 & B_2 \end{pmatrix} \quad (\text{C.13})$$

To complete the present study, we think it interesting to add a discussion regarding the CS level $k=2$ of the holographic dual of Narain CFT built out of the $SU(3)$ lattices $R_k^{\text{su}_3}$ and $W_k^{\text{su}_3}$. These lattices are given by *the Figures 20-21*. The characteristic matrices of the three lattices $\Lambda_2^{\text{su}_3}$, $\Lambda_{2C}^{\text{su}_3}$ and $\Lambda_2^{\text{su}_3^*}$ are given by eqs(C.12,C.13). Holographically, the dual Narain CFT based on $\Lambda_{2C}^{\text{su}_3}$ is described by the AB-action (B.1) that reads in our notations like

$$\mathcal{S}_{\text{CS}} + \mathcal{S}_{\text{BND}} = \frac{i}{2\pi} \int_{\mathcal{M}} \text{Tr} (\mathbf{A} \wedge d\mathbf{B} + \mathbf{B} \wedge d\mathbf{A}) + \int_{\partial\mathcal{M}} \text{Tr} (\mathbf{A}_z \tilde{K} \mathbf{A}_{\bar{z}} + \mathbf{B}_z K \mathbf{B}_{\bar{z}}) \quad (\text{C.14})$$

In this expression, the potentials \mathbf{A} and \mathbf{B} are given by linear combinations of the old potential pairs $(\mathcal{A}_1, \mathcal{A}_2)$ and $(\mathcal{B}_1, \mathcal{B}_2)$ as follows

$$\begin{aligned} \mathbf{A} &= \mathcal{A}^1 \tilde{\alpha}_1 + \mathcal{A}^2 \tilde{\alpha}_2 & \tilde{\alpha}_i &= \sqrt{\frac{k}{3}} \alpha_i \\ \mathbf{B} &= \mathcal{B}_1 \tilde{\lambda}^1 + \mathcal{B}_2 \tilde{\lambda}^2 & \tilde{\lambda}^i &= \sqrt{\frac{3}{k}} \lambda^i \end{aligned} \quad (\text{C.15})$$

In these relations, we have $\mathcal{A}^i = \tilde{\lambda}^i \cdot \mathbf{A}$ and $\mathcal{B}_i = \tilde{\alpha}_i \cdot \mathbf{B}$; in terms of the matrices (\tilde{A}_i^j) and (\tilde{B}_j^i) given by eqs(3.5,3.8) with $k=2$, we also have $\mathcal{A}^i = (\tilde{B}_j^i) \mathcal{A}^j$ and $\mathcal{B}_i = (\tilde{A}_i^j) \mathcal{B}_j$. For this holographic dual, the dimension of the Hilbert space is $\dim \mathcal{H} = k^2$; it is generated by

the wave functions $\Psi_{\mathbf{a},\mathbf{b}}(\xi, \zeta)$ labeled by $\mathbf{a} = a\tilde{\boldsymbol{\alpha}}_2$ and $\mathbf{b} = b\tilde{\boldsymbol{\lambda}}_2$ with $a, b = 0, 1 \pmod 2$. These multi-holomorphic functions are defined in terms of the path integral as

$$\Psi(\xi, \bar{\zeta}) = \int_{(\xi, \bar{\zeta})} [DADB] e^{-\mathcal{S}_{\text{CS}} + \mathcal{S}_{\text{BND}}} \quad (\text{C.16})$$

where $(\xi, \bar{\zeta})$ encode the boundary conditions of the CS potentials \mathcal{A}^i and \mathcal{B}_i on the boundary $\partial\mathcal{M} = \mathbb{T}^2$ [21]. For solid torii, their explicit expressions coincide with by the genus-one partition functions of the $\mathbb{Z}_2 \times \mathbb{Z}_2$ Narain CFTs with $c_{L/R} = 2$. They read like

$$\Psi_{\mathbf{a},\mathbf{b}}(\xi, \zeta) = \frac{1}{|\eta(\tau)|^2} \sum_{\mathbf{n}, \mathbf{m}} e^{i\pi\tau P_L^2 - i\pi\bar{\tau} P_R^2 + 2i\pi(P_L\xi - P_R\bar{\zeta}) + \frac{\pi}{2\tau_2}(\xi^2 + \zeta^2)} \quad (\text{C.17})$$

where $\eta(\tau)$ is the usual Dedekind eta function and where ($k = 2$) the left/right momenta $p_{L/R}$ are given by [with $P_1^i = (P_L^i + P_R^i)/2$ and $P_2^i = (P_L^i - P_R^i)/2$],

$$\begin{aligned} P_L^i &= \frac{1}{\sqrt{2k}} \left[\tilde{A}_j^i (a^j + kn^j) + (b_j + km_j) \tilde{B}_i^j \right] \\ P_R^i &= \frac{1}{\sqrt{2k}} \left[\tilde{A}_j^i (a^j + kn^j) - (b_j + km_j) \tilde{B}_i^j \right] \end{aligned} \quad (\text{C.18})$$

with \tilde{A}_j^i and \tilde{B}_i^j as in (C.12). The integers n^j describe the KK modes and the m_j 's are windings. In terms of the simple $\boldsymbol{\alpha}_i$ and the fundamental $\boldsymbol{\lambda}^i$, we have $\mathbf{P}_{L/R} = \frac{1}{2}[(a^i + 2n^i)\boldsymbol{\alpha}_i \pm (b_i + 2m_i)\boldsymbol{\lambda}^i]$. For the ground state for which $n^i = m_i = 0$, the associated momenta are given by $\hat{\mathbf{p}}_{L/R} = \frac{1}{2}(a\boldsymbol{\alpha}_2 \pm b\boldsymbol{\lambda}_2)$; then we have $\mathbf{P}_{L/R} = \hat{\mathbf{p}}_{L/R} + \mathbf{p}_{L/R}$ with excitations $\mathbf{p}_{L/R} = n^i\boldsymbol{\alpha}_i \pm m_i\boldsymbol{\lambda}^i$. Moreover, the complex ξ^i and ζ^i , interpreted in terms of fugacities in conformal field theory, can be respectively parameterised like

$$\begin{aligned} \xi^i &= \sqrt{\frac{k}{2}} (\tilde{A}_j^i u^j + v_j \tilde{B}_i^j) \\ \zeta^i &= \sqrt{\frac{k}{2}} (\tilde{A}_j^i \bar{u}^j - \bar{v}_j \tilde{B}_i^j) \end{aligned} \quad (\text{C.19})$$

For $k=3$, the manifestation of the $\text{SU}(3)$ symmetry is given by $K = A^T A$ and $\tilde{K} = B B^T$ where K is the Cartan matrix and \tilde{K} its inverse ($K\tilde{K} = I$). Further developments in this direction and in link with lattice topological matter with Dirac points will be reported in a future occasion.

References

- [1] Wen, X. G. (2004). Quantum field theory of many-body systems: From the origin of sound to an origin of light and electrons. Oxford university press.
- [2] Fradkin, E. (2013). Field theories of condensed matter physics. Cambridge University Press.

- [3] Kitaev, A. Y. (2003). Fault-tolerant quantum computation by anyons. *Annals of physics*, 303(1), 2-30.
- [4] Dymarsky, A., & Shapere, A. (2021). Solutions of modular bootstrap constraints from quantum codes. *Physical Review Letters*, 126(16), 161602.
- [5] Dymarsky, A., & Shapere, A. (2021). Quantum stabilizer codes, lattices, and CFTs. *Journal of High Energy Physics*, 2021(3), 1-84.
- [6] Buican, M., Dymarsky, A., & Radhakrishnan, R. (2023). Quantum codes, CFTs, and defects. *Journal of High Energy Physics*, 2023(3), 1-37.
- [7] Moriwaki, Y. (2021). Code conformal field theory and framed algebra. arXiv preprint arXiv:2104.10094.
- [8] Sang, S., Hsieh, T. H., & Zou, Y. (2024). Approximate quantum error correcting codes from conformal field theory. *Physical Review Letters*, 133(21), 210601.
- [9] Ando, K., Kawabata, K., & Nishioka, T. (2024). Quantum subsystem codes, CFTs and their \mathbb{Z}_2 -gaugings. *Journal of High Energy Physics*, 2024(11), 1-44.
- [10] Kawabata, K., Nishioka, T., & Okuda, T. (2024). Narain CFTs from quantum codes and their \mathbb{Z}_2 gauging. *Journal of High Energy Physics*, 2024(5), 1-56.
- [11] Kusuki, Y. (2024). Modern Approach to 2D Conformal Field Theory. arXiv preprint arXiv:2412.18307.
- [12] Alam, Y. F., Kawabata, K., Nishioka, T., Okuda, T., & Yahagi, S. (2023). Narain CFTs from nonbinary stabilizer codes. *Journal of High Energy Physics*, 2023(12), 1-38.
- [13] Henriksson, J., Kakkar, A. & McPeak, B. Narain CFTs and quantum codes at higher genus. *J. High Energ. Phys.* 2023, 11 (2023). [https://doi.org/10.1007/JHEP04\(2023\)011](https://doi.org/10.1007/JHEP04(2023)011).
- [14] Kawabata, K., Nishioka, T., & Okuda, T. (2024). Narain CFTs from quantum codes and their \mathbb{Z}_2 gauging. *Journal of High Energy Physics*, 2024(5), 1-56.
- [15] Saidi, E. H., & Sammani, R. (2024). Classification of Narain CFTs and Ensemble Average. arXiv preprint arXiv:2412.13932.
- [16] Ando, K., Kawabata, K., & Nishioka, T. (2025). Gauging \mathbb{Z}_N symmetries of Narain CFTs. arXiv preprint arXiv:2503.21524.
- [17] Förste, S., Jockers, H., Kames-King, J. et al. Ensemble averages of \mathbb{Z}_2 orbifold classes of Narain CFTs. *J. High Energ. Phys.* 2024, 240 (2024). [https://doi.org/10.1007/JHEP05\(2024\)240](https://doi.org/10.1007/JHEP05(2024)240).
- [18] Yahagi, S. Narain CFTs and error-correcting codes on finite fields. *J. High Energ. Phys.* 2022, 58 (2022). [https://doi.org/10.1007/JHEP08\(2022\)058](https://doi.org/10.1007/JHEP08(2022)058)

- [19] Henriksson, J., Kakkar, A. & McPeak, B. Classical codes and chiral CFTs at higher genus. *J. High Energ. Phys.* 2022, 159 (2022). [https://doi.org/10.1007/JHEP05\(2022\)159](https://doi.org/10.1007/JHEP05(2022)159)
- [20] Dymarsky, A., Henriksson, J., & McPeak, B. (2025). Holographic duality from Howe duality: Chern-Simons gravity as an ensemble of code CFTs. arXiv preprint arXiv:2504.08724.
- [21] Aharony, O., Dymarsky, A. & Shapere, A.D. Holographic description of Narain CFTs and their code-based ensembles. *J. High Energ. Phys.* 2024, 343 (2024). [https://doi.org/10.1007/JHEP05\(2024\)343](https://doi.org/10.1007/JHEP05(2024)343)
- [22] Yahagi, S. (2022). Narain CFTs and error-correcting codes on finite fields. *Journal of High Energy Physics*, 2022(8), 1-21.
- [23] Dymarsky, A., Shapere, A. Quantum stabilizer codes, lattices, and CFTs. *J. High Energ. Phys.* 2021, 160 (2021). [https://doi.org/10.1007/JHEP03\(2021\)160](https://doi.org/10.1007/JHEP03(2021)160)
- [24] Henriksson, J., Kakkar, A. & McPeak, B. Narain CFTs and quantum codes at higher genus. *J. High Energ. Phys.* 2023, 11 (2023). [https://doi.org/10.1007/JHEP04\(2023\)011](https://doi.org/10.1007/JHEP04(2023)011)
- [25] Seiberg, N., & Witten, E. (2016). Gapped boundary phases of topological insulators via weak coupling. *Progress of Theoretical and Experimental Physics*, 2016(12), 12C101.
- [26] Kapustin, A., & Seiberg, N. (2014). Coupling a QFT to a TQFT and Duality. *Journal of High Energy Physics*, 2014(4), 1-45.
- [27] Andrianopoli, L., Cerchiai, B., D'Auria, R. et al. -extended $D = 4$ supergravity, unconventional SUSY and graphene. *J. High Energ. Phys.* 2020, 84 (2020). [https://doi.org/10.1007/JHEP01\(2020\)084](https://doi.org/10.1007/JHEP01(2020)084)
- [28] Drissi, L. B., Saidi, E. H., & Bousmina, M. (2010). Electronic properties and hidden symmetries of graphene. *Nuclear Physics B*, 829(3), 523-533.
- [29] Drissi, L. B., Saidi, E. H., & Bousmina, M. (2011). Four-dimensional graphene. *Physical Review D Particles, Fields, Gravitation, and Cosmology*, 84(1), 014504.
- [30] Sénéchal, D. (2004). An introduction to bosonization. In *Theoretical Methods for Strongly Correlated Electrons* (pp. 139-186). New York, NY: Springer New York.
- [31] E. Miranda, Introduction to Bosonization, *Brazilian Journal of Physics*, vol. 33, no. 1, March, 2003.
- [32] R.Shankar, *Acta Physica Polonica B*. Vol 26 (1995), N 12.
- [33] Fruchart, M., & Carpentier, D. (2013). An introduction to topological insulators. *Comptes Rendus. Physique*, 14(9-10), 779-815.

- [34] Haldane, F. D. M. (1988). Model for a quantum Hall effect without Landau levels: Condensed-matter realization of the "parity anomaly". *Physical review letters*, 61(18), 2015.
- [35] Schnyder, A. P., Ryu, S., Furusaki, A., & Ludwig, A. W. (2008). Classification of topological insulators and superconductors in three spatial dimensions. *Physical Review B Condensed Matter and Materials Physics*, 78(19), 195125.
- [36] L. B Drissi, E. H Saidi, From orthosymplectic structure to super topological matter, *Nuclear Physics B*, Volume 989, April 2023, 116128.
- [37] Saidi, E. H., Fassi-Fehri, O., & Bousmina, M. (2012). Topological aspects of fermions on hyperdiamond. *Journal of mathematical physics*, 53(7).
- [38] Drissi, L.B., Mhamdi, H. & Saidi, E.H. Anomalous quantum Hall effect of 4D lattice QCD in background fields. *J. High Energ. Phys.* 2011, 26 (2011).
[https://doi.org/10.1007/JHEP10\(2011\)026](https://doi.org/10.1007/JHEP10(2011)026).
- [39] Drissi, L.B., Lounis, S. & Saidi, E.H. Higher-order topological matter and fractional chiral states. *Eur. Phys. J. Plus* 137, 796 (2022).
<https://doi.org/10.1140/epjp/s13360-022-02975-2>
- [40] Drissi, L. B., & Saidi, E. H. (2020). A signature index for third order topological insulators. *Journal of Physics: Condensed Matter*, 32(36), 365704.
- [41] Altland, A., & Zirnbauer, M. R. (1997). Nonstandard symmetry classes in mesoscopic normal-superconducting hybrid structures. *Physical Review B*, 55(2), 1142.
- [42] Witten, E. (2016). Fermion path integrals and topological phases. *Reviews of Modern Physics*, 88(3), 035001.
- [43] Witten, E. (2016). Three lectures on topological phases of matter. *La Rivista del Nuovo Cimento*, 39, 313-370.
- [44] Chiu, C. K., Teo, J. C., Schnyder, A. P., & Ryu, S. (2016). Classification of topological quantum matter with symmetries. *Reviews of Modern Physics*, 88(3), 035005.
- [45] Saidi, E. H. (2019). Gapped gravitinos, isospin particles, and partial breaking. *Progress of Theoretical and Experimental Physics*, 2019(1), 013B01.
- [46] Benalcazar, W. A., Bernevig, B. A., & Hughes, T. L. (2017). Quantized electric multipole insulators. *Science*, 357(6346), 61-66.
- [47] Drissi, L. B., Saidi, E. H., & Bousmina, M. (2011). Four-dimensional graphene. *Physical Review D—Particles, Fields, Gravitation, and Cosmology*, 84(1), 014504.

- [48] Borici, A. (2008). Creutz fermions on an orthogonal lattice. *Physical Review D Particles, Fields, Gravitation, and Cosmology*, 78(7), 074504.
- [49] Creutz, M., Kimura, T., & Misumi, T. (2010). Index theorem and overlap formalism with naive and minimally doubled fermions. *Journal of High Energy Physics*, 2010(12), 1-23.
- [50] Drissi, L. B., & Saidi, E. H. (2011). Dirac zero modes in hyperdiamond model. *Physical Review D Particles, Fields, Gravitation, and Cosmology*, 84(1), 014509.
- [51] Drissi, L. B., Lounis, S., & Saidi, E. H. (2022). Higher-order topological matter and fractional chiral states. *The European Physical Journal Plus*, 137(7), 796.
- [52] Asboth, J. K., Oroszlany, L., Palyi, A., (2016). Berry phase, chern number. *A Short Course on Topological Insulators: Band Structure and Edge States in One and Two Dimensions*, 23-44.
- [53] Weisbrich, H., Klees, R. L., Rastelli, G., & Belzig, W. (2021). Second Chern number and non-Abelian Berry phase in topological superconducting systems. *PRX Quantum*, 2(1), 010310.
- [54] Angelinos, N., Chakraborty, D. & Dymarsky, A. Optimal Narain CFTs from codes. *J. High Energ. Phys.* 2022, 118 (2022). [https://doi.org/10.1007/JHEP11\(2022\)118](https://doi.org/10.1007/JHEP11(2022)118)
- [55] Sammani, R., Boujakhrou, Y., Saidi, E. H., Laamara, R. A., & Drissi, L. B. (2023). Higher spin AdS 3 gravity and Tits-Satake diagrams. *Physical Review D*, 108(10), 106019.
- [56] Sammani, R., Boujakhrou, Y., Laamara, R. A., & Drissi, L. B. (2024). Finiteness of 3D higher spin gravity Landscape. *Classical and Quantum Gravity*, 41(21), 215012.
- [57] Sammani, R., & Saidi, E. H. (2025). Higher spin swampland conjecture for massive AdS₃ gravity. *SciPost Physics*, 18(6), 173.
- [58] Sammani, R., Saidi, E. H., & Laamara, R. A. (2025). Black hole solutions of three dimensional E6-gravity. *Journal of Mathematical Physics*, 66(2).
- [59] Boujakhrou, Y., Saidi, E. H., Ahl Laamara, R., & Btissam Drissi, L. (2023). 't Hooft lines of ADE-type and topological quivers. *SciPost Physics*, 15(3), 078.
- [60] Boujakhrou, Y. (2022). On exceptional't Hooft lines in 4D-Chern-Simons theory. *Nuclear Physics B*, 980, 115795.
- [61] Boujakhrou, Y., Saidi, E. H., Laamara, R. A., & Drissi, L. B. (2023). Embedding integrable superspin chain in string theory. *Nuclear Physics B*, 990, 116156.
- [62] Gouba, L. A. U. R. E., Avossevou, G. Y., Govaerts, J., & Hounkononou, M. N. (2004, December). Fermionisation of a two-dimensional free massless complex scalar field. In

Contemporary Problems In Mathematical Physics-Proceedings Of The Third International Workshop (p. 233). World Scientific.

- [63] Kawai, H., Lewellen, D. C., & Tye, S. H. H. (1987). Construction of fermionic string models in four dimensions. *Nuclear Physics B*, 288, 1-76.
- [64] Tudor D. Stanescu, *Introduction to Topological Quantum Matter & Quantum Computation*, ISBN 9781032126524, 442 Pages 84 B/W Illustrations. Published July 2, 2024 by CRC Press
- [65] Saidi, E. H. (2012). On flavor symmetry in lattice quantum chromodynamics. *Journal of mathematical physics*, 53(2).
- [66] Misumi, T., Kimura, T., & Ohnishi, A. (2012). QCD phase diagram with two-flavor lattice fermion formulations. *Physical Review D Particles, Fields, Gravitation, and Cosmology*, 86(9), 094505.
- [67] Ashwinkumar, M., Kidambi, A., Leedom, J. M., & Yamazaki, M. (2023). Generalized Narain Theories Decoded: Discussions on Eisenstein series, Characteristics, Orbifolds, Discriminants and Ensembles in any Dimension. arXiv preprint arXiv:2311.00699.
- [68] Datta, S., Duany, S., Kraus, P. et al. Adding flavor to the Narain ensemble. *J. High Energ. Phys.* 2022, 90 (2022). [https://doi.org/10.1007/JHEP05\(2022\)090](https://doi.org/10.1007/JHEP05(2022)090).
- [69] Dymarsky, A., & Shapere, A. (2021). Comments on the holographic description of Narain theories. *Journal of High Energy Physics*, 2021(10), 1-26.
- [70] Afkhami-Jeddi, N., Cohn, H., Hartman, T., & Tajdini, A. (2021). Free partition functions and an averaged holographic duality. *Journal of High Energy Physics*, 2021(1), 1-43.
- [71] Maloney, A., & Witten, E. (2010). Quantum gravity partition functions in three dimensions. *Journal of High Energy Physics*, 2010(2), 1-58.
- [72] Sammani, R., Saidi, E.H., Laamara, R.A. et al. Fluctuating ensemble averages and the BTZ threshold. *Eur. Phys. J. C* 85, 467 (2025). <https://doi.org/10.1140/epjc/s10052-025-14181-2>